EMBL

RESEARCH REPORTS 1977

TABLE OF CONTENTS

DIVISION OF CELL BIOLOGY

Non-histone chromosomal proteins

Member: E. Jost

Fellow: S. Ely

Technical assistants: M. Klein*, A. d'Arcy*

The efforts of this group are directed towards an understanding of the structure of the eukaryotic chromosome and the control of gene expression in higher organisms. It is generally agreed that histones play the important role in packing DNA inside the cell nucleus but are not directly involved in regulating gene expression. Non-histone chromosomal proteins are concentrated in template-active portions of the genome and hence considered to be involved in gene expression, but to a lesser extent in the structure of the chromosome. A more specific way in which non-histone proteins might contribute to gene regulation is by recognizing specific sequences of the DNA, which requires sensing the molecule in the minor or the major groove. We have a method of testing more specific recognition of the DNA by non-histones by using intercalating agents as "reporter" molecules. We have chosen intercalating agents with large side groups protruding into the minor groove of the DNA, and we have found that although the majority of the non-histone chromosomal proteins bind DNA only a minor fraction seems to bind by recognizing the minor groove. The arrangement of these proteins on the histone/DNA complex is under investigation.

Non-histone proteins may also contribute to the structure of chromosomes. Studies of their role in maintaining the loops in eukaryotic DNA are being undertaken. As an experimental system we use structures which may be released from cells by gentle lysis in solutions containing non-ionic detergents and high concentrations of salt. These "nucleoids" contain superhelical DNA and retain some of the morphological features of nuclei. The DNA inside the "nucleoids" exhibits the behaviour of circular, supercoiled molecules. Constraints which prevent the free rotation of the strands of the double helix have been found to be sensitive to RNAase and protease. Only about 7 major proteins are associated with "nucleoids" that contain these intact DNA molecules. The first three of these proteins have been isolated and identified as proteins belonging to the proteinaceous lamina attached to the nuclear pore complex underlying the inner nuclear membrane. Employing preparative

---

* part of the year

SDS-polyacrylamide electrophoresis to separate the proteins, we have excized discrete bands from gels and used the subsequently-eluted proteins to immunize chickens. Monospecific antibodies have been prepared. Ouchterlony double diffusion analysis, double immunoprecipitation, and indirect immunofluorescent microscopy have been used to characterize the antisera and to localize the proteins in cells and "nucleoids". All three antisera crossreact with one other and present a similar staining pattern. Characteristic changes of the protein distribution have been recognized during the cell cycle; at metaphase the proteins which had been concentrated at the nuclear membrane disassemble and are distributed over the whole cytoplasm, whereas at telophase the antigens gradually shift to the location of the chromosomes. We propose that the proteins are part of a biological polymer constituting the proteinaceous lamina of the nuclear pore complex. This complex is disassembled and reassembled during the cell cycle.

Plate I

The proteinaceous lamina of the nuclear pore complex is also present in "nucleoids". Therefore "nucleoids" remain intact structures with histone-free and unravelled but supercoiled DNA inside. These proteins are therefore essential for the structural integrity of the "nucleoids". Four other proteins are present in large amounts in "nucleoids"; these have also been isolated and antibodies are being prepared. Their distribution in supercoiled DNA will be studied.

Using double labelling techniques, we have compared (in cooperation with P.R. Cook (Oxford)), at different salt concentrations, the amounts and types of protein associated with human "nucleoids" containing superhelical DNA or relaxed DNA. We find that the slightly lysine-rich histones (H2A and H2B), but not the arginine-rich histones (H3 and H4), dissociate more slowly from "nucleoids" containing superhelical DNA than from relaxed DNA. A protein of apparent molecular weight 22,000 also binds more tightly to the superhelical DNA; we conclude that this protein and the slightly lysine-rich histones convert the free energy of supercoiling into binding energy when they bind to superhelical DNA.

Control of morphogenesis in hydra

Members: H.C. Schaller, C. Grimmelikhuijzen

Student: T. Schmidt

Visiting workers: H. Bode*, F. Bode* (part-time)

Technical assistants: K. Flick, C. Francke* (part-time)

Pattern formation in hydra is controlled by at least four substances: an activator and an inhibitor of head formation and an activator and an inhibitor of foot formation. We have developed quantitative assays for these substances and are able to separate them free of contamination by each other in relatively few steps with little loss of material. Our aim is to characterize them chemically and to investigate how they act and interact to control growth and differentiation, and thus morphogenesis, in hydra.

Isolation of the four morphogens

We have processed 100 kg of sea anemones to obtain somewhat larger amounts as starting material for the chemical analysis. To be able to isolate all four substances in high yield, it was necessary to develop new purification procedures applicable to large-scale preparation.

Head activator in rat intestine

Like a number of other hypothalamic hormones we found that the "head activator" peptide of the mammalian system is present in the intestine as well. Since larger amounts are present in the intestine than in the brain, the intestine may be the better source for a large-scale preparation of the mammalian peptide.

Morphogenetic mutants of hydra

We have analyzed four morphogenetic mutants of hydra for their content of and response to the above four "morphogens" from hydra. As expected these mutants show changes in morphogen concentration and/or action. For example *aberrant*, a mutant with a very low head forming potential and few tentacles per head (4 instead

Plate II (a)

Plate I

Distribution of a protein of the fibrous lamina/ nuclear pore complex system in different cell-cycle stages of mouse L cells, as determined by indirect immunofluorescent microscopy. The predominant 3 polypeptides (MW 71, 68 and 66K dalton) that occur in association with the nuclear pore complexes underlying the inner nuclear membrane, were isolated and monospecific antibodies prepared. The plate shows the distribution in mouse L cells of the protein with apparent MW 68K dalton. Immunofluorescent staining of cells in different stages of the cell cycle (interphase, metaphase and telophase cells can be seen) indicates that the protein is part of a biological polymer that is assembled at the nuclear membrane at interphase. Following the breakdown of the nuclear membrane at pro-metaphase the protein is distributed homogeneously over the whole cell cytoplasm. Subsequent reassembly of the nuclear membrane at late telophase leads to a reassembly of the protein at the site of the nuclear membrane. This envelope is formed on the chromosomes of the daugther cells.

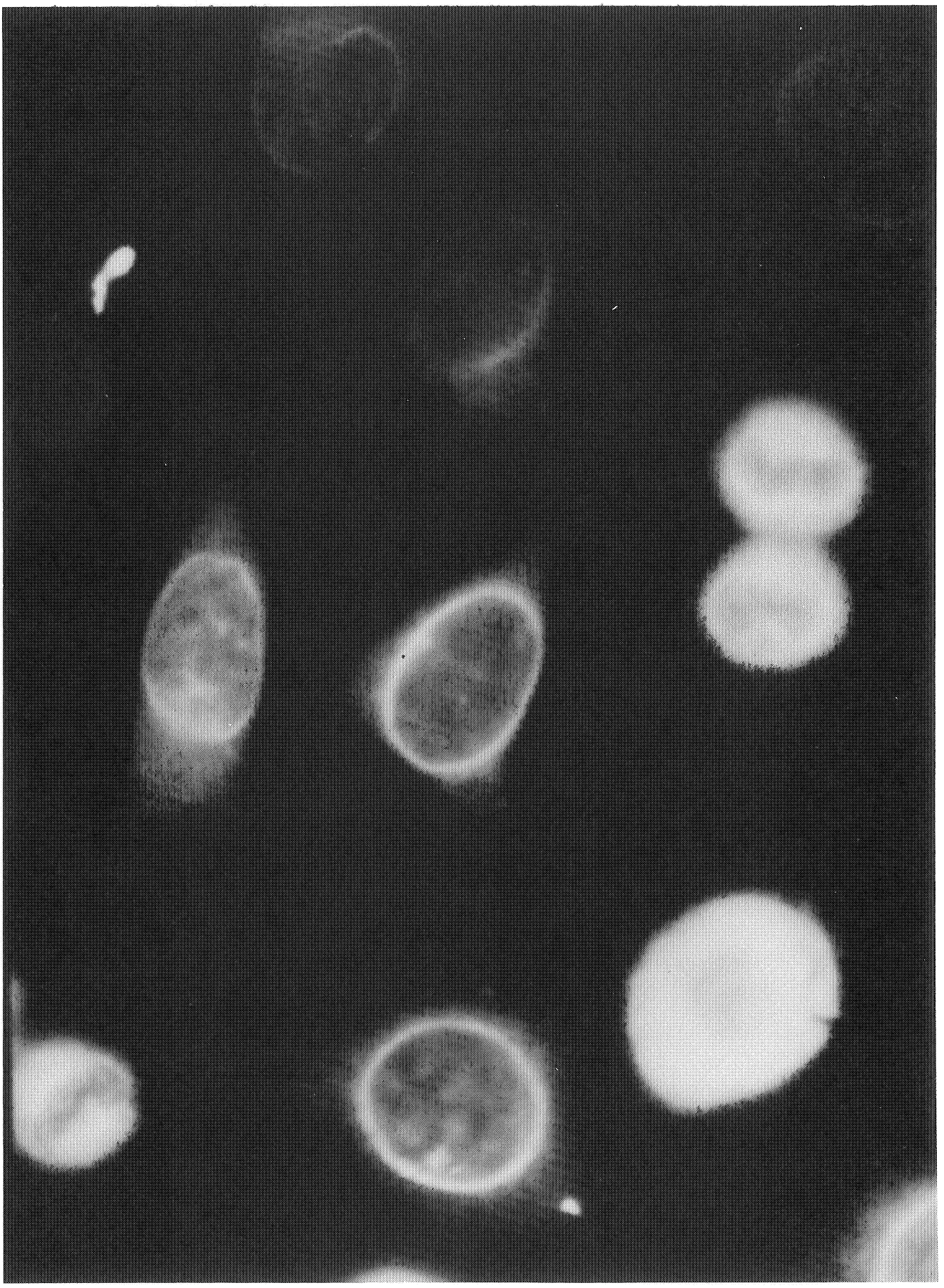

of 6) contained among other abnormalities reduced amounts of the head activator. The morphogenetic defects due to this could accordingly be complemented by treatment with purified head activator. Another mutant, which is distinguished by an excessive tentacle and hypostome production, contained increased amounts of the head factors. A very interesting pair of mutants is *mini* and *maxi* which have an altered size regulation. The small size of the *mini* is due to the fact that the animal starts budding at an extremely early stage. This change is probably caused by too low levels of head inhibitor. *Vice versa* the *maxi* only forms its first bud when the mother animal has reached an enormous size. We attribute this inability to bud to too high levels of head inhibitor.

Plate II (c)

Plate III

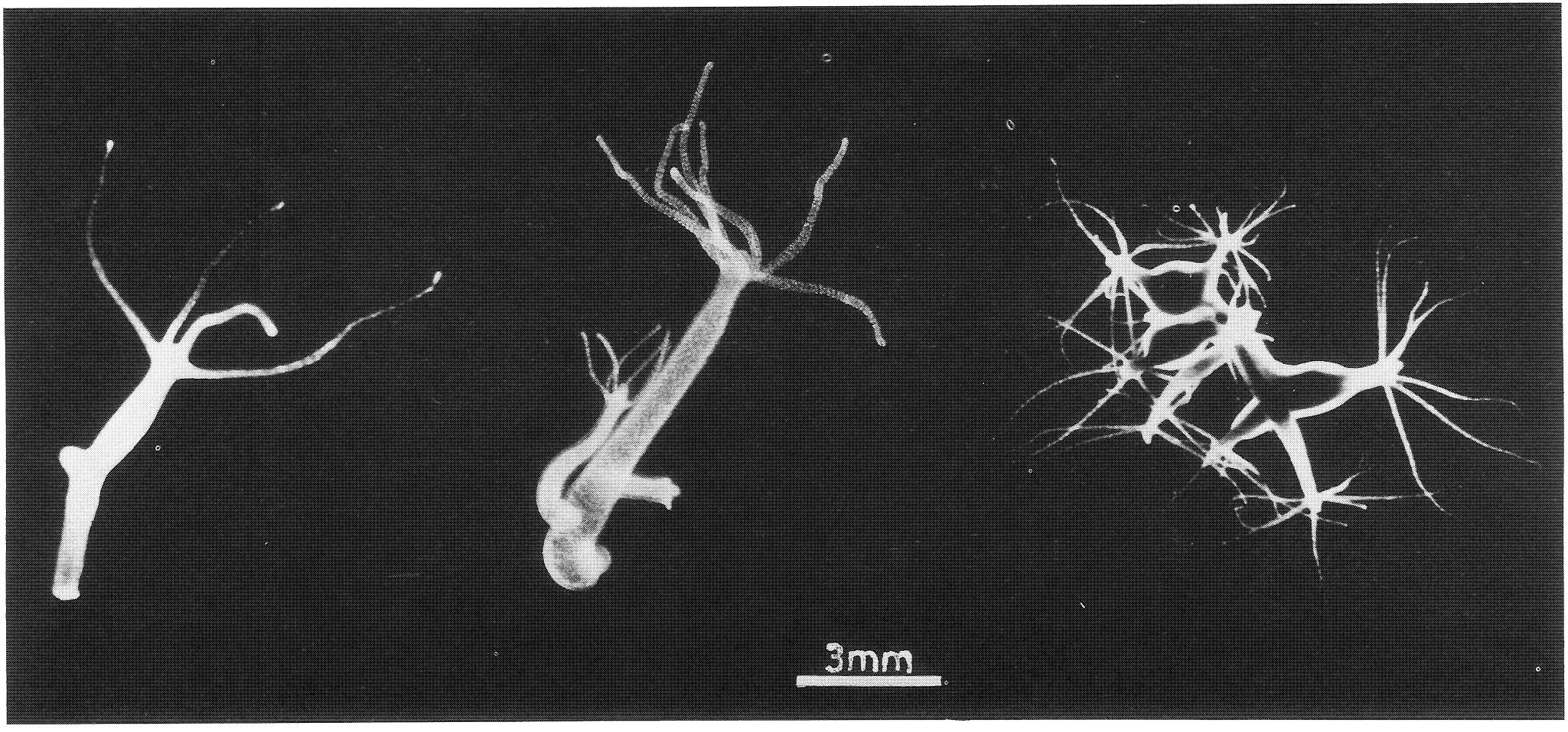

Plate II

Hydra and hydra mutants with changes in morphogenesis
(a) *aberrant*,
(b) wild-type *Hydra attenuata*,
(c) non-budding mutant

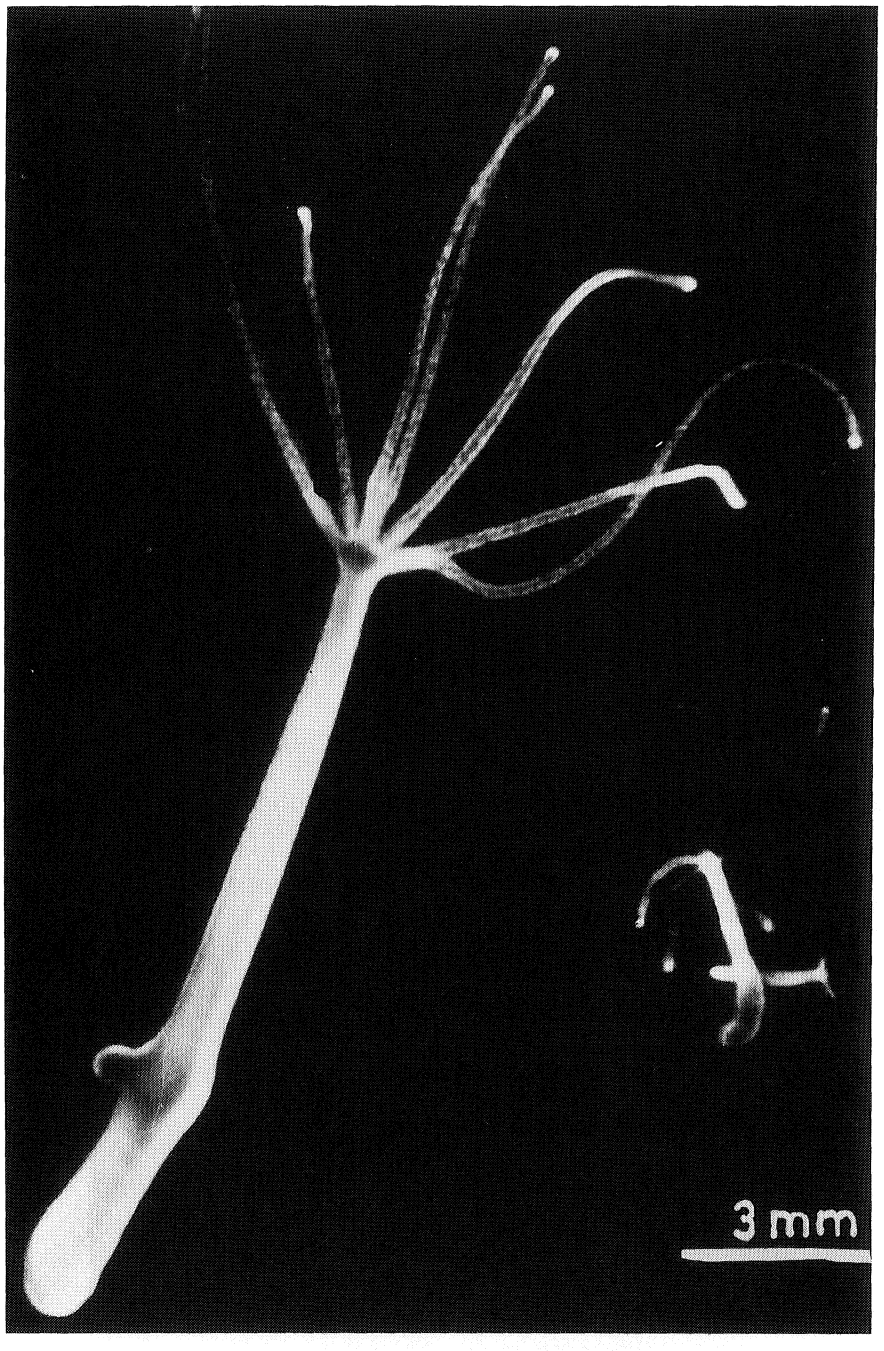

Plate III

Hydra mutants *maxi* and *mini*

Viruses, vaccines and membranes

Members: K. Simons, H. Garoff, A. Helenius

Fellows: E. Fries, B. Morein*, M. Sarvas*, A. Ziemiecki

Visiting workers: M.J. Gething*, H. Söderlund*, C. Terhorst*, M. Waterfield*

Technical assistants: K. Goldmann, E. Kiko, H. Virta

We have continued our studies of Semliki Forest virus to probe into the structure, function and synthesis of biological membranes. This animal virus is composed of a nucleocapsid assembled in the cytoplasm of the host cell, and a membrane that is acquired when the nucleocapsid buds out from the host cell plasma membrane. A number of significant developments have taken place during the year. Our biochemical studies have shown how the virus membrane proteins are oriented in the membrane, and work on the primary structure of these proteins has begun. A cell-free system for their synthesis has been constructed that has permitted detailed studies on the insertion of the proteins into the membrane. Most important, our hopes of crystallizing the virus have now been realized. Studies of the mechanism by which the virus enters into the host cells have reached the molecular level. We have been able to identify the host cell receptor for Semliki Forest virus, this being the first receptor for animal viruses to be described. It turned out that the major histo-compatibility antigens, HLA in human cells and H_2 in mouse cells, are in fact receptors for Semliki Forest virus.

Our work to develop methodology for handling and reconstitution of membrane proteins has led to a potentially important application. It is well known that the vaccines available against most enveloped viruses, e.g. influenza, are inefficient and usually not free from side-effects. The ideal vaccine should be a preparation of isolated viral spike proteins. Two new spike protein preparations of this type, spike protein micelles (octamers of the spikes) and virosomes (reconstituted viral envelopes) were tested in mice with dramatic results. The protective effect of these vaccines against Semliki Forest virus encephalitis was orders of magnitude higher than previously found for subunit vaccines.

Work on our second membrane system, the penicillinase secretion in *Bacillus licheniformis*, has been concerned with the structure of precursors of secreted penicillinase. These have turned out to be of a novel type for membrane ectoproteins. They have an amino-terminal hydrophobic extension apparently preceded by a signal sequence, whereas other ectoproteins so far studied (characterized by a large external hydrophobic domain attached to the lipid bilayer by a small hydrophobic segment) have been found to be attached to the membrane by their carboxy-terminal ends rather than their amino-terminal. This is the case for example, for the Semliki Forest virus spike glycoproteins.

Semliki Forest virus

Structure and synthesis

The spikes of Semliki Forest virus have a three-chain structure consisting of one chain each of the polypeptides E1 (MW 49×10^3), E2 (52×10^3) and E3 (10×10^3). Both E1 and E2 have short hydrophobic segments at their carboxy-terminal ends, attached to the lipid bilayer (in collaboration with H. Söderlund, University of Helsinki). The hydrophobic segment from E2 has been shown to penetrate the membrane, and it seems likely that the same may be true of the others. The amino-terminal amino-acid sequences of the polypeptides have been partially elucidated by automatic sequencing methods. We are planning to sequence all the structural proteins of the virus, not, however, by protein sequencing but by sequencing the cDNAs produced from their mRNAs.

We have been able to obtain crystals of the virus (in collaboration with R. Leberman), the largest being about 0.1 mm in the largest dimension but only about 0.02 mm in the smallest. These are still too small for x-ray crystallography, but attempts to obtain bigger crystals will be intensified. For this purpose it will be necessary to increase the potentiality for virus production and purification.

Plate IV

All four polypeptides of the virus, the nucleocapsid (C) and the spike polypeptides, are translated from a single initiation point on the 26S mRNA in the order C-E3-E2-E1. The C protein is removed from the nascent chain and remains in the cytoplasm, whereas the E polypeptides are inserted into the endoplasmic reticulum. In collaboration with B. Dobberstein we have been able

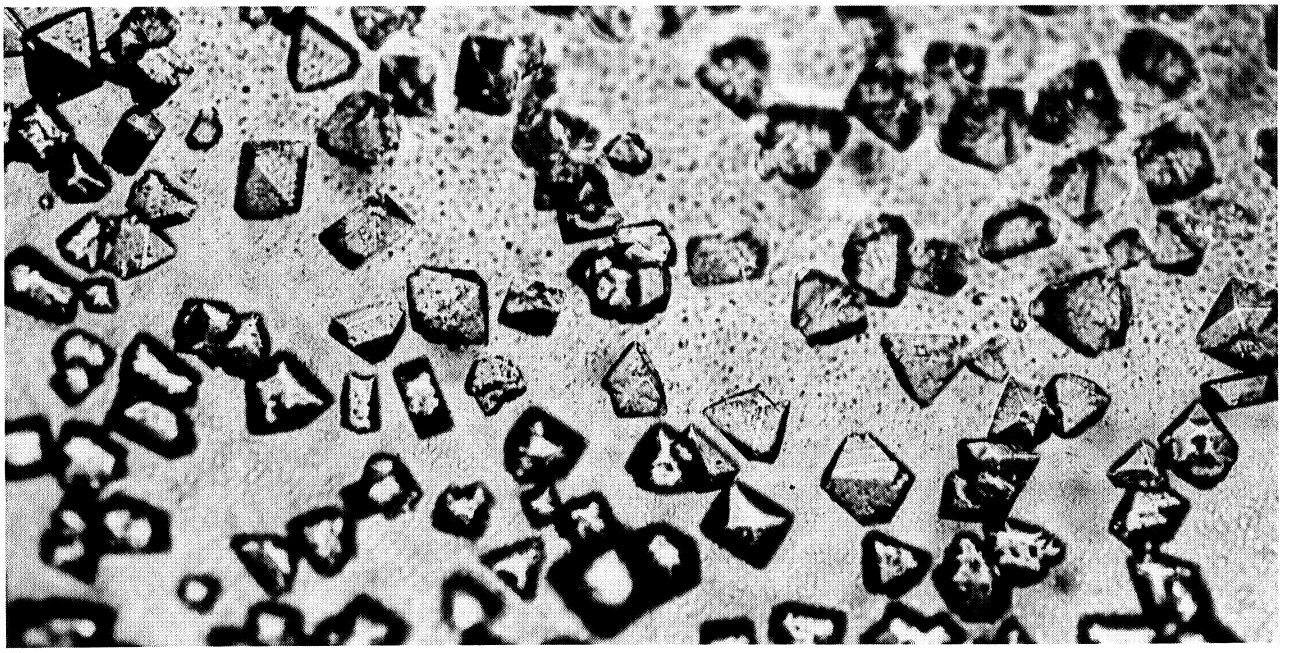

Plate IV

Crystals of Semliki Forest virus (the largest crystal dimension is about 0·1 mm)

to construct a cell-free protein synthesizing system which, with the 26S RNA as messenger, will make C protein and a $97x10^3$ molecular weight protein which contains the E3, E2 and E1 sequences. When microsomes are added to this system the E polypeptides are inserted into the membrane in their correct orientation, and are then glycosylated and cleaved between E2 and E1. The capacity for membrane insertion persists only until about 100 amino-acids of the amino-terminus of E3 have been made. The cleavage between E3 and E2 does not take place in the endoplasmic reticulum but shortly before budding at the plasma membrane. The problem now is to find out whether the sequence at the amino-terminus of E3, that is revealed when the C-protein is cleaved off, is equivalent to the signal sequences present in secretory proteins. Tunicamycin, an antibiotic which completely blocks the glycosylation of glycoprotein (including E1, E2 and E3), had no effect on the insertion of the spike glycoproteins into the endoplasmic reticulum nor was the cleavage between E2 and E1 affected. Further transport to the cell surface was blocked, however.

The receptors on the cell surface

We have initiated a long-term study to find out how Semliki Forest virus penetrates into host cells. In general little is known about the early interaction of animal viruses with host cells, but the first step in the entry process is the attachment of the virus to receptors on the cell surface. Using the octameric form of the Semliki Forest virus spike proteins, the 29S complex, which is water-soluble when lipid- and detergent-free, we have been able to count the number of receptors present on different cells. By a chance observation we found that, when the 29S complexes are attached to P815 mouse cells, an antiserum to their H2 antigens was not able to lyse the cells in the presence of complement. This first indication that the receptors for the virus might be the H2 antigens has been followed up both with mouse and human cells, in collaboration with C. Terhorst and J. Strominger at Harvard University and with P. Robinson and V. Schirrmacher at the Deutsches Krebsforschungszentrum in Heidelberg. Using a combination of immunofluorescent, immunochemical and biochemical methods, the major proteins present on the cell surface binding Semliki Forest virus 29S complexes have been shown to be the HLA antigens in human cells, and the H2 antigens in mouse cells. Pure HLA glycoprotein has been reconstituted into lipid vesicles that bind to the virus. Further work will

attempt to construct a cell-free system in which virus entry can be studied. Semliki Forest virus has a very wide host range, infecting both vertebrate and invertebrate cells in culture. The histocompatibility antigens are known to have a very conservative structure (except for the hypervariable region) in mammals and birds, and it will be interesting to find out whether invertebrates have histocompatibility antigens with a similar structure.

Vaccines against Semliki Forest mouse encephalitis

The present generation of subunit vaccines against enveloped viruses consist of spike proteins solubilized with detergents. The effect of these has been equivocal. We have tested the octameric 29S complexes and the spike protein reconstituted into egg lecithin vesicles (virosomes) at high protein-to-lipid ratios. 10 µg of the vaccines were given to Balb/c mice in a single intraperitoneal injection, and after two weeks the mice were challenged with a strain of Semliki Forest virus which causes lethal encephalitis in mice. The LD_{50} (the number of infectious virus particles needed to kill half the mice) was $10^{2.1-2.6}$ in unvaccinated controls. The Semliki Forest virus spike protein-Triton X-100 complex (monovalent) gave only slight protection, the LD_{50} increasing to $10^{2.7-3.4}$. With the 29S complexes and the virosomes the protective effect was dramatic, the LD_{50} increased to more than 10^{7}. These results are based on an extensive study in which Balb/c mice were used. Two factors may serve to explain the poor efficiency of spike proteins solubilized with detergents. The first is that this type of preparation needs detergent to keep the protein soluble, and if the detergent has not been removed before injection, at the least the detergent will then dissociate from the protein, which may precipitate or stick to any available surface by hydrophobic interactions; the antiserum content then available for interaction with the immune system is beyond anyone's guess. The second factor is that these antigens are monovalent, at least before they precipitate. In nature the immune system is confronted with microbial surfaces where the potential antigens normally occur in multiple copies. The "natural" multivalency of the 29S complexes and the virosomes may be the key to their effectiveness.

Whether spike protein micelles or virosomes from other enveloped viruses will prove as efficient as vaccines remains to be seen.

Penicillinase from *Bacillus licheniformis*

The penicillinase enzyme occurs as a hydrophobic protein intermediate that is attached to the cytoplasmic membrane, and also as a water-soluble extracellular secreted form. The extracellular penicillinase is released from the cell by proteolytic cleavage. Our earlier work has shown that the membrane penicillinase has an amino-terminal hydrophobic peptide extension which attaches the protein to the membrane. As soon as it is cleaved off, this hydrophobic extension aggregates irreversibly. The fact that the extension is amino-terminal makes it interesting; intestinal aminopeptide is another ectoprotein that is known to attach through its amino-terminus to its membrane (Maroux and Louvard, 1976), and this type of orientation must be accounted for in the mechanism proposed for membrane protein biosynthesis (Rothman and Lenard, 1977).

We have found a precursor of membrane penicillinase by using a λ phage DNA (obtained from K. Murray, Edinburgh), which contains the penicillinase gene cloned from *B. licheniformis*, to program a transcription-translation assay system (in collaboration with P. Hirth and E. Fuchs, Heidelberg University). The precursor presumably contains a signal sequence attaching the ribosome to the cytoplasmic membrane. We know from studies in collaboration with L. Randall (University of Uppsala), that penicillinase is translated by membrane-bound ribosomes, and we are now trying to construct a cell-free system coupled with "inside-out" vesicles of the cytoplasmic membrane to study the vectorial transfer of penicillinase through the membrane. The mapping of this process will hopefully be assisted by mutants of *B. licheniformis* with defective penicillinase secretions.

References

Maroux, S. and Louvard, D.(1976). *Biochem. Biophys. Acta*, *419*, 189-195.

Rothman, J.E. and Lenard, J. (1977). *Science*, *195*, 743-753.

Transfer of newly synthesized proteins across membranes

Member: B. Dobberstein

Visiting workers: B. Hock*, H. Walk*

Technical assistant: H. Heinz*

This group has continued work on the characterization of the membrane proteins involved in the transfer of secretory proteins across membranes. In addition we have begun to study the biosynthesis, membrane insertion and cotranslational modification of a membrane glycoprotein.

It has long been recognized that secretory and at least some membrane proteins are synthesized on membrane-bound ribosomes. So for both types of proteins the ribosome membrane interaction, and as we think the nescent polypeptide chain itself, play a major role in determining the fate of these proteins.

In the signal hypothesis it was postulated that proteins to be secreted contain at their amino-terminal end an amino-acid sequence termed the signal sequence which directs the ribosomal complex to the endoplasmic reticulum membrane. There the nascent polypeptide chain traverses the membrane and the signal sequence is cleaved off.

Little is known about the membrane proteins that are involved in conveying the growing polypeptide chain across the membrane. Some must be involved in recognizing and binding the signal sequence and ribosomal complex to the membrane, others might be needed to form a channel across the membrane. Our aim is to dissect the microsomal membrane into components that can be reassembled subsequently into a functional entity. This would allow the purification and characterization of components involved in protein transfer.

In these studies we are using *in vitro* protein synthesizing systems, mRNA for the light chains of immunoglobulin or for pancreatic secretory proteins and rough microsomes from canine pancreas.

MODEL FOR THE TRANSFER OF SECRETORY PROTEINS ACROSS MEMBRANES

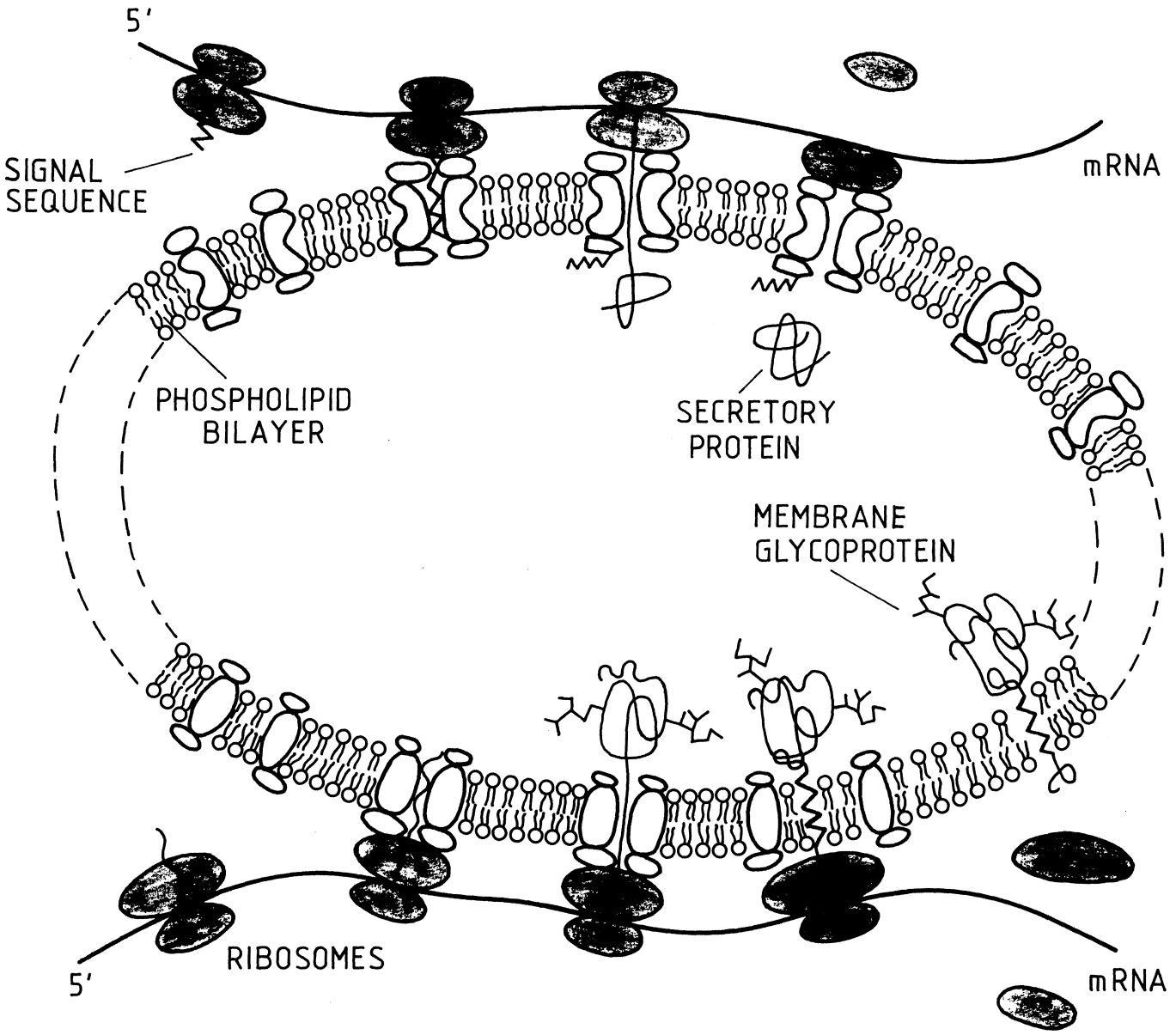

MODEL FOR THE INSERTION OF MEMBRANE GLYCOPROTEINS INTO A MEMBRANE

Plate V

In collaboration with G. Warren we have found that peripheral membrane proteins extracted from the microsomes with 0·5 M KCl are needed for the transfer of secretory proteins across the membrane. They can restore transfer activity to inactive salt-washed vesicles. They are proteins bound to the cytoplasmic side of the microsomal membrane and probably do not span the membrane. This location would suggest that they are involved in the binding of the signal peptide and the associated ribosomal complex to the membrane. For further purification of the proteins in the salt extract, we have devised a rapid assay for the restoration of transfer activity to salt-washed vesicles. This assay takes advantage of the fact that proteins which have been transferred across the membrane into the intracisternal space of the microsomes are resistant to added protease.

To study the biosynthesis and insertion of membrane glycoproteins into the membrane we have used as a model system the glycoproteins of Semliki Forest virus (SFV). (This work was done in collaboration with H. Garoff and K. Simons.)

As membrane insertion only occurs during translation we had to construct an *in vitro* protein synthesizing system. The SFV 26S mRNA codes for viral capsid protein and the viral membrane glycoproteins E3, E2 and E1 in that order (total 130K dalton). To achieve complete translation of such a long mRNA a Hela cell-free system was modified. Translation of 26S mRNA resulted in the synthesis of viral capsid protein and a 97K dalton protein containing the protein moiety of the glycoproteins E3, E2, E1. By adding canine rough microsomal membranes to the *in vitro* translation system we could demonstrate that these heterologous membranes are capable of correctly inserting, proteolytic processing, and glycosylating the viral glycoproteins. Insertion of the glycoproteins into the membrane can only take place during translation before 80-100 amino-acid residues of the amino-terminal end of the glycoproteins are completed. Proteolytic processing of the glycoproteins to give rise to p62 (the precursor of E3 and E2) and E1 takes place on the nascent chain shortly after the cleavage site has emerged from the ribosome. Glycosylation is also occurring on the nascent chain.

It should be emphasized that for this study use has also been made of pancreatic membranes which transfer

secretory proteins with the same efficiency. The question which arises from these experiments is: do secretory proteins and membrane proteins use the same transfer mechanism for their transfer or insertion? It is quite conceivable that the signal sequence of secretory proteins and an amino-terminal region of membrane ectoproteins are recognized by the same postulated membrane receptor.

Structural studies of neuronal assemblies

Members: N.J. Strausfeld, G. Geiger, G. Griffiths*

Fellows: N.R. Singh*, J. Bacon*

Visiting workers: E. Aubele*, J.A. Campos-Ortega*
H. Fraser-Rowell*, C. Goodman*, K. Hausen*,
J. Kien*, M. Land*, F.W. Schürmann*

Technical assistants: M. Obermayer, H. Cambier*

The resolution of neuronal assemblies in wild-type and mutant neuropils

Chronic application of cobalt salts into the brain and thoracic ganglia of insects results in its uptake by many interneurons (see 1976 Research Reports) as well as its transport between contiguous nerve cells. In conjunction with K. Hausen (Max-Planck-Institut für Biologische Kybernetik, Tübingen) a technique has been designed to resolve consistent patterns of neuronal arrangements throughout the central nervous system. In spite of its simplicity (Strausfeld and Hausen, 1977) this technique is proving to be the most effective method for resolving brain structure in many species of insect; it is superior to the Golgi methods, as well as to the more recent structural techniques which employ either radioactive amino-acids or horseradish peroxidase. In essence, cobalt salts that are injected directly into the neuropil are incorporated by many nerve cells. These invariably comprise one or more entire populations of one or more species of neuron. The number of populations resolved depends upon a critical timing of an injection phase, followed by a period of cobalt diffusion through the tissue as well as the location of the injection site. Manipulations of these parameters make possible the demonstration of arrangements between many neural elements in a consistent fashion. The same set of neurons can be resolved in many individuals, and each element of the set corresponds to the branching structure of single neurons that were hitherto recognized only from random and unpredictable selective impregnation (Strausfeld and Blest, 1970).

The present method has demonstrated that although each region of the optic lobes is complex, in terms of the shapes of its constituent neurons and their synaptic connectivities (Strausfeld and Campos-Ortega, 1977),

arrangements of nerve cells are in fact simple and limited to only three modes of neuronal assembly (Strausfeld and Hausen, 1977). All assemblies are precisely and characteristically mapped to coincide with the retinotopic pathways from the retina. The modes of assembly can be simply summarized as follows.

Plate VI

(1) Isomorphic assemblies of neurons extend across the whole retinotopic projection and thus subserve the entire visual field. Some graded differences of structure are apparent in some assemblies where, between the upper and lower, or frontal and posterior, poles there exist graded differences between the number of dendritic spines and hence the possible number of postsynaptic sites subtending peripherally derived channels.

(2) Local isomorphic assemblies comprise sets of identical neurons which are mapped so as to subserve a special segment of the retinotopic input and, hence, a characteristic portion of the visual field.

(3) Single neurons, or constellations of non-identical neurons, comprise sets of so-called "unique cells" that also subserve specific areas of the receptor mosaic. These elements are similar to outgoing nerve cells from the brain in that they are represented by paired elements rather than a multitude of identical columnar units.

These studies have also revealed that, superimposed upon the discrete homolateral columnar structure of each optic lobe, there exists a bilaterally symmetrical columnar projection which represents a map of the upper anterior region of binocular overlap from the contralateral eye. This assembly constitutes a dorsoventral binocularity "supercolumn" reminiscent of arrangements in mammalian visual cortices.

The present method is exceedingly simple to carry out and is thus being extensively used for studying the development of neuropils as well as the study of mutations that are expressed within the thoracic ganglia of *Drosophila*. The former project, which will be carried out in collaboration with D.R. Nässel (EMBO fellow, 1978) will initially map the locations of all neuron cell bodies that contribute to the motion-sensitive neuropils of the lobula complex. This will be performed prior to resolving the development of these regions in larvae and pupae, using both the technique described above and autoradiography. In addition it is intended to apply cobalt incorporation to developing complex non-columnar

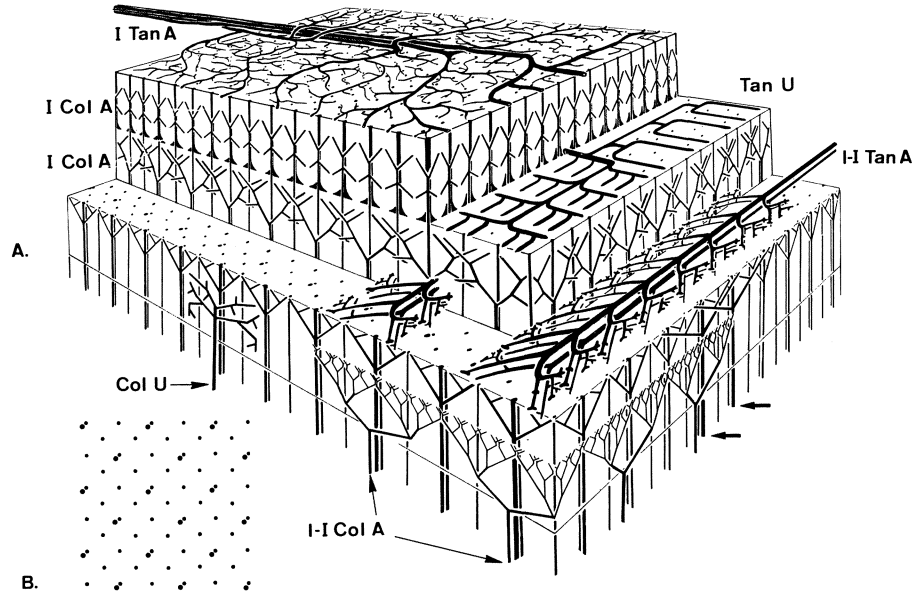

Plate VI

A. Schematic summary diagram of retinotopic neuropil which has been derived from observations of 240 populations of interneurons in lobula neuropil. Layers have been exposed stepwise to show periodic arrangements of inputs (outer layer) concomitant with an isomorphic columnar assembly (I Col A) whose elements are arranged 1:1 with the retinotopic mosaic. Below this is shown a bistratified isomorphic assembly (I Col A) whose elements are arranged as a subperiod of the mosaic. This assembly shows a local perturbation at its inner stratum (arrowed p). A local isomorphic columnar assembly (1-I Col A) is also shown at this level with a unique columnar neuron (Col U) nearby. An isomorphic tangential assembly (I Tan A) is shown at the upper surface of the neuropil and two pairs of tangential neurons illustrate typical arrangements of local isomorphic tangential assemblies (1-I Tan A). A unique tangential neuron (Tan U) is shown at the level of the input terminals.
B. The basic plan of the retinotopic mosaic, viewed normal to the long axes of columns, on which is superimposed a sub-periodic array at the double points.

neuropils of the thoracic ganglia. Experiments initiated by M. Obermayer have demonstrated that larval neurons also incorporate cobalt in concert and that their arrangements are similar to those detected in imago optic lobes.

R.N. Singh prepared several hundred diffusions of sensory and motor projections into the thoracic ganglia of *Calliphora* to reveal sensory and motor neuronal mappings as well as the dispositions of contiguous interneurons. This information has proved invaluable for the present studies of *Drosophila* neuropil: although the shapes of the nerve cells appear relatively simple in this species their lay-out with respect to the sensory input patterns are homologous. Using information collected from *Calliphora* and wild-type (Oregon) *Drosophila* J.A. Campos-Ortega (University of Freiburg) and N.J. Strausfeld are investigating the structure of sensory projections and transsynaptically stained neurons in bx^3 and bx^{34e} bithorax mutants in which the anterior half of the metathoracic cuticle, and appendages, have been transformed to the equivalent mesothoracic structures. Projections from the transformed halteres superficially appear as a chimeric geometry with structural properties characteristic of both wild-type anterior wing and posterior (wild-type) haltere. However, parts of projections from the wings, and interneurons associated with these, are constrained to ganglionic areas that correspond to the transformed meta- to meso-thoracic(and normal mesothoracic) periphery. Using the most sensitive silver enhancement procedures it has been possible to resolve corresponding alterations in contiguous interneurons within this class of mutants. We intend to continue these studies to include a range of mutants and genetic mosaics. One consequence of these studies has been the initiation of an Atlas of the wild-type nervous system which is intended to cover both central and peripheral neuronal arrangements in the brain and ventral ganglia of *Drosophila*.

Neuronal reconstitution by computer graphics

The process of sectioning histological material breaks up structural contiguity, and thus sets the requirement for its reconstitution to the original branching pattern. In the case of a small nervous system, such as that of *Drosophila*, there is a need for an automated realignment procedure to correct distortions that may be incurred

during preparation. P. Speck of the Computer Group is working in close collaboration with us in devising software for tracing profiles and reconstituting these as three-dimensional structures that can subsequently be rotated. Up to the present time programs have been devised to construct stick-diagrams from tree-like structures as one step towards comparison and averaging neuronal assemblies in mutant and wild-type tissue respectively. These programs supplement initial data-smoothing routines, and methods for serial section reconstitution, three-dimensional rotation, and elimination of hidden lines are now in an advanced stage. The basic software for a MOP graphics tablet has been written, allowing rapid input and digitizing of contours from prealigned photomicrographs. We have opted for relatively simple digitizing and display hardware, and have chosen to concentrate on more sophisticated software procedures in order that the final package of programs may be made available to other workers with fewer resources than our own.

Structure and behaviour

It is possible to describe visual tracking and fixation behaviour as the superimposition of two systems, one of which is directionally sensitive to motion, and another which is insensitive. Both systems reside beneath an identical optical array but they probably differ from one another in their nerve cell constituents and synaptic connectivities. Although there is much information about the behaviour of these two systems, in terms of cybernetic theory, relatively little is known about their internal structure. One technique for its analysis is that of electrophysiological recording followed by the structural identification of the recorded neuron (Hausen, 1977). We have, however, chosen an alternative approach; namely that of selectively removing parts of the system, either by discrete ablations within the matured brain or by selective destruction of neuroblasts in the developing nervous system. Instrumentation for these operations has been designed and constructed by G. Geiger in conjunction with the Division of Instrumentation; in principle it consists of a dye pulse laser the beam from which is directed into the optical pathway of a microscope. Tissue is viewed either by interference phase contrast illumination (in the case of embryonic and larval tissue) or by incident illumination. A low energy ruby laser provides a reference target marker and the actual event of ablation is viewed *via* a video system. Although some

technical problems are still to be surmounted, such as the relative insensitivity of some types of cells, the apparatus functions well on a variety of test gels, tissues and blood cells. Lesions with diameters of 0.5 μm can be achieved routinely. Destruction of a cell can be effected at the surface of the tissue, or deep within it, without incurring damage to cells beneath or above the site of lesion. Routine use of this instrument, in conjunction with developmental studies, will be initiated in 1978.

In order to evaluate specific deletions in terms of their effect on behaviour, G. Geiger has designed and constructed a laser torque transducer for measurements of in-flight responses to visual stimuli. The prototype works satisfactorily and is somewhat more sensitive, and faster, than mechanical transducers used elsewhere. This system will eventually be interfaced with the ND 178 computer during 1978, and not to a ND 240, as envisaged in last year's Report.

Glia fine structure and receptor axon degeneration

The role of satellite glia microtubules in the degenerative process of visual receptor axons is being investigated by G. Griffiths, using cytochemical assays for the lysosomal marker enzyme, acid phosphatase (AcPase). AcPase reaction products are associated with smooth endoplasmic reticulum (SEM) and the cytoskeleton of glia microtubules. The latter pack the glia cells, and are generally oriented parallel to each other and perpendicular to the adjacent receptor axons. High resolution microscopy and scanning transmission microscopy indicate that an extensive SEM network is possibly cross-linked to the microtubules. Shortly after onset of receptor axon degeneration AcPase staining is much enhanced, indicating a relationship between the SEM system and the packaging of lysosomal enzymes within primary lysosomes.

References

Hausen, K. (1977). In *Life Sciences Research Report 6. Dahlem Konferenzen* (Stent, G.S., ed.), pp. 111-138.

Strausfeld, N.J. and Blest, A.D. (1970). *Phil. Trans. Roy. Soc. (Lond.) B*, 258, 81-134.

Strausfeld, N.J. and Campos-Ortega, J.A. (1977). *Science*, 195, 894-897.

Strausfeld, N.J. and Hausen, K. (1977). *Proc. Roy. Soc. (Lond.) B*, 199, 463-476.

DIVISION OF BIOLOGICAL STRUCTURES

Bacterial polypeptide elongation factor

Members: R. Leberman, D. Suck*

Fellows: Z. Acosta-Reyes*, W.H. Gast*

Student: W.H. Gast*

Technical assistant: B. Antonsson*

In the past year our structural studies on the bacterial polypeptide elongation factor EF-Tu have continued on two fronts: chemical and physico-chemical solution studies with the thermostable factor from *Bacillus stearothermophilus*, and an x-ray diffraction study of crystals of the *Escherichia coli* factor.

The solution studies on the *B. stearothermophilus* factor have been mainly physico-chemical measurements of the interaction of the protein with the low molecular weight components of the system viz. GDP, GTP, Mg^{2+}. The advantage of the *B. stearothermophilus* factor for these studies is that it is reasonably thermostable without bound ligand (Wittinghofer and Leberman, 1976). We have studied the effects of Mg^{2+}, GDP, and MgGDP on the reactivity of various functional groups within the protein, protection against trypsinolysis, and thermostability. Thus, it appears that Mg^{2+} ions play an important role in stabilizing the protein or maintaining its tertiary structure. This is shown, for example, by the fact that when they are present they partially protect the nucleotide-free protein against trypsin digestion. Using the nucleotide-free factor we are also redetermining the affinity constants for GDP and GTP by equilibrium dialysis; doubts exist as to the validity of similar data obtained by filter-binding studies and realiable values are required for a description of the cycle of reactions involving EF-Tu.

X-ray diffraction studies have continued on crystals of controlled trypsin-degraded EF-Tu·GDP from *E. coli*. It was previously believed that the crystals contained only the major tryptic fragment (fragment A - M.W. *ca.* 39,000), however, it now appears that they also contain the smaller fragment D (M.W. *ca.* 5,000). These crystals were produced from protein treated with trypsin for 20 min. at 0°C. Crystallizations were carried out at room temperature using polyethylene glycol 6000 as the precipitant. The crystals diffract to 2.5 Å resolution, belong to the space group $P2_12_12_1$ with two molecules in the asummetric unit, and have cell dimensions a = 144 Å, b = 93 Å, c = 69 Å.

6 Å data were collected on a Syntex diffractometer for the native crystals, and three heavy-atom derivatives were obtained by soaking the crystals in solutions of methyl mercury acetate (two derivatives) and $Pt^{II}(en)Cl_2$. An electron density map was calculated using multiple isomorphous replacement phases based on these three derivatives, the mean figure of merit being 0.71 (Kabsch *et al.*, 1977).

A model of the protein was constructed by averaging the electron density of the two dyad-related molecules in the asymmetric unit. Even at this low resolution the protein can be seen to have some very interesting properties. The overall dimensions of the molecule are 75 Å x 50 Å x 35 Å. It consists of a compact globular head of about 40 Å diameter which appears to contain a fair amount of α-helix, and a curled tail, which probably has little α-helical structure, 55 Å long and 25 Å diameter. Between the head and the tail is a second connection such that the molecule forms a ring, the diameter of the hole being approximately 12 Å.

Plate VII

A balsa wood model of the molecule is illustrated. The hole in the structure is a very unusual feature and to show that this was not due to a significant loss of protein in the crystals and that it is not an artefact of the analysis, the protein mass represented by the electron density was determined in the following manner: the balsa wood model was weighed and compared with the weights of similar available models of adenylate kinase and glutathione reductase. By this method the molecular weight of the protein represented by the model could be estimated, and values of 43,800 and 42,400 were obtained. The molecular weight of EF-Tu is 44,000 , therefore the model represents over 95% of the intact molecule and strongly suggests that the hole is a genuine structural feature.

The head and tail regions together present a structure with dimensions and shape reminiscent of the structure of $tRNA^{Phe}$ (Jack, Ladner and Klug, 1976). Bearing in mind that the structure we have is of partially degraded EF-Tu·GDP and not EF-Tu·GTP, and that the tRNA structure is not of an aminoacylated tRNA, we compared the two structures to see how well they could fit together.

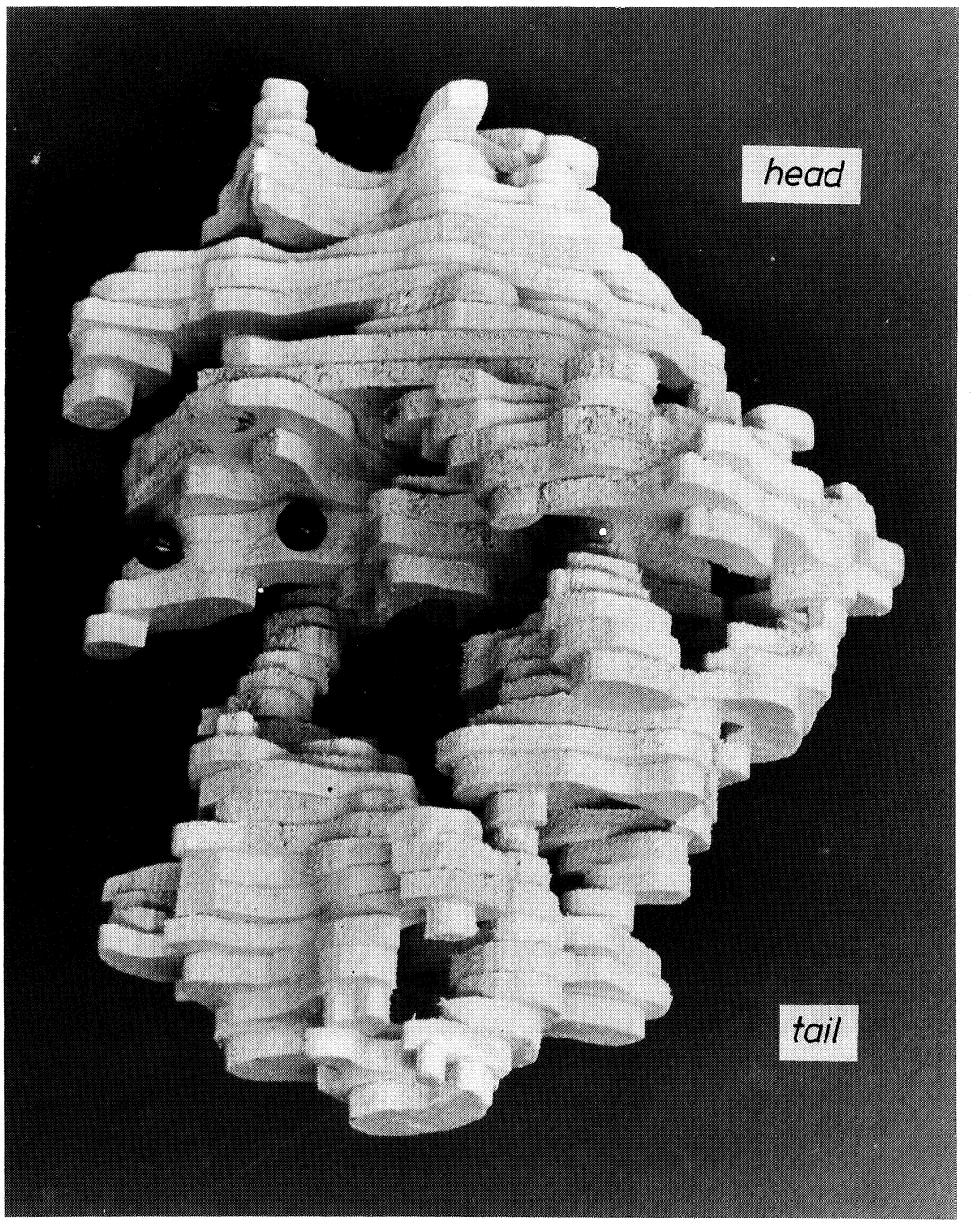

Plate VII

Balsa wood model of the partially trypsin-degraded EF-Tu·GDP molecule at 6 Å. resolution, derived from the averaged electron density map.

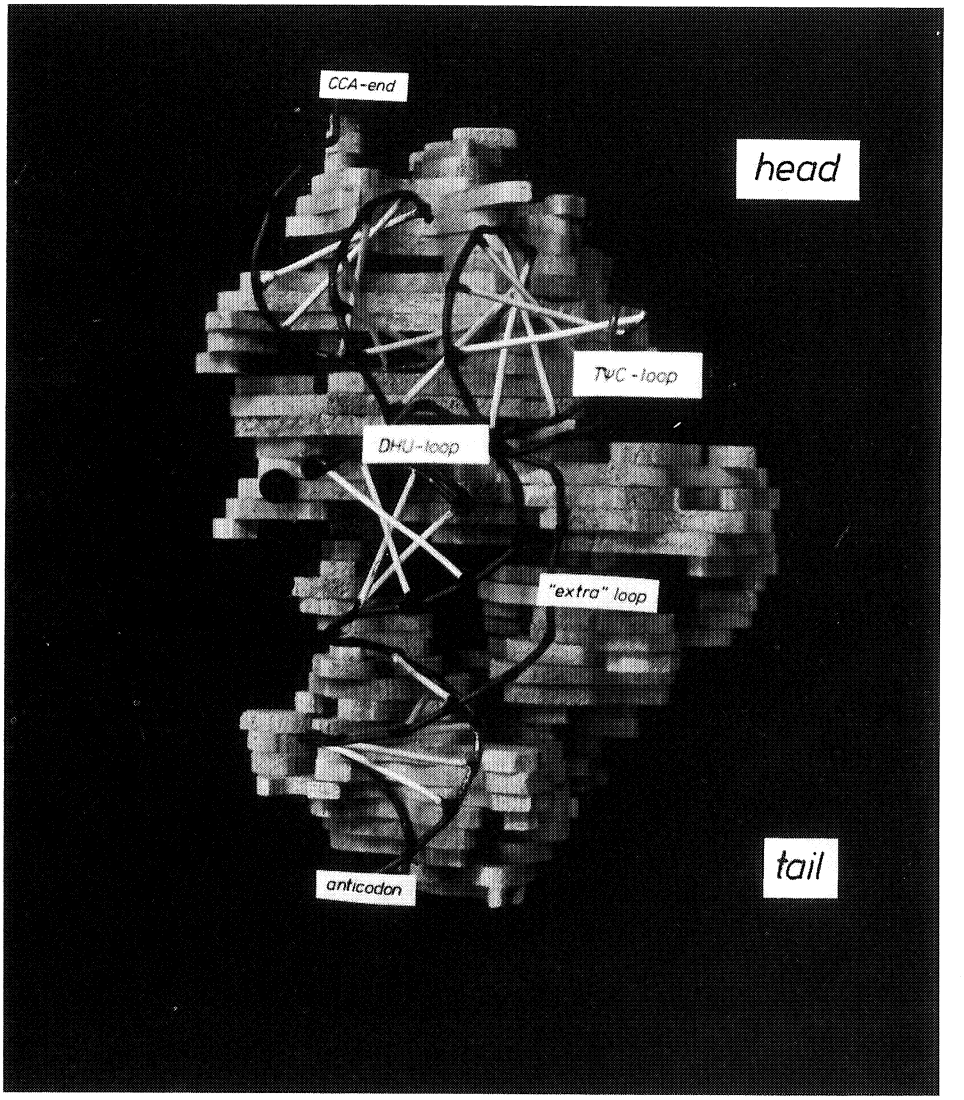

Plate VIII

Example of a possible fit between a wire model of yeast $tRNA^{Phe}$ and the balsa wood model of EF-Tu·GDP. The two models are on the same scale and in this example their general L-shapes are parallel.

Plate VIII

An example of such a fit is illustrated; it takes into account many of the known properties of the ternary complex. Thus the two molecules form a compact structure, the maximum dimension of which is still that of the protein molecule consistent with the observation that the Stokes' radii of both EF-Tu·GTP and the ternary complex are very similar; the aminoacylated 3'-terminus of the tRNA could interact with the protein, the anticodon of the tRNA would not be protected in the ternary complex, and the TψC loop would be available for interaction with ribosomal 5S-RNA.

The production of large crystals of the EF-Tu·EF-Ts complex and the crystallization of the ternary complex EF-Tu·GTP·aa-tRNA have not yet been successfully achieved; the problem is to produce enough material to study a large range of crystallization parameters.

The evolutionary relationships between proteins are currently under discussion. Owing to some similarities in their biological reactions and properties such a relationship has been proposed for actin and EF-Tu (Rosenbusch, Jacobsen and Jaton, 1976). This question could be answered by structural studies of the two proteins. Crystals, suitable for an x-ray diffraction study, of the complex formed by actin and DNAase I have been obtained (Mannherz, Kabsch and Leberman, 1977).

References

Jack, A., Ladner, J.E. and Klug, A. (1976). *J. Mol. Biol.*, *108*, 619-649.

Kabsch, W., Gast, W.H., Schulz, G.E. and Leberman, R. (1977). *J. Mol. Biol.*, *117*, 999-1012.

Mannherz, H.G., Kabsch, W. and Leberman, R. (1977). *FEBS Letters*, *73*, 141-143.

Rosenbusch, J.L., Jacobsen, G.R. and Jaton, J.-C. (1976). *J. Supramol. Res.*, *5*, 391-396.

Wittinghofer, A. and Leberman, R. (1976). *Eur. J. Biochem.*, *62*, 373-382.

Structural basis of the control mechanisms of allosteric enzymes

Member: M.F. Moody*

Technical assistant: A. Foote*

This group, established in July 1977, is studying conformational changes in the enzyme aspartate transcarbamylase (ATCase) from *E. coli*, which has been extensively studied as a model allosteric enzyme. Its substrates, carbamyl phosphate and aspartate, produce a cooperative activation of the enzyme, which is inhibited by CTP and facilitated by ATP. Studies by various workers have shown that the enzyme's properties are too complex to be explained in terms of only two conformational states, as postulated by a simple version of the theory of Monod, Wyman and Changeux. But Gerhart has suggested that there are just two major conformational states (differing in quaternary structure), each state comprising a variety of tertiary structures. If this is true, the two-state aspects of ATCase behaviour would be revealed by a technique specifically sensitive to the quaternary structure of the molecule in solution.

Work done before joining the EMBL demonstrated that the x-ray scattering patterns of ATCase solutions show substantial reversible changes (extending out to about .055 $Å^{-1}$) following activation with the substrate analogues carbamyl phosphate and succinate, or with the transition state analogue N-(phosphonacetyl)-L-aspartate (PALA). These changes indicate that, after ligation, the molecules in solution have a different quaternary structure, becoming larger and more anisotropic. Both changes are in agreement with Gerhart and Schachman's (1968) finding that ligation reduces the sedimentation coefficient by 3.5%.

ATCase is known to form a dimer in solution, and the process of dimerization should produce a change in x-ray scattering pattern at very low angles, of the same general type as that seen after ligation. Although results obtained by other workers have indicated that a ligand-induced dimerization is unlikely, it is clearly desirable to investigate this point more fully,

especially since contamination with dimer would hinder structural interpretation of the very low angle portion of the scattering curve. Since joining the EMBL, purified monomer and dimer have been prepared by gel chromatography. At concentrations of at least 20 mg/ml., and over the period required for an x-ray scattering experiment, the purified monomer and dimer are each stable in either the presence or absence of PALA. So it is very unlikely that ligand-induced dimerization could be responsible for the x-ray pattern changes seen at higher concentrations.

The purified monomer has been used for studies of the very low angle scattering pattern of ATCase in the presence and absence of PALA (studies made in collaboration with P. Vachette, Centre de Génétique Moléculaire, C.N.R.S., Gif-sur-Yvette). Some preliminary measurements have also been made with partially purified dimer, but this is more difficult to obtain in large quantities. These studies, in combination with electron microscopy, should provide considerable information concerning the structural change accompanying the allosteric transition, particularly since an atomic model of the unligated form is nearing completion in the laboratory of Prof. W.N. Lipscomb (Harvard University).

However, even without a structural interpretation of the x-ray scattering pattern changes, these can be used rather in the manner of a difference spectrum, but with the advantage that they are specifically sensitive to alterations of quaternary structure. For example, work done before joining the EMBL has shown that it should be possible to obtain titration curves of the quaternary structure change following ligation, and has also given evidence for the existence of a new kind of expanded quaternary state at high pH. Finally, some preliminary calculations suggest that the scattering pattern changes may be sufficiently large to permit study of the kinetics of the allosteric transition using a synchrotron radiation source of x-rays. (Equipment for this type of experiment is under construction at the Outstation at Hamburg.) Besides yielding the relaxation time of the major structural change, rather than of the various precursors and effects of it, such a study might provide information about the intermediate structures through which the enzyme passes.

A multiprotein complex from mitochondria: ubiquinone-cytochrome c oxidoreductase of *Neurospora crassa*

Members: H. Weiss, P. Wingfield*

Fellows: E. Herz*, B. Ziganke*

Visiting worker: M. Claisse*

Technical assistants: B. Juchs, A. Scharm

The group is studying the structure, function and biogenesis of ubiquinone-cytochrome c oxidoreductase. This is a multiprotein complex which catalyzes electron transport from reduced ubiquinone to ferricytochrome c and the transformation of the electronic energy into a form suitable for ATP synthesis. The oxidoreductase is a constituent of the mitochondrial inner membrane and amounts to about one tenth of the inner membrane protein.

The fungus *Neurospora crassa* is used as the source of mitochondria, because the protein, phospholipid and haem can be selectively labelled by *in vivo* incorporation of labelled precursors, and because modified and mutated strains are available. Furthermore, in *Neurospora crassa* the subunits of the ubiquinone cytochrome c oxidoreductase are relatively weakly associated with each other, and thus the isolated oxidoreductase can be resolved stepwise under mild conditions and (so far partially) reconstituted again.

The oxidoreductase is isolated from Triton X-100 solubilized membranes by affinity-binding to immobilized ferricytochrome c (which can be regarded as the substrate of the oxidoreductase) and subsequent affinity release by reducing ferricytochrome c to ferrocytochrome c (which can be regarded as a product). This affinity chromatographic procedure offers the advantage of isolation according to biological function and, most importantly, can be performed at low ionic strength.

A monodisperse preparation of the oxidoreductase is obtained. It consists of two cytochromes b (M_r each 30,000), cytochrome c_1 (M_r 31,000) and iron-sulfur protein (M_r 25,000) and five subunits without known

prosthetic groups (M_r 50,000, 45,000, 14,000, 12,000, 8,000). The preparation binds one ferricytochrome c per two cytochromes b with high affinity ($K_d < 10^{-7}$M); it does not bind ferrocytochrome c ($K_d > 10^{-5}$M). The isolated oxidoreductase is readily incorporated into phospholipid bilayers by ultracentrifugation on a sucrose density gradient containing lecithin liposomes. The electron transport activity is thereby restored.

The isolated oxidoreductase can be resolved as follows. (a) By reduction with ascorbate, bound cytochrome c is released. (b) By slightly increasing the ionic strength the iron-sulfur protein is removed. (c) By further increasing the ionic strength the remaining complex (M_r 250,000, Triton X-100 binding 0.3 g/g protein) dissociates into a water-soluble part (M_r 150,000, no Triton X-100 binding) which contains one 50,000 M_r and two 45,000 M_r subunits, and a membrane part (M_r 110,000, Triton X-100 binding 0.6 g/g protein) which contains the two cytochromes b, cytochrome c_1 and the 14,000, 12,000 and 8,000 M_r subunits. (d) At an even higher ionic strength (in the presence of antimycin) the water-soluble part dissociates into its constituent subunits and the membrane part loses the 12,000 M_r subunit. The remaining membrane part (M_r 100,000, Triton X-100 binding 0.65 g/g protein) retains the high affinity binding site for ferricytochrome c. (e) By treatment of the membrane part with deoxycholate at high ionic strength cytochrome c_1 and the 14,000 and 8,000 M_r subunits are removed. A dimeric cytochrome b (M_r 55,000, deoxycholate binding 0.3 g/g protein) remains. The cytochrome c binding is abolished by this step. So far conditions have been worked out for making the steps (a) to (c) reversible.

The close neighbourhoods of the subunits have been investigated by using intramolecular crosslinking reagents, and the arrangement of the subunits in the membrane by using surface labelling reagents. Apparently, the ubiquinone-cytochrome c oxidoreductase consists of a hydrophobic membrane section and two hydrophilic "water soluble" sections. The membrane section contains the dimeric (possibly even tetrameric) cytochrome b; cytochrome c_1 and cytochrome c are located nearer to the cytoplasm surface of the mitochondrial inner membrane: and a colourless complex which contains the 50,000 M_r and 45,000 M_r subunits is located at or near the matrix surface.

By means of protein labelling experiments, namely *in vivo* incorporation of radioactive amino-acids in the presence of inhibitors of either cytoplasmic protein synthesis or mitochondrial protein synthesis, the two cytochrome b subunits have been shown to be translated on mitochondrial ribosomes, the other subunits on cytoplasmic ribosomes.

It is hoped that the outcome of these studies will be a detailed picture of arrangement and interaction of the individual subunits within ubiquinone-cytochrome c oxidoreductase, and their contribution to the overall function of the multi-subunit enzyme. This should eventually lead to an understanding of the way electronic energy is transduced and conserved in the mitochondrial inner membrane. An additional aspect of the studies is to develop new techniques for the isolation and handling *in vitro* of membrane proteins.

Intracellular transport of newly synthesized plasma membrane components

Member: G. Warren*

Recent studies on plasma membrane proteins have shown that their synthesis is initiated in eukaryotic cells on ribosomes bound to the membrane of the endoplasmic reticulum. The growing polypeptide chain is transferred across the membrane and specific carbohydrate residues are added to those parts of the protein that emerge on the cisternal side of the reticulum. Addition of carbohydrate continues during transfer to the Golgi complex and the proteins are finally transported through the cell cytoplasm to the cell envelope.

There are two main features of this process that are of interest to this group (which will be joined by Dr. Brigitte Jockusch in January 1978).

(1) The newly-synthesized plasma membrane proteins are embedded in the reticulum bilayer together with membrane proteins indigenous to this membrane and those destined for other membranes in the cell: how are the plasma membrane proteins separated from these other membrane components? We are examining the possibility that there are lectin-like proteins in the endoplasmic reticulum membrane. These would recognize specific carbohydrate residues and possibly even specific sequences and so collect together in the plane of the membrane a certain class of membrane proteins destined for a particular membrane in the cell. The carbohydrate residues added to newly-synthesized membrane proteins would then determine their final location in the cell. Some recently published work supports this hypothesis. First, when the addition of carbohydrate residues to certain plasma membrane proteins is inhibited, they are synthesized and inserted into the endoplasmic reticulum membrane but do not appear at the cell surface. Second, several workers have clearly demonstrated the existence of lectin-like proteins in animal cells; they all appear to be membrane-bound.

    We shall concentrate initially on examining endoplasmic reticulum membranes for these lectin-like proteins, particularly those that can be shown to interact with specific plasma membrane glycoproteins.

(2) Once the plasma membrane proteins have been separated from other components in the endoplasmic reticulum and Golgi complex, they must be transported through the cytoplasm to the cell surface. This could be achieved by the formation of small "inside-out" vesicles which may be attached to contractile elements of the cytoskeleton (such a transport mechanism is also assumed for secretory vesicles). By following the synthesis and transport of selected plasma membrane proteins we hope to ascertain whether a specific association occurs between contractile proteins and plasma membrane proteins. For identification and intracellular localization of such complexes, antibodies seem to provide the best experimental approach. Specific antibodies against cytoskeletal proteins have already been prepared, and antibodies against several plasma membrane proteins are available.

Ultimately we hope to provide a molecular model for the transport of newly synthesized membrane proteins from the endoplasmic reticulum to their correct location in the cell.

Structure of filamentous bacterial viruses

Members: D.A. Marvin, J.E. Ladner, C. Nave*

Fellows: W. Folkhard*, C. Gray*, D. Gray*

Technical assistants: S. Malsey, H. Siegrist, H. Kabsch* (part-time), F.J. Marvin*(part-time)

The filamentous bacterial virus system is a model minimal system that carries out fundamental biological processes and is accessible to study at the level of molecular structure. The virion is a rod-shaped nucleoprotein containing single-stranded circular DNA encapsulated at the core of a helical array of coat protein subunits (Marvin and Wachtel, 1976). It adsorbs to host bacteria *via* a minor protein at one end which attaches to the tip of the pilus, a rod-like protein appendage of male bacteria. Adsorption of the virion is thought to trigger a retraction of the pilus, and therewith the virion, through the bacterial membrane into the cell. The infecting DNA is then converted to a double-stranded form that replicates and produces single-stranded circular progeny DNA under control of the viral gene 5 protein. The gene 5 protein forms linear intracellular nucleoprotein complexes with the progeny DNA. Assembly of the completed progeny virion involves placing the viral coat protein in the bacterial membrane, its 50-residue α-helix extending across the membrane. During assembly the gene 5 protein is displaced from the DNA and replaced by the coat protein as the DNA passes through the membrane without lysing or otherwise killing the cell.

Several structures involved in the virus life-cycle are accessible to analysis by diffraction methods. These include the virion itself, the coat protein in the membrane, the DNA-gene 5 protein complex, and the pilus. We hope that a study of the detailed molecular structure of each of these components will reveal general principles of static and dynamic interaction between DNA, protein and membrane. Knowledge of these structural principles will help us to understand such biologically important processes as transport across membranes, control of DNA replication, and control of cell division.

The virion

The coat protein molecules can be represented as rods of α-helix about 70 Å long and 10 Å in diameter. Their long axes are directed roughly along the virion axis, but they also slope radially so as to overlap each other and form a helical array with a pitch of 15 Å. There has been some uncertainty whether the number of units per 15 Å turn is 4.4 or 5.4. X-ray diffraction pictures of appropriately tilted well-ordered fibres show strong meridional intensity at 3.4. Å but not at 2.8 Å, as expected for 4.4 (rather than 5.4) units per turn.

Plate IX

The virion is not just a static array of subunits. Mild treatments modify the parameters of the helix and the orientation of the subunits within the helix (Wachtel, Marvin and Marvin, 1976). One treatment is simply alteration in temperature. At room temperature the virion has 4.4 units per turn; lower temperatures promote a coupled change in local packing to give 4.5 units per turn. This small structural change, when extended over the whole virion, increases the length of the virion by almost 10% and causes a rotation of one end of it with respect to the other by more than ten turns around the virion axis. We call this phenomenon "allosteric amplification". Treatment of the virion with ether causes a more dramatic rearrangement of subunits. Brief treatment converts virions to tubes about 3-fold fatter but 10-fold shorter than virions (Amako and Yasunaka, 1977). We have found that longer treatment with ether causes these tubes to swell into spheres and then to collapse into flat sheets. X-ray diffraction of orientated samples of sheets indicates that they are about 70 Å thick, as expected for planar arrays of the coat protein molecule having the α-helix axis perpendicular to the plane of the sheet. The sheets are models for the arrangement of coat protein in the membrane during the early stage of assembly.

Plate X

Plate XI

These structural transitions illustrate the geometrical basis of polymorphism. Structural biology has traditionally used classical coordinate systems, such as the Cartesian or the cylindrical-polar system, as frames of reference. But biological changes are often coupled in ways that are easier to describe as distortions of a coordinate system within which the

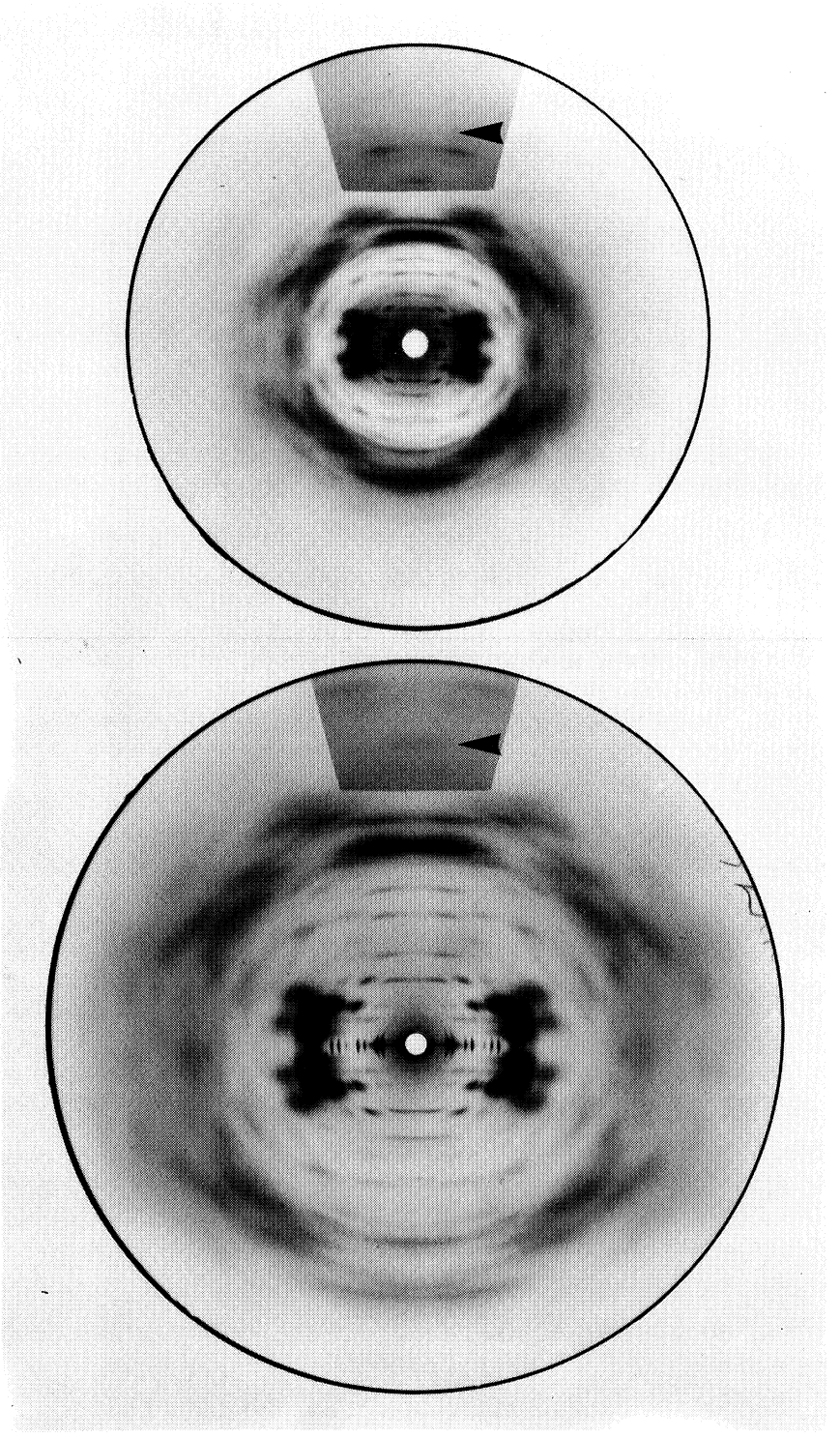

Plate IX

X-ray fibre diffraction patterns of the Pf1 strain of filamentous virus at 75% relative humidity. Fibre axis vertical. Fibre G128C, 4.4 units per turn. Bottom, film 3231, tilted 13° away from normal to the x-ray beam to show the meridional reflexion at 3.4 Å (arrow). Top, film 3247, tilted 16° away from normal to the x-ray beam to show absence of a meridional reflexion at 2.8 Å (arrow). The meridional region is more heavily exposed, to bring out weaker reflexions.

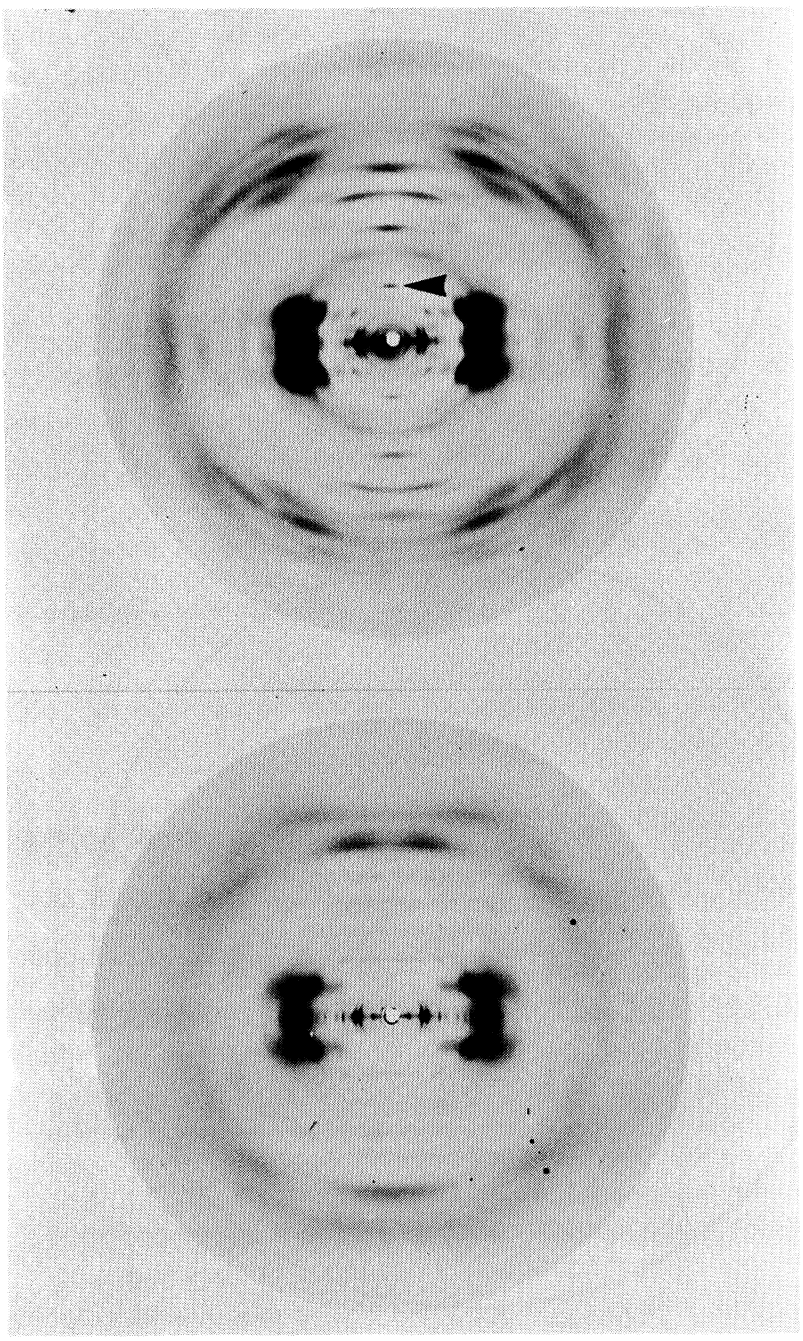

Plate X

X-ray fibre diffraction patterns of filamentous phage with 4.5 units per turn, at 75% relative humidity. Fibre axis vertical. Top, fd strain: fibre 187, film 552. Arrow indicates the 16 Å meridional reflexion. Bottom, Pf1 strain: fibre G15OA, film 3429.

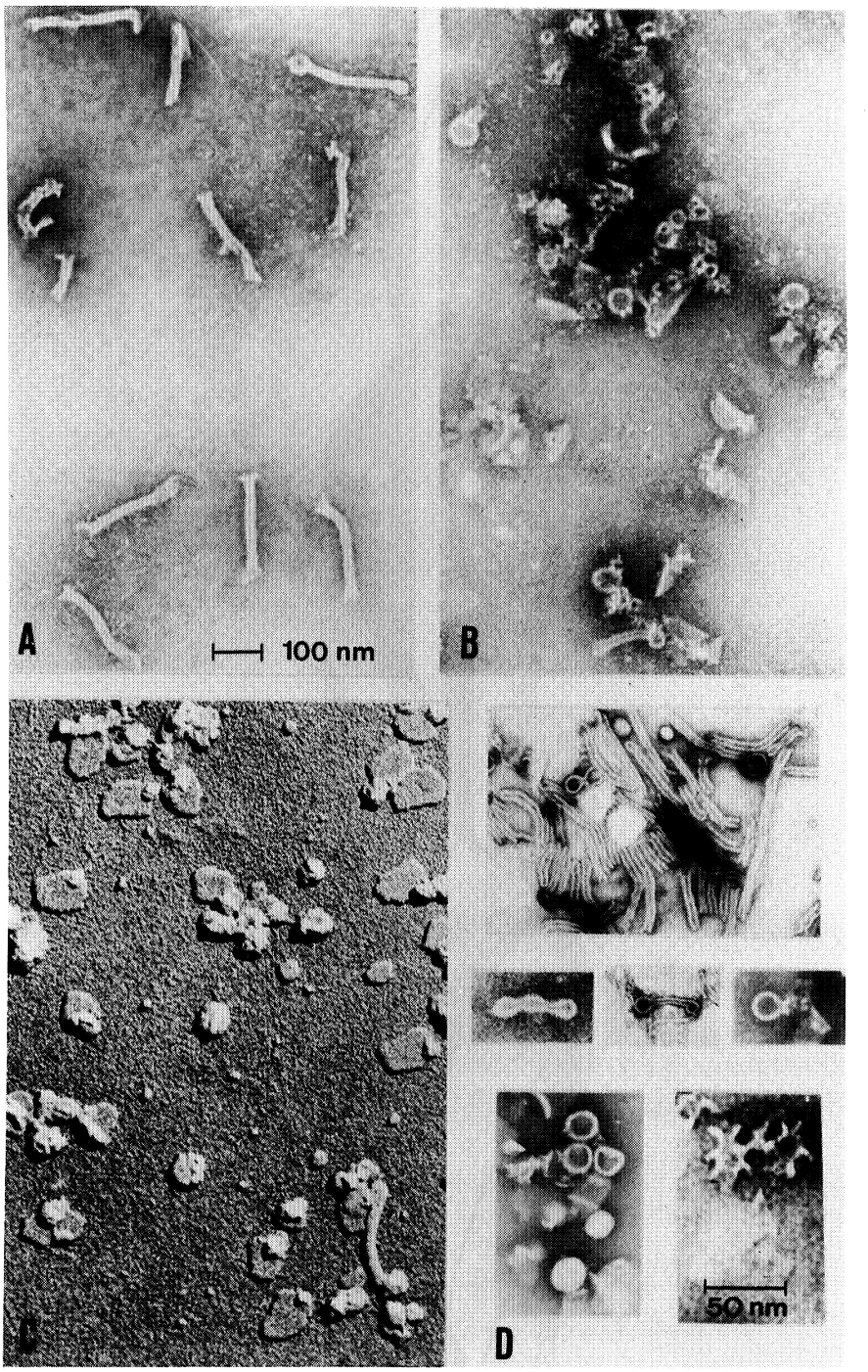

Plate XI

Electron micrographs of Pf1 treated with ether. Samples were gently mixed with excess ether, incubated at room temperature for the indicated time, diluted 100-fold into 0.01% glutaraldehyde, and negatively stained (fields (a), (b), (d)), or shadowed at a 20° angle (field (c)). (a) 1 min; (b) and (c) 10 min; (d) selected fields. Enlargement as (a) except where indicated. Experiment in collaboration with T. Arad and K. Leonard.

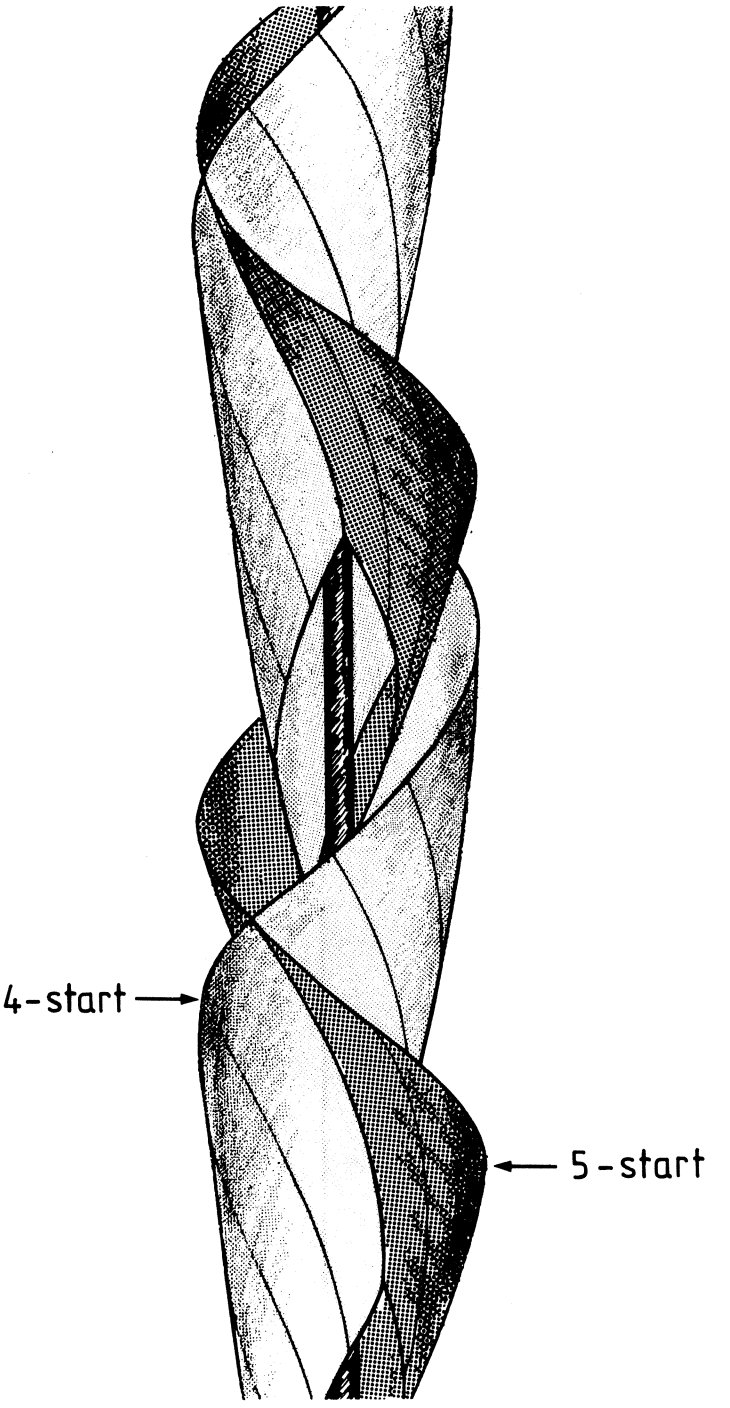

Plate XII

Representative of the symmetry of the filamentous phage virion by the intersections of two helicoids. The short curves represent the α-helix axes of protein subunits arranged along the 4-start (right-handed) and 5-start (left-handed) helicoids, for the model of Marvin and Wachtel (1976). One helicoid in each of these two sets is shown; in the complete structure there are four 4-start helicoids intersecting five 5-start helicoids around the axis. The dark vertical line represents DNA in the core of the virion.

parameters of the structure remain constant: a picture of a basset hound drawn on a rubber sheet and stretched vertically becomes a picture of a fox hound. We have used the techniques of differential geometry to approach this problem. We replace each α-helix subunit in the virion by a curve representing the α-helix axis. If we move one such curve smoothly through successive subunit positions in the virion helix, it will sweep out a twisted ribbon, or helicoid. The subunits may then be represented by the intersections of helicoidal surfaces. The positions observed experimentally for the arrangement of subunits in the virion are in fact those predicted for the intersections of orthogonal helicoids. The surfaces which divide space can be defined by a few parameters which can vary continuously to describe the conversion of a helical array into virions of different symmetry or into tubes, spheres or sheets.

Plate XII

One previously difficult technical problem was to obtain large well-ordered specimens of virions for diffraction studies. J. Torbet and G. Maret at Grenoble, who have been collaborating with us, have now found that samples of virions can be oriented in a strong magnetic field, which probably acts on the α-helix.

Our detailed analysis of the virion using x-ray diffraction and model-building methods is continuing. We have implemented a suite of computer programs (in collaboration with the Computer Group) that should be generally useful in x-ray fibre diffraction. X-ray films are measured using the Optronics film scanner on-line to the Nord-10 computer. The array of intensities can be displayed, all or in part, at any magnification, on a Tektronix terminal using shades of grey, points above a threshold, or contours. Using the cursor, a box may be drawn around any spot or region of intensity; single instructions then give centre of gravity and/or integrated intensity of the spot. In particular, appropriate spots can be used to calculate specimen-to-film distance, centre of the film, or tilt of the fibre in the x-ray beam. We have also modified programs of L. Makowski (Brandeis University) to produce plots of intensity along a layer line, corrected for disorientation, and to separate overlapping layer lines. Further programs make possible the generation of molecular models, calculation of stereochemical constraints, calculation of Fourier transforms, and calculation of electron density maps. R. Ladner, of the Computer Group, is developing an interactive molecular graphics program using the Evans and Sutherland graphics system.

In order to narrow the range of models that need to be considered we are using the STEM in collaboration with R. Freeman to determine the mass per length of unstained samples.

The gene 5 protein-DNA complex

Our approach to determining the structure of the complex between viral DNA and the gene 5 DNA-binding protein has been the same as our approach to determining the structure of the virion. Low resolution data from x-ray fibre patterns or electron micrographs must be supplemented by high resolution data on the structure of the subunit in the complex. In the case of the virion, the large α-helix content of the subunit defines the structure sufficiently to give an initial model. In the case of the gene 5 protein-DNA complex, it is necessary to determine the structure of the subunit as a single-crystal project. To this end, we collaborated several years ago with W. Konigsberg to determine the primary sequence of the gene 5 protein, and with R. Fletterick and T. Steitz (all at Yale) to attempt to crystallize the protein. Since then A. McPherson and A. Rich at M.I.T. have been successful in crystallizing the protein, and in collaboration with R. Leberman we have repeated the crystallization, but we plan to concentrate on determination of the structure of the complex of protein with DNA.

Plate XIII — X-ray fibre diffraction patterns of the gene 5 protein-DNA complex show strong equatorial intensity at about 75 Å, and some detail in the 10-20 Å region. Neutron scattering experiments (in collaboration with J. Torbet at Grenoble) show a radius of gyration of about 35 Å. Density matching using D_2O/H_2O mixtures has not enabled us to distinguish between the radius of the DNA and the radius of the protein, probably because the amount of DNA in the complex is relatively small. To determine the relative radii of DNA and protein it will be necessary to label one of these components with deuterium.

Plate XIV — Preliminary electron microscopy of the complex promises detailed structural information.

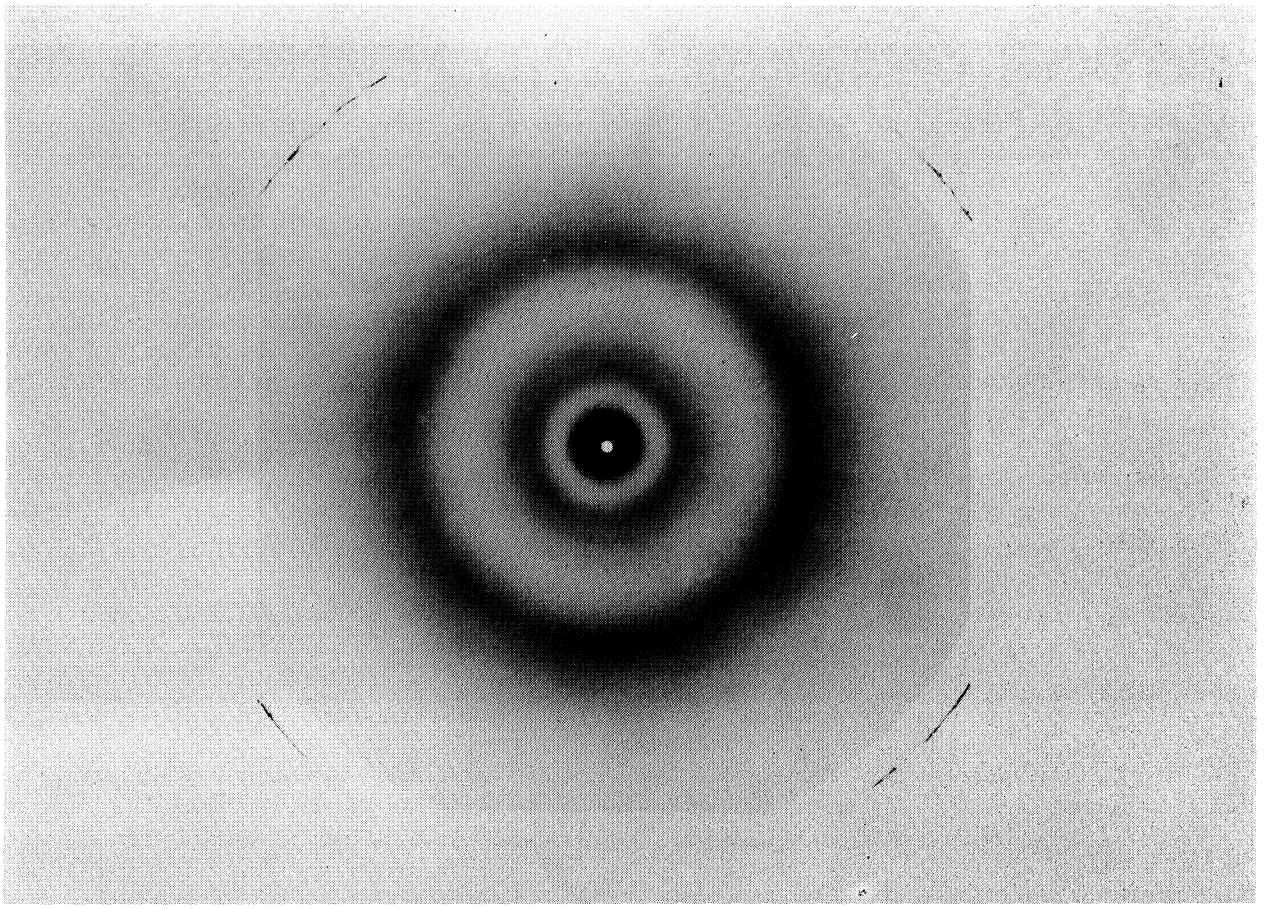

Plate XIII

X-ray diffraction pattern of a fibre of the complex between viral DNA and gene 5 protein from the filamentous bacterial virus strain fd. Fibre axis vertical.

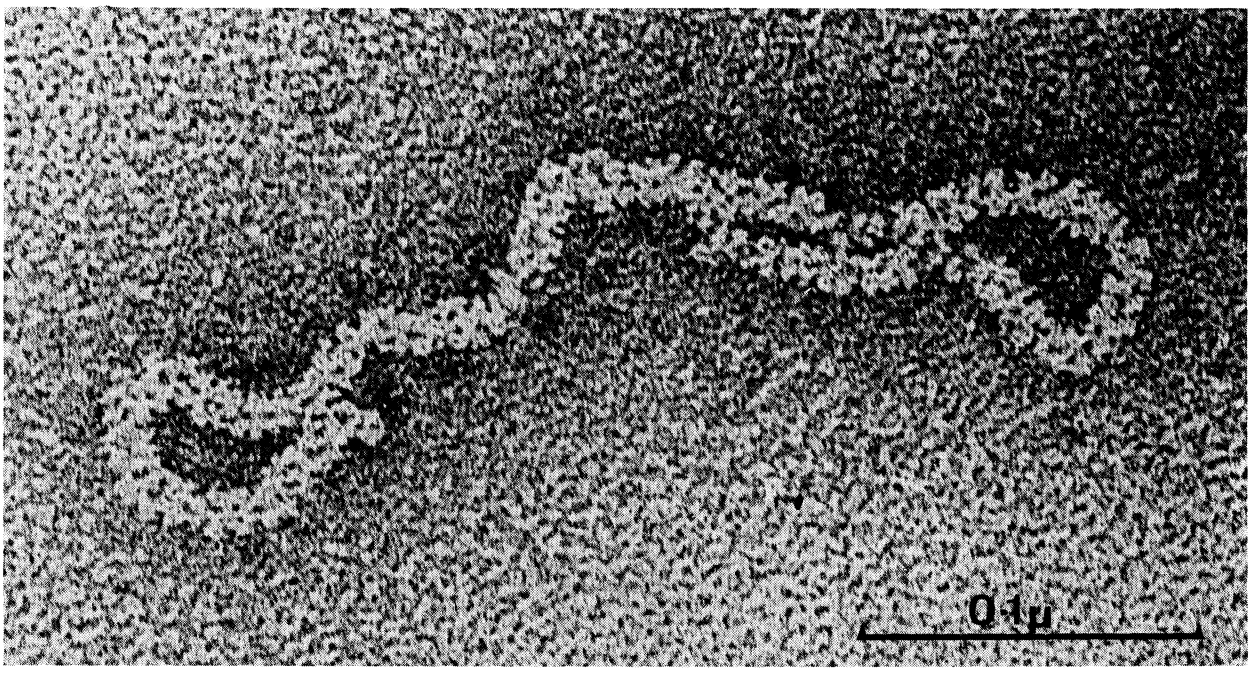

Plate XIV

Electron micrograph of the complex of gene 5 protein and fd DNA, isolated from fd-infected cells. The structure visualized here is more highly organized than previously observed for the *in vivo* complex. Specimens were adsorbed to a freshly exposed carbon surface and stained with 1% uranyl acetate. Bar is 0.1 μm long.

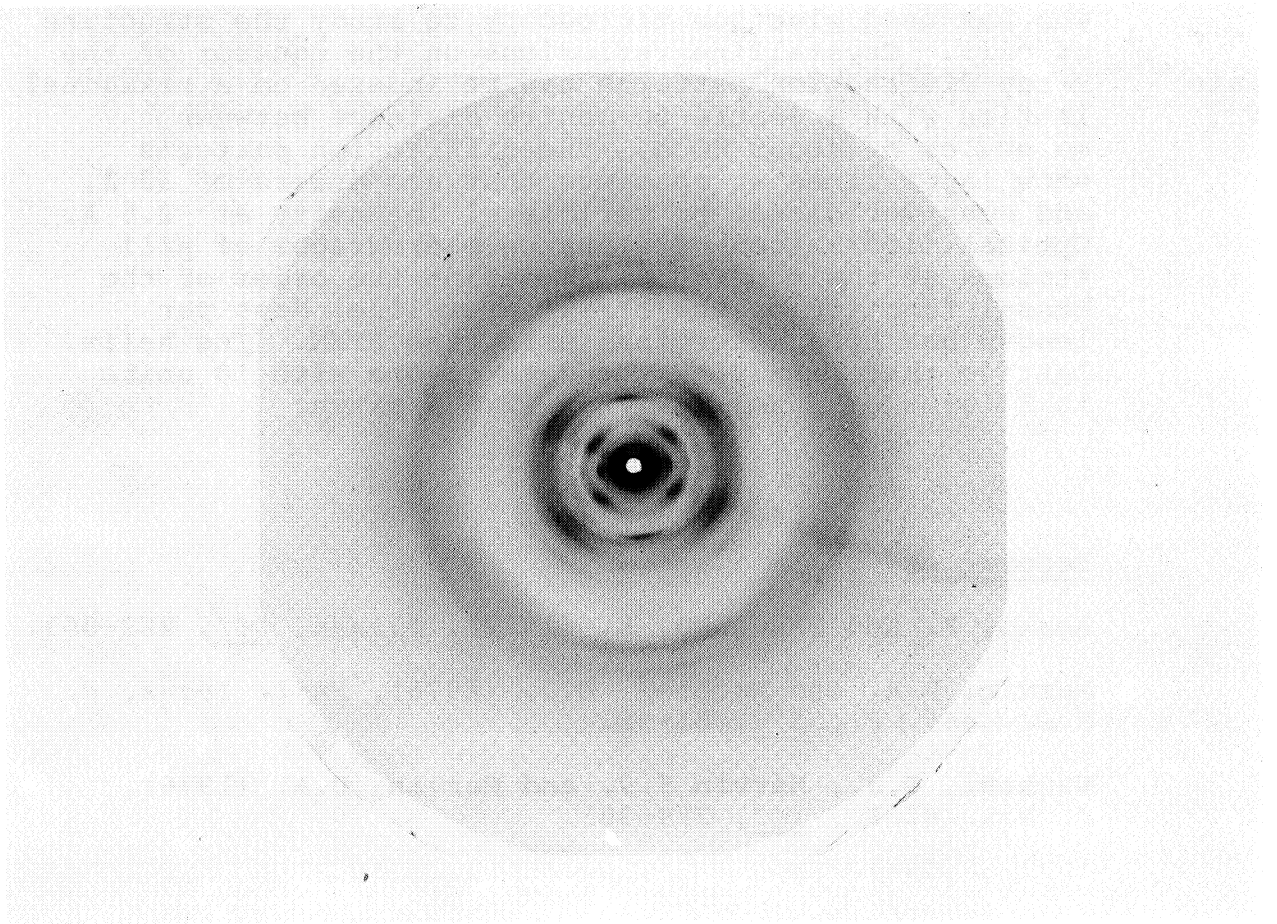

Plate XV

X-ray diffraction pattern of a fibre of F-pili. Fibre axis vertical.

F-pili

We have begun a study of the structure of F-pili using x-ray fibre diffraction, in collaboration with M. Achtman (Berlin); and with J. Dubochet (Zürich*), who has used electron microscopy to study the structure of pili. Crystalline reflexions on the equator of the x-ray diffraction patterns can be indexed on a hexagonal lattice with a centre-to-centre distance between molecules of about 80 Å. The diffraction patterns show layer lines at spacings that are orders of 32 Å, and near-meridional or meridional intensity at 2.5 Å. Optical diffraction of electron micrographs of pili stained at their outer radii define the order of the Bessel function on the first layer line. Mass per length has been determined using the STEM. The helix lattice that best fits the data is one with 18 units in 5 turns of a helix with a 12.5 Å pitch.

Plate XV

References

Amako, K. and Yasunaka, K. (1977). *Nature*, *267*, 862-863.

Marvin, D.A. and Wachtel, E.J. (1976). *Phil. Trans. R. Soc. (Lond.) B.*, *276*, 81-98.

Wachtel, E.J., Marvin F.J. and Marvin, D.A. (1976). *J. Mol. Biol.*, *107*, 379-383.

---

* joining EMBL staff on 1 May, 1978

Electron microscopy of nucleic acids

Members: H. Delius, B. Koller*

Technical assistant: M.-T. Sagne

This group uses the cytochrome spreading procedure (Kleinschmidt technique) for the electron microscopic analysis of nucleic acids.

Results:

(a) An important tool for the characterization of recombinant DNAs is heteroduplex analysis; when a mixture of single-stranded DNAs is reannealed only complementary base sequences will form duplex strands. These can be measured to determine the extent of homologies in DNAs of different origins. The major problem in the application of this method is caused by the difficulty of obtaining preparations of intact single-stranded DNA. Agarose gel electrophoresis of single-stranded DNA permits a separation of intact molecules from fragments, and in favourable cases also the separation of the two complementary strands. A method has been developed to isolate DNA from agarose gel bands in quantities and concentrations suitable for electron microscopy. This method makes use of the electrophoretic elution of the DNA onto a new adsorbent, malachite green coupled to polyacrylamide beads (developed by H. Bünemann and W. Müller, Bielefeld).

Plate XVI — The Plate shows an example of heteroduplexes prepared from the separated complementary strands of $T7^+$ DNA and the DNA of a T7 deletion mutant (D53) used as a model system. It demonstrates that by using this method it is possible to obtain a high yield of intact heteroduplexes.

(b) The analysis of $\phi 80$ phage DNA carrying insertion sequences with promoter and anti-promoter activity (in collaboration with J. Besemer, Köln) is continuing. Difficulties that arose from fragmented DNA and a high content of helper phage DNA in the original sample will hopefully be overcome by the purification procedure described above. Accurate measurements for one of the deletion mutants were obtained by stepwise reannealing and complex formation with T4 gene 32 protein.

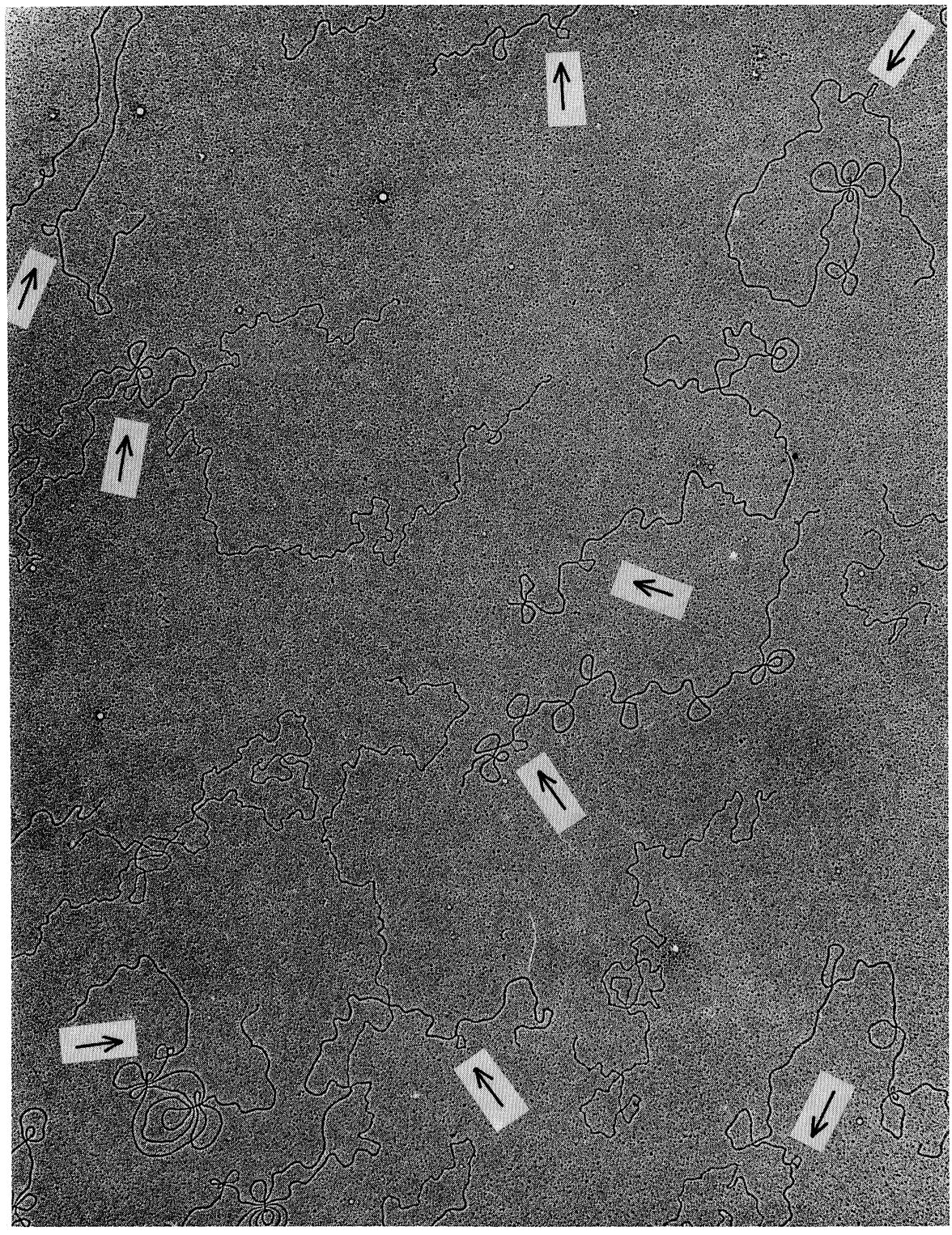

Plate XVI

Complementary strands of $T7^+$ DNA and of DNA from the deletion mutant D53 (gifts from H. Priess, Munich) were purified by agarose gel electrophoresis, reannealed, and prepared for electron microscopy by the cytochrome spreading procedure. A high yield of intact heteroduplexes was obtained. The arrows point to the single-stranded deletion loops.

(c) In collaboration with D. Stüber and H. Bujard (Heidelberg) a map of the promoters for transcription of T5 phage DNA by *E. coli* RNA polymerase was established. *In vitro* synthesized RNA was complexed with T4 gene 32 protein, and the length, position, and number of RNA chains on the template DNA determined. Approximately 45 promoters were located; therefore the number of promoters derived earlier from initial transcript experiments must be doubled. The distribution of promoters on the T5 DNA is asymmetrical. The majority of promoters are found in the region of early transcription, while only eight promoters are located in the late transcriptional region. Two promoters each were found in the pre-early sequences which constitute the two redundant ends of the phage DNA. Not all of the promoters show the same affinity for RNA polymerase. At polymerase concentrations of less than one active enzyme per promoter certain sites compete less efficiently for the enzyme than others, as expressed in the lower number of RNA chains initiated. The analysis of the transcription complexes also permits the determination of the direction of synthesis initiated at the different promoter sites. One prominent switch of the direction of transcription is observed in a position which might coincide with the location of the major origin of replication in T5 DNA.

(d) The partial denaturation patterns of the DNAs from a transforming (B95-8) and a non-transforming (HR-1) strain of Epstein-Barr virus were compared (with G. Bornkamm, Erlangen). The partial denaturation of the DNA isolated from strain HR-1 revealed a heterogeneity within the population of DNA molecules. One group of partial denaturation maps comprising the majority of DNA molecules showed a denaturation pattern that could be correlated with the pattern obtained from the partially denatured B95-8 DNA. The comparison of the two patterns leads to the assumption that extensive stretches of DNA about 12 kilobases in length were inserted and deleted at different positions in the two viral genomes, respectively.

High resolution electron microscopy

Member: K.R. Leonard

Visiting workers: W. Hofmann*, D.S. Hulmes*, M. Reedy*, H.G. Schramm*

Technical assistant: T. Arad

The aim of this group is to obtain, by both conventional transmission electron microscopy (CTEM) and scanning transmission electron microscopy (STEM), together with analogue or digital data processing, high resolution structural information for biological materials. This also includes work being done to minimize the damaging effects of specimen preparation (mainly dehydration) and electron beam irradiation.

(a) Electron microscopy

Considerable progress has been made with STEM mixed signal operation for the imaging of very low contrast speciments (see STEM Group report, p. 65, for technical and operational details). Thin sections of plastic-embedded specimens, containing no heavy metal fixative or stain, including insect flight muscle and fly optic neuropil (see Plate, internal collaboration with G. Griffiths) have been observed at a resolution approaching that obtained for conventionally stained material in the CTEM. Image contrast, for an acceptable signal-to-noise ratio, can be adjusted to a level equivalent to that for stained specimens. In the absence of heavy metals, it is possible to observe the natural contrast corresponding to the distribution of biological material in the specimens. Unstained specimens of filamentous bacteriophage, whole-mounted on thin carbon films, have also been used for measurement of mass distribution. A visit was also made to the factory of Messrs. VG Microscopes Ltd. to carry out tests on biological samples of the x-ray microanalysis equipment which is scheduled to be installed early in 1978. These were very promising and indicated that a microanalytical capacity will be an important accessory for the STEM.

Plate XVII

Plate XVIII

A number of projects has been carried out with the Philips EM 400 CTEM, including both internal and external collaborative work. With the group of D. Marvin,

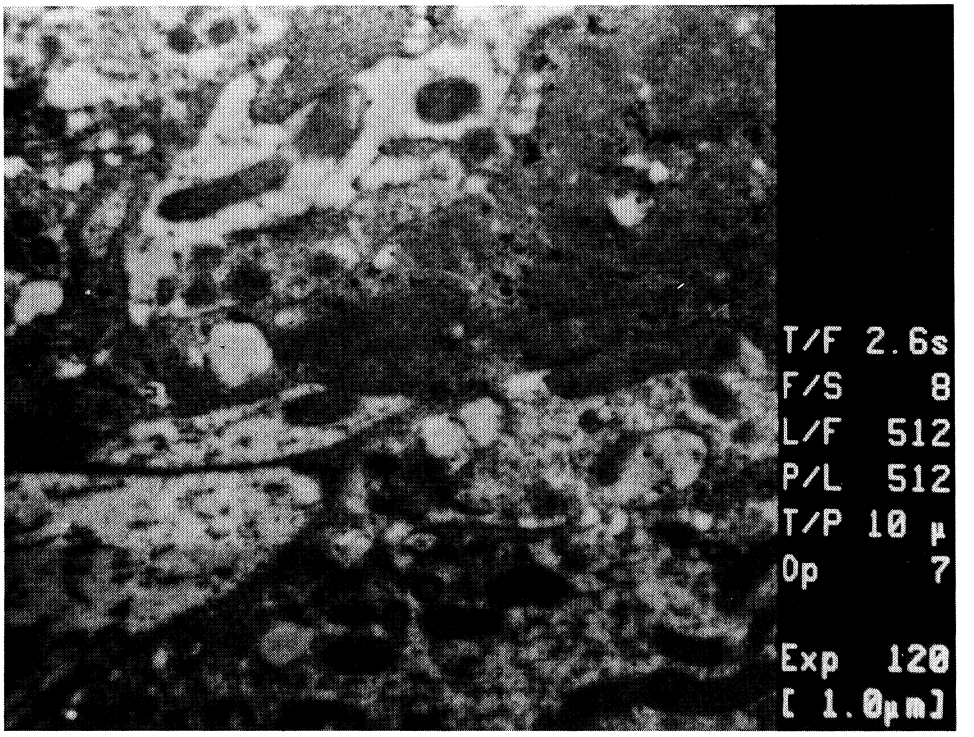

Plate XVII

STEM mixed signal image of unstained fly optic neuropil, taken with the EMBL digital scan generator. The alpha-numerics are displayed with the image and give all essential imaging conditions.

(a)

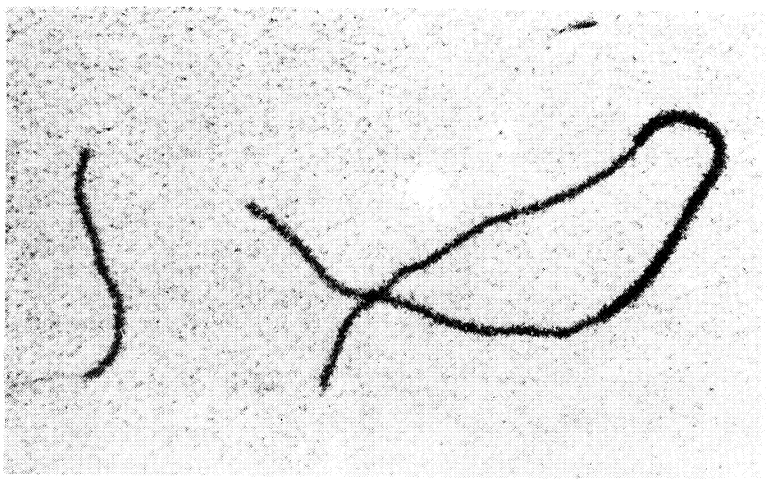

(b)

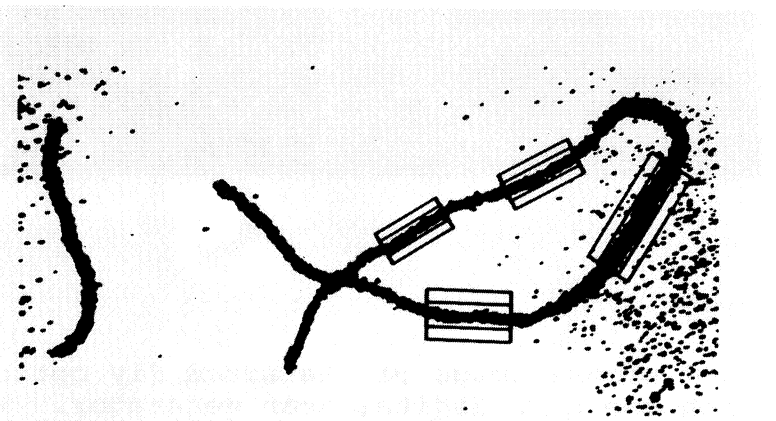

Plate XVIII

(a) STEM mixed signal image of unstained filamentous bacteriophage Pfl. A conformational change has occurred over part of the length of the right hand particle, resulting in an increase in mass per unit length.
(b) After digitization, the image has been displayed on a Tektronix computer terminal and computer integration of selected lengths of the particle was carried out. Selection of the integration boxes is carried out interactively by the terminal operator. (program EMGUCK, J. Ladner).

we have investigated conformational changes occurring in bacteriophage Pf1 on treatment with ether (see Plate XIII and report of D. Marvin, p. 41). Work has also continued with the groups of K. Simons (on the structure of viral membrane protein complexes) and H. Weiss (on the structure of mitochondrial membrane proteins). Electron microscopy and optical diffraction analysis of negatively stained insect flight muscle proteins has been carried out in collaboration with B. Bullard (Department of Zoology, Oxford University).

(b) Specimen preparation

Work has concentrated mainly on the preparation of specimens for STEM where self-contamination by the specimen is a particular problem. This has been fairly well overcome by the combination of clean techniques for preparing the supporting carbon film and sample, and if necessary by pre-baking the sample to a moderate temperature under ultra-high vacuum. A cryo-ultramicrotome was installed in the latter part of the year, and preliminary work has been carried out on the cutting of thin frozen sections of muscle and protein crystals.

(c) Electron microscope image processing by computer

A set of programs has been developed for image processing on the EMBL mini-computer system, principally for two-dimensional Fourier filtering of periodic structures. Software has mainly been developed by the Computer Group (P. Taylor); see Computer Group report (p. 72) and Plate XIX. Electron micrographs are digitized on the Optronics drum densitometer and stored on disc files. These use the file format standardized by the Computer Group and can be output to various devices - Tektronix terminal, electrostatic plotter or film - after correction for contrast (gamma function). Two-dimensional Fourier transforms of up to 1024 x 1024 data points selected from the digitized image can be carried out on the Nord 10 computer, the transformed data being output numerically or as a diffraction pattern image which can be displayed (Plate XIX b). Peak selection and masking can be carried out interactively at the Tektronix terminal using this pattern, followed by inverse Fourier transformation of the selected data to give a noise-filtered image (Plate XIX c). Alternatively, the inverse transformation of selected peak Fourier terms

Plate XIX

(a)

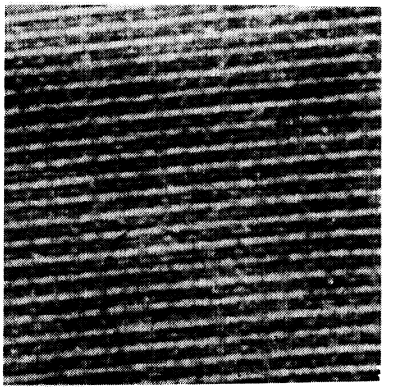

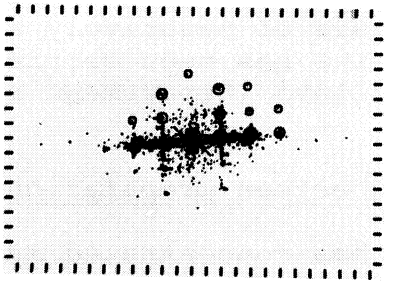

(b)

(c)

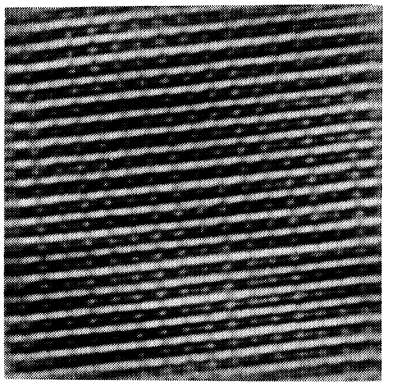

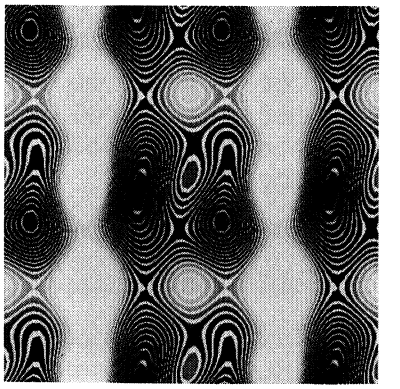

(d)

Plate XIX

(a) STEM image of unstained insect flight muscle. This has been digitized at 256x256 picture points and computer-written on to film using 64 grey levels. The image density has been inverted so that protein appears lighter.
(b) Tektronix display of a computer-calculated 256x256 Fourier transform of the image in (a). Peaks for integration have been selected in the upper half of the transform. The size of the "window" around each peak corresponds to the size of the small circles.
(c) Inverse Fourier transform of the selected data from (b) to give a noise-filtered image.
(d) A peak-averaged filtered image of a STEM micrograph of a negatively stained phosphorylase-b microcrystal. Density has been reversed so that protein is dark. The projected density is displayed as a 10-level grey scale contour map.

can be carried out, to give an averaged picture of the unit cell (Plate XIX d). An interactive Tektronix program has also been developed by J. Ladner for the display and numerical integration of optical density in selected regions of images. This is being used for the analysis of mass density in STEM electron micrographs of unstained specimens (Plate XVIII b).

E/M Application Group

Member: R. Freeman*

Technical assistant: E.-M. Bolzau*

It was decided during the year to establish an Electron Microscope Applications Group, the functions of which would be

(1) to collaborate with other research groups needing to use electron microscopy as a research tool, but not themselves including professional electron microscopists;

(2) to assist in the exploitation of instruments of new types, in the first instance the STEM, under development in the Division of Instrumentation;

(3) to make available sophisticated methods for preparing specimens, e.g. freeze-fracture and thin sectioning, and to collaborate with the Division of Instrumentation in developing new specimen-preparation techniques.

Dr. R. Freeman was appointed first scientific member of the group on 1st June 1977 and has so far for the most part been concerned with developing the applications of the STEM.

DIVISION OF INSTRUMENTATION

STEM development

Members: A.V. Jones, J.-C. Homo, B.M. Unitt

STEM development this year has concentrated on four main projects.

(1) The assessment and extension of the analogue image-processing facilities.
(2) The development of the necessary electronics to permit the STEM to be interfaced to a Nord-10 computer for digital image processing.
(3) The design and fabrication of a cryo-stage to operate initially at liquid nitrogen temperature.
(4) The development of specimen pre-treatment to minimize electron-beam damage.

Analogue image processing

The impetus for this work came from our initial success in imaging unstained insect flight muscle. The essential instrumental factors in producing these images were:

(1) the use of the "single-shot" operating techniques and image storage facilities developed in the latter part of 1976.

(2) the ability to mix simultaneously bright and dark field signals to produce a composite image.

Single-shot operation has now become our standard technique. Basically, the microscope operating parameters (focus, astigmatism etc.) are set up on an area adjacent to the area of interest, by using the beam shift controls. The scan is then switched off, automatically blanking the electron beam, and the beam shift controls are reset to the preselected specimen area. The image is then simultaneously stored on the scan converter and recorded photographically. (The camera system has been modified to provide dual recording facilities; all photographs are recorded on 35 mm film, and a beam-splitting mirror allows selected photographs to be recorded either on Polaroid or on 70 mm film for improved image quality.)

Variations of this technique have been developed by the different operators to suit their own personal requirements, but the principle of single-shot operation is always adhered to since a significant increase in image degradation has been found to occur between the first and second scans of a particular area.

The central factor, however, has been the use of mixed signals to produce adequate contrast from unstained materials.

The video mixing unit can accept up to three input signals. These signals can be added (or subtracted) in any chosen ratio to form two independent composite signals. These signals are then fed to a divider to produce the ratio of the two composites. All intermediate mixed signals are available as possible output signals.

The scan converter storage facilities can be used to advantage in setting up the mixing parameters by providing a side-by-side comparison of processed and unprocessed images. To avoid specimen irradiation during this setting-up process, the primary inputs can be stored and fed via the mixer to the displays.

The original mixing unit supplied with the STEM had inadequate bandwidth for this operation, and has been replaced by our own design which is operable at television rates for flicker-free viewing.

The most useful combination of signals found so far is:

$$\frac{\text{Bright field - Dark field}}{\text{Bright field + Dark field}}$$

with the ratios chosen to provide minimum contrast in the denominator. This has the additional advantage of suppressing electron beam noise. The resultant image is pseudo-bright-field in appearance and has high contrast.

The technique has since been applied by Drs. Leonard, Freeman and Griffiths to fly optic nerves. The ability to image unstained material has also been used in mass measurement studies by Drs. Leonard and Freeman (see p. 56).

Accurate setting-up of the various units is essential for best results. To simplify these procedures the STEM has been fitted with a video step-wedge generator and video monitor to display graphically the effect of altering the various parameters.

Digital image processing

The usual method of adding digital image processing to a scanning microscope is to interface the microscope directly to a mini-computer of limited power, operated basically as a data retrieval system with restricted image processing capabilities. Data is archived on magnetic tape for transfer to a central computer facility for processing.

The EMBL computer facility is built around distributed medium size computers with no large central computer. For this reason it was decided to concentrate all image processing facilities in a task-oriented computer linked on-line to the STEM and operable in a multi-user mode either directly from the STEM or from terminals with grey scale displays for off-line operation with archived data and data read-in from an optical scanner. A priority system allows the STEM immediate access when requested.

This computer will have 192 Kbytes of main store, two 66 Mbyte discs, a tape drive, and a line printer, and it will be fitted with an array processor to provide increased speed for matrix arithmetic.

Because of the multi-user operation, control functions normally carried out by the data-retrieval computer had to be incorporated in the STEM itself. This is done using a micro-processor-based digital scan generator (designed by B. Unitt) which can operate either in computer-linked or stand-alone modes to maximize access to the computer for off-line users. This scan generator is completed and is now under test.

Cryo-stage

The need for a cryo-stage is two-fold. First, the success with unstained sections suggests the elimination of the conventional embedding medium as a logical next step, and this is done by cryo-sectioning pre-frozen specimens which then must be imaged while still frozen. Secondly, work in the other laboratories suggests that specimen damage can be reduced by lowering specimen temperatures.

No commercially produced cryo-stage exist for the HB5 STEM, and one has therefore been designed (by J.-C. Homo) and built and is about to be tested.

Specimen pre-treatment

Preliminary tests have indicated that decreased self-contamination occurs when specimens are gently heated in ultra-high vacuum prior to insertion in the STEM. Facilities to carry out this heating routinely will be incorporated in a UHV freeze-fracture unit (designed by Dr. J. Escaig of the CNRS Laboratoire de Microscopie Electronique, Paris) which is at present under construction.

The Computer Group

Members: R. Herzog, C. Boulin, F. Herzog (part-time), R.C. Ladner, P.T. Speck, P. Taylor*

1977 saw the firm establishment of image processing capacity, with the completion of the on-line micro-sensitometry and film writing systems and the interactive x-ray and E/M image-processing systems. The neuroanatomy graphics project was begun, and the molecular model-building system was nearly completed. In parallel, software and hardware tools were developed for the two Nord 10 mini-computers belonging to the Laboratory. Evaluation of a high speed graphics system and an array processor were carried out, and contracts have been written; delivery is expected in mid-1978.

All the software development carried out in the Group relies on computer/human interactions. The biological computer systems are not yet well defined and most of our efforts are aimed at developing better displays of results, and in leaving to the user the decision what should be done next, and where. This presupposes time-sharing systems with very short response, and interactive graphics terminals.

Standard large batch computing is not provided by the Computer Group, but is available *via* the Max-Planck-Institute for Nuclear Physics in Heidelberg (DEC 10), and for Plasma Physics in Garching (IBM 360/91 and Amdahl).

System development and support

Plate XX

This work has been carried out on the two Nord 10 computers belonging to the Laboratory, the configuration of which is illustrated. About one third of the Group's activity consists in developing or improving software tools for the user community, as well as setting up internal standards. The most noteworthy projects in 1977 have been:

- a string processing package for the manipulation of character strings and symbols in FORTRAN programs. This package is the foundation of tools like RUNOFF, the wiring list system (see later), or utilities like batch editors, sorts, symbolic files and transformations.

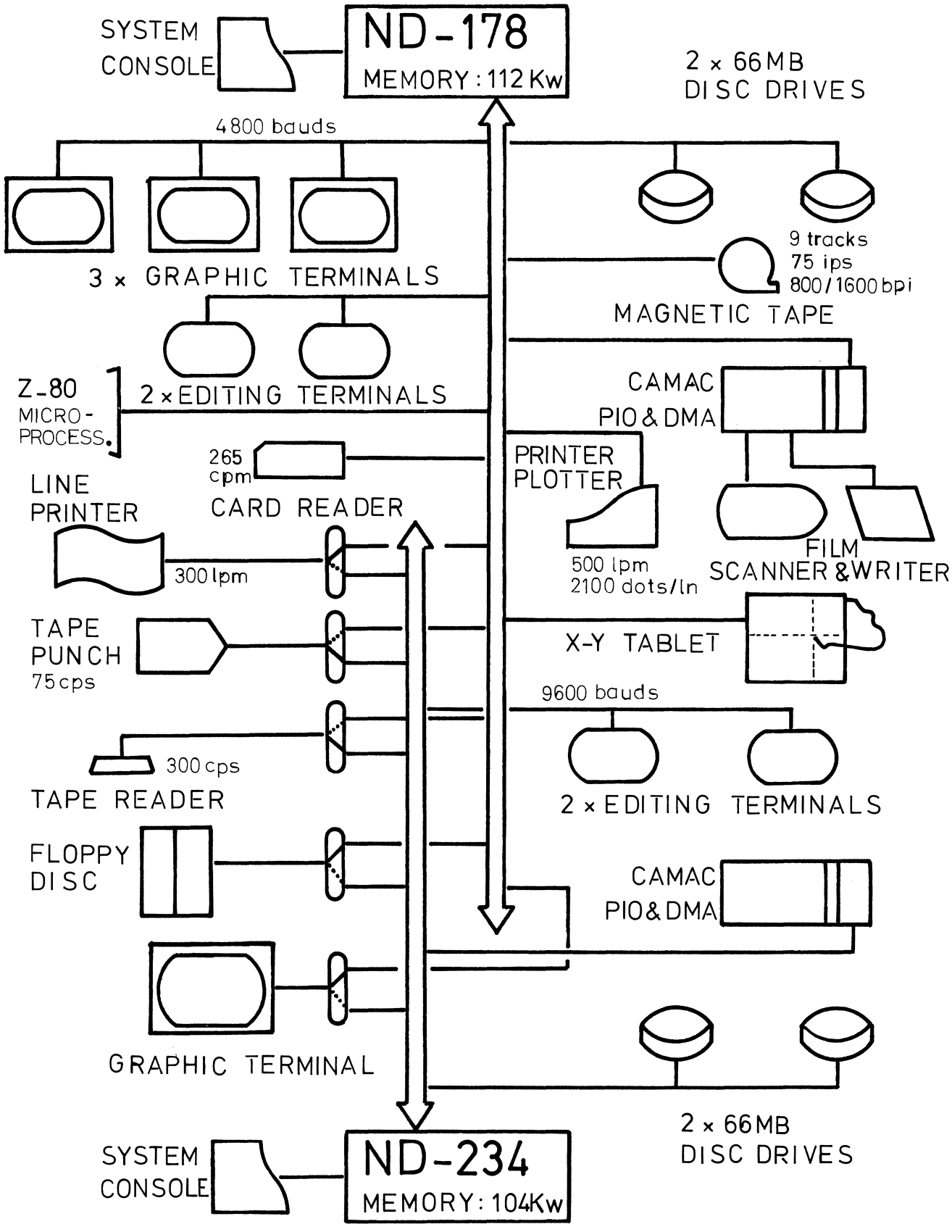

Plate XX

EMBL minicomputer systems at the end of 1977

- an interactive terminal character input/output package that allows FORTRAN programs to use simple and standard interactive menu selection.
- a documentation program, RUNOFF, for the maintenance of the Group's documentation.
- a microprocessor development system (in collaboration with B. Unitt of the STEM Group) whereby software for stand-alone microprocessors can be developed on the Nord 10 time-sharing system and downloaded to the microprocessor for immediate execution and debugging. Established programs are later written in PROM using the CAMAC system. This very flexible system allows efficient software development while keeping the microprocessor peripheral equipment minimal (i.e. a teletype line).
- the adaptation to 32-bit floating point of a PASCAL system developed at the PS Division of CERN. PASCAL is a high level language which is very suitable for algorithm development and documentation; developed at the E.T.H. (Zürich), it is now internationally used and available on most recent computers. It is planned to use it extensively in the neuroanatomy project, and in all areas involving artificial intelligence.
- a wiring list system for the establishment and functional verification of electronic circuit wiring lists. This allows speedier and more accurate development than with manual methods, and makes it possible to maintain the documentation whenever changes are made.

Microdensitometry and film writing

The prototype CAMAC interface for the Optronics film scanner and film writer was completed early in 1977. This development of real-time programs for the control and data transfers was carried out with some advice from the EP division of CERN. Operation on a trial basis has been available to the E/M and x-ray groups since April 1977, while software improvements in the interests of reliability and speed took place throughout the rest of 1977 as new problems were uncovered. A reader/writer installation was established at the Grenoble Outstation in September 1977, all the software developed in Heidelberg being transportable since the Grenoble Outstation uses a Nord 10/CAMAC system.

Basic image processing support

Plate XXI

To obtain video images from scanning processes, images are displayed or recorded on the storage screen terminals (Tektronix 4000 series), on the printer plotter, or on film. The data files are usually very large (128 Kbytes to 16 Mbytes) and require a minimum set of utility programs for their efficient manipulation. Such a package has been created, starting with the precise definition and strict enforcement of the file structure, and followed by utility programs to create, extract, print, copy, analyse and acquire images. The file structure has been defined so as to be easily transportable to other systems, by the use of a symbolic header file. For efficient local operation on the Nord computers a binary header file is maintained.

This package forms the foundation of image processing for both the E/M and x-ray groups. Strictly enforced standards have so far avoided duplication of programs, and have speeded up development by making powerful tools available for manipulating the file structure.

Image processing for E/M work

This was was carried out for Dr. K. Leonard of the E/M Group, and is described in the report of that group (p. 56). It consists of a suite of programs for the interactive performance of two-dimensional Fourier filtering.

Image processing for x-ray fibre work

Computer Group involvement in this program was mainly software support and the provision of advice to the x-ray group. The development of interactive storage tube display programs by Dr. J. Ladner (x-ray group) has provided a general mechanism for the display of video images on the Tektronix terminals, providing threshold, contour or density display.

A feature of the neuroanatomy project, allowing interactive input of closed contours and integration over closed contours, has been included in both the E/M and x-ray analysis programs (for details see p. 25).

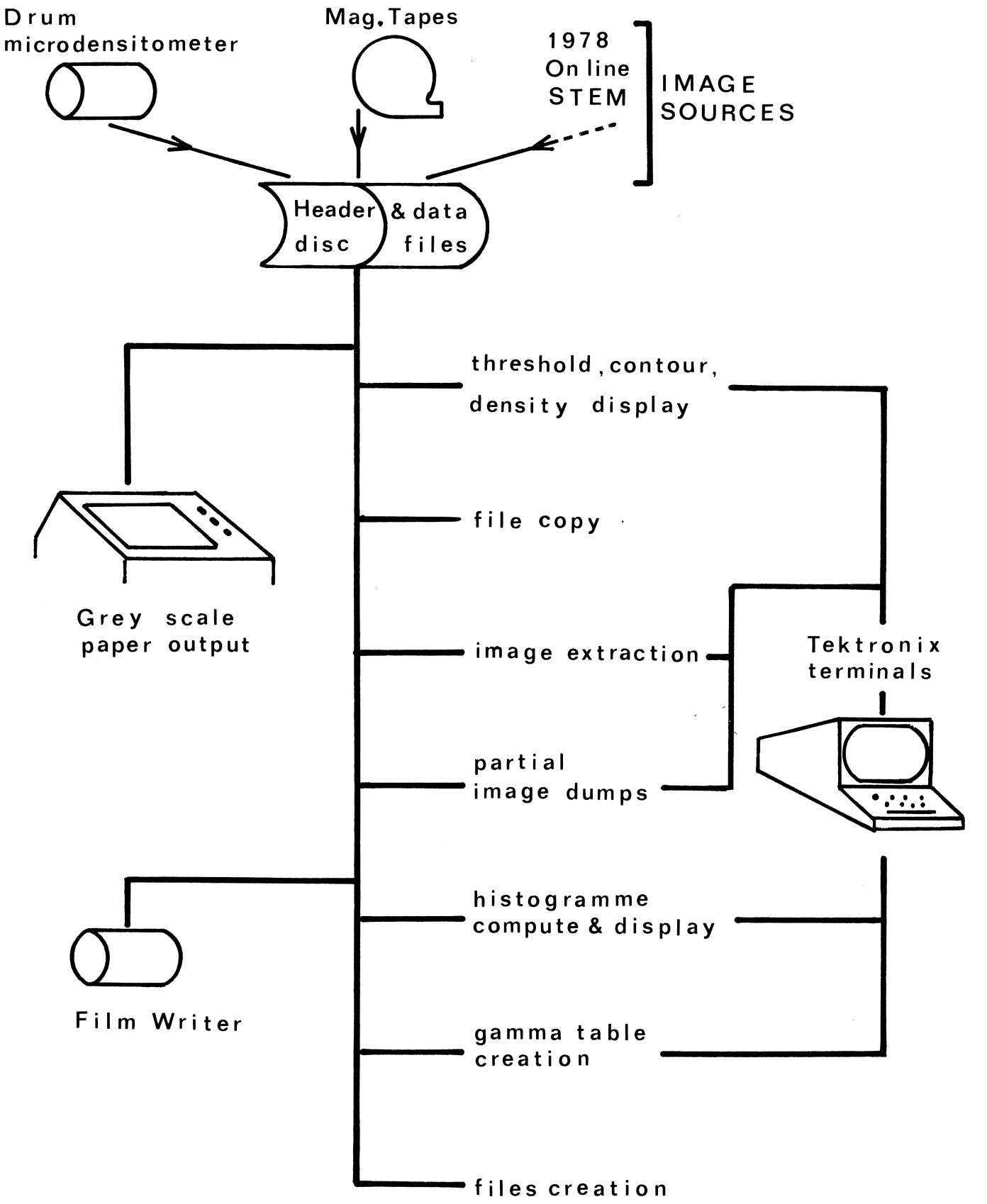

Plate XXI

Basic image-processing facilities

STEM interfacing

Owing to shortage of manpower, this project has been transferred almost completely to Dr. B. Unitt of the STEM Group. The Computer Group has, however, provided support for hardware design (the wiring list system) and microprocessor software development, as well as general advice. It is hoped to resume the project in 1978.

Computer graphics for neuroanatomy

This project was begun in January 1977 for the neuroanatomy group. Investigation of existing systems, and measurements of some sample data, led to the development of data-smoothing procedures. Data originating from digitizing processes, e.g. contour entries from micrographs, are ill-suited for storage or processing, so they are fitted with polygonal sequences that are allowed to deviate from the original points within a given tolerance. This treatment not only provides smoother outlines but also requires much less storage and therefore provides faster display and processing. The internal vertex coordinates are simply kept in full 16-bit words.

Another tool for graphical data processing is an algorithm that finds the "skeleton" of an arbitrary two-dimensional contour. The method uses the topological properties of a set of grid points superimposed on the contour. Skeletons can be simplified and then used as "stick models" to study the topological properties of dentrite structures. An example is illustrated.

Plate XXII

Software support for a digitizing tablet allowing backward projection now makes available manual digitizing of contours from micrographs (35 mm slides).

The future development of programs will be stimulated by the availability of the high level language PASCAL.

Molecular modelling

A long term goal is to use real-time computer graphics to study the structure and dynamics of biological structures. In the 1976 Research Report we discussed plans for a set of computer-graphics molecular-model building (molecular graphics) programs; these have now

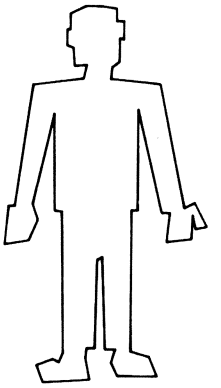

(a)

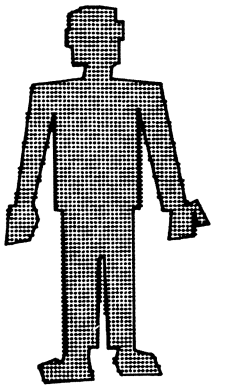

(b)

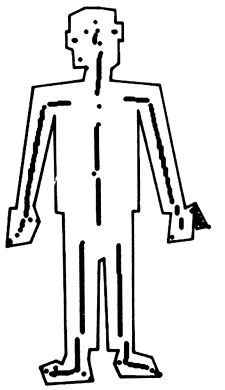

(c)

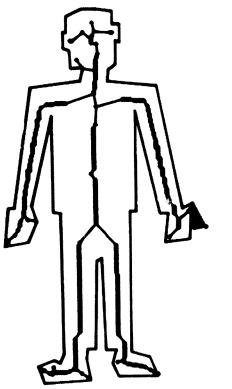

(d)

Plate XXII

An example of the method of "skeletonizing" two-dimensional contours
(a) The original polygon.
(b) Superposition of an orthogonal grid.
(c) Skeleton vertices "shrunk in" from the grid.
(d) The final skeleton is the shortest tree spanning the vertices.

been implemented on the PDP 11/40 - Evans and Sutherland (E&S) Picture System 1 in the Deutsches Krebsforschungszentrum in Heidelberg. A first version of the molecular graphics package is running, and will soon be in use on the filamentous virus Pf1 coat problem. The current program allows the user to build, display, and manipulate up to 200 atoms from one stretch of a protein, nucleic acid, or polysaccharide. Electron density maps can also be displayed and the structure manipulated to improve the fit between model and map. Coordinates of atoms not being displayed are kept on disc.

The coat Pf1 consists of about 2000 copies of a 46 amino-acid polypeptide. Fibre diffraction x-ray data are available to about 3.0 Å, but comprise only about 200 independent reflexion intensities. The protein chains are thought to have a distorted α-helical conformation and to pack in a larger, left-handed helix to make a sheath for the DNA. Because of the small amount of x-ray data and the lack of tertiary structure, the stereochemical constraints on the packing of the helices to form a virus, and the side-to-side packing of virus particles, are at least as important as fitting the observed transform.

The programs obtained in 1976 from R. Diamond (MRC Laboratory, Cambridge) have been modified to allow the display of 200 atoms and an arbitrary number of repetitions of up to four different symmetry operations. This allows us to examine the intermolecular contacts over about 3 turns of α-helix. With so much molecule on the screen the usual "stick figure" of all the atoms can become confusing. Therefore several alternative representations have been developed, thus the plate shows 11 copies of 30 residue sections of the backbones of Pf1 α-helices shown as 3-start helices drawn through the carbonyl carbon atoms. The conformation of the molecule or of the standard groups can be changed by changing the bond angles or dihedral angles.

Plate XXIII

A second version of the program is under development that will permit handling about 300 atoms from several different stretches of sequence. This will be important in studying larger, more folded molecules. The electron-density display can include dashed and blinking contours which will be useful in studying difference maps, or in comparing two maps.

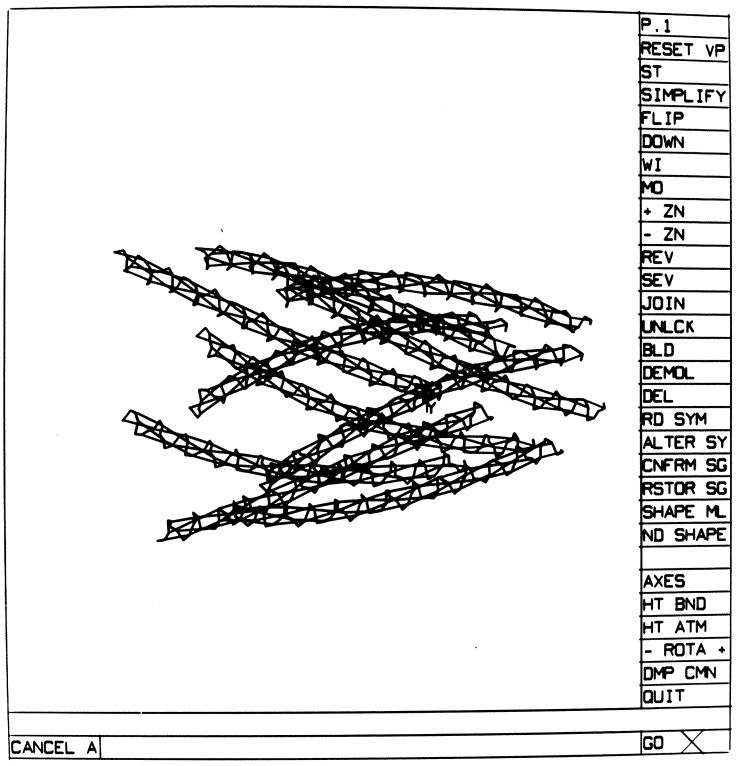

Plate XXIII

A partial model of the filamentous bacterial virus Pfl. 30-residue stretches of the backbones of 11 α-helices are shown as 3-start helices drawn through the carbonyl carbon atoms.

It was decided in December 1977 to buy an E&S Picture System 2 for attachment to a Nord 10 computer. This will make the Laboratory independent of the E&S/PDP system now used in the DKFZ; it is due to arrive in April 1978 and should become operational in June 1978. The programs from the PDP 11 will need some modification to run on the Nord, but much of this will be mechanical and development should proceed much faster on the Nord.

Position-sensitive detectors

Member: A. Gabriel

Technical assistant: F. Dauvergne

Area detectors

The main activity of the group, at present located at the Grenoble Outstation, has been the setting up of the area detector referred to in last year's Report on the synchrotron beam at the DESY Outstation in Hamburg. Extensive precautions were needed because of parasitic radiation, but the detector is now linked to a mini-computer (Intertechnique IN90) and is in routine operation.

A small number of other 200 x 200 mm area detectors has been constructed, adapted to different read-out systems.

Linear detectors

This system has been in routine operation at DESY for six months; its original characteristics have been maintained and there is no evidence of radiation damage.

Circular detectors

This type has been fully tested though not yet used for experimental purposes. It is envisaged that it may be converted to a two-dimensional detector locating incident photons in polar co-ordinates.

Channel plates

First tests have been carried out.

Future plans

A linear detector is being built, 200 mm long and with one wire per mm. Read-out is to an amplifier attached to each wire, and the counting rate will be 10^5 counts/sec given suitable data storage electronics.

THE OUTSTATIONS

The Outstation at DESY, Hamburg

Head: H. Stuhrmann

Members: P. Clout*, H. Fürst*, A. Harmsen, J. Hendrix, M. Koch*, G. Rosenbaum

Fellows: J. Milch*, Z. Rek*

Visiting workers: J. Barrington Leigh*, C. Berthet*, J. Bordas*, F. Dauvergne*, J. Drenth*, P. Duke*, W. Faruqi *, A. Gabriel*, P. Gill*, R. Goody*, R. Hendricks*, R. Hester*, W. Hildebrand*, K. Holmes*, H. Huxley*, G. Johnsen*, A. Jones*, J. Lowy*, T. Matsuo*, A. Miller*, M. Moody*, I. Munro*, F. Parak*, R. Pettifer*, F. Poulsen*, Sir John Randall*, G. Reitz*, H. Riedel*, R. de Roos*, S. White*, J. Worgan*, Z. Kam*

Technical assistants: W. Behrens*(†), P. Bendall, E. Dorrington R. Kläring*, H. Ludwig, V. Renkwitz, B. Robrahn

The main activity during the year was a major effort to develop instrumentation. In general the plans outlined in the previous report have been followed, with some modifications in the light of experience. The design of instruments is primarily dictated by the special properties of synchrotron radiation, but of course paying due regard to the possible applications in molecular biology. Table 1 summarizes the special features of synchrotron x-radiation and their applications.

I. Development of instruments

(a) General concept

The number of instruments which can simultaneously receive radiation is given by the ratio between the beam cross section and the size of the optical elements (mirrors, monochromators). The beam has a horizontal width of 25 cm. As the vertical divergence of x-ray synchrotron radiation is about 0.2 milliradian, the vertical width of the beam at the entrance of the hall is about 0.5 cm.

---

† deceased

The spectrum of the radiation depends on the energy of the accelerated electrons (or positrons) and on the radius of curvature of the orbit. At the synchrotron (DESY) the particle energy is very often 7 GeV, whereas at the storage ring (DORIS) our laboratory receives radiation from positrons with energies of 4 GeV. The wavelength spectra are, however, almost identical because the radius of the orbit at DORIS (12.12 m) is almost three times smaller than that of the synchrotron (31.7 m). The intensity of synchrotron radiation per wavelength unit reaches a maximum at about 0.6 Å.

The design of instruments must be adapted to the given circumstances that the Outstation is mainly a parasitic user of synchrotron radiation produced by high energy physics experiments. This means the optical elements should be designed for a wavelength region from 0.3 to 3 Å. As the incident angles may become rather small, very large mirrors and monochromators would be needed in order to accept a major part of the beam. In practice mirrors 160 cm long are used for vertical focussing, and bent monochromators of 7 cm length demagnify the beam in the horizontal plane. Therefore not more than 5 cm horizontal width are allotted to each instrument, and since 25 cm total horizontal beam width are available, five instruments can be operated simultaneously in each laboratory. The installation of five or more independent instruments in the hall has been guided by the following principles. In order to minimize spatial interference, the instruments should be distributed homogeneously over the area or, preferably, the volume of the hall. Each user should have independent access to his instrument, either by way of an elaborate remote control system for alignment of the camera and sample control, or by introducing radiation shielding. For obvious reasons we have adopted the second alternative whenever possible, after discussing the design of the shielding with the DESY radiation protection group.

(b) The optical layout

The line-shaped beam, 25 cm long in the horizontal plane, is divided into five sections. The central part and the extreme outer parts are reflected by quartz mirrors at grazing incidence. The eight quartz mirrors in each of the three sections are 20 cm long, 5 cm wide, and 2 cm thick; they are aligned to form tangents of an ellipse in order to achieve focussing in the vertical direction.

Depending on the angle of incidence only wavelengths beyond a critical value will be reflected. The outer beams are deflected by the monochromator crystals to the right and to the left respectively (Ge_{111} reflexion); as the crystals are cut asymmetrically and bent, a point-line monochromatic beam, useful for diffraction experiments, is obtained. The central beam has a broad wavelength distribution; it is used for diffuse small angle scattering and spectroscopic experiments.

Plates XXIV and XXV

The beams between the mirrors are deflected upwards by crystal monochromators. Second monochromators, 130 cm and 190 cm above the central beam respectively, direct the beam back into the horizontal plane. The second monochromators are fixed to H-section girders, 6 m long and parallel to the central beam; the displacement of the crystal along a girder with concomitant rotation permits change of wavelength without changing the direction of the beam emerging from the second monochromator. The upward deflection of the beam does not lead to any losses because of its polarization, even at large angles, where horizontal deflection of the almost linearly polarized beam would lead to a dramatic decrease of intensity.

Plate XXVI

(c) Shielding of instruments and radiation protection

Instruments along the central beam line, and the movable optical benches, are remotely controlled. Shielding would decrease the degrees of freedom of movable optical benches close to the central "white" beam, and though it is not impossible to shield the central beam line at the storage ring, it cannot be done at the synchrotron. We therefore preferred to build tunnels around the main beam. Instruments in the tunnel can be reached through small holes in the concrete for sample control and exchange. The tunnels cover a part of the beam path; they are 2 m high, have an interior width of 1.8 m with 0.4 m thick walls. The roofs of the tunnels form an upper floor on which instruments using the upward deflected beams are installed. Instruments on this first floor need no remote control, nor do some of the instruments on the ground floor that are shielded against radiation by concrete walls.

Plates XXIV, XXV, XXVI

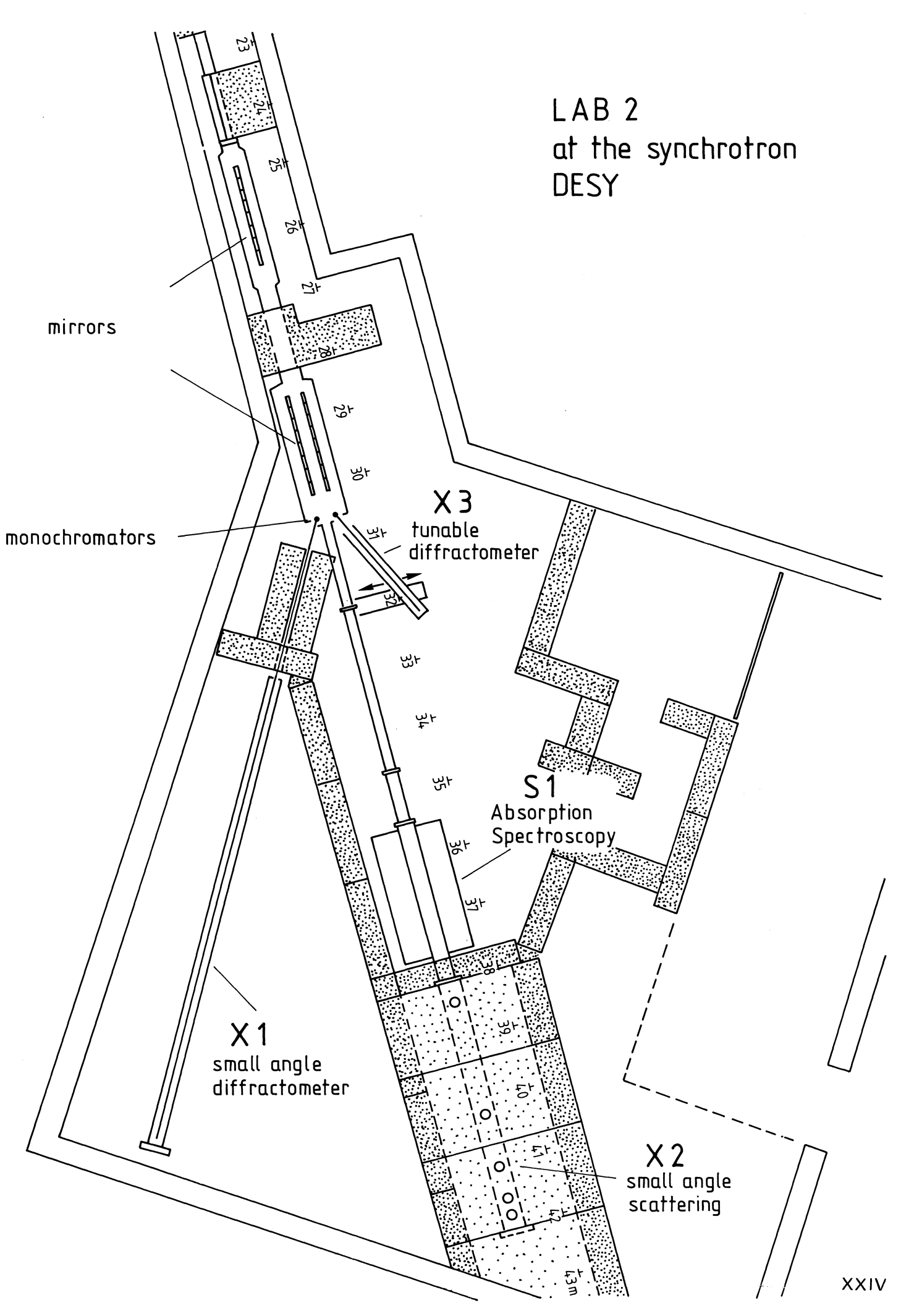
LAB 2
at the synchrotron
DESY
mirrors
monochromators
X3
tunable
diffractometer
S1
Absorption
Spectroscopy
X1
small angle
diffractometer
X2
small angle
scattering
23
24
25
26
27
28
29
30
31
32
33
34
35
36
37
38
39
40
41
42
43m

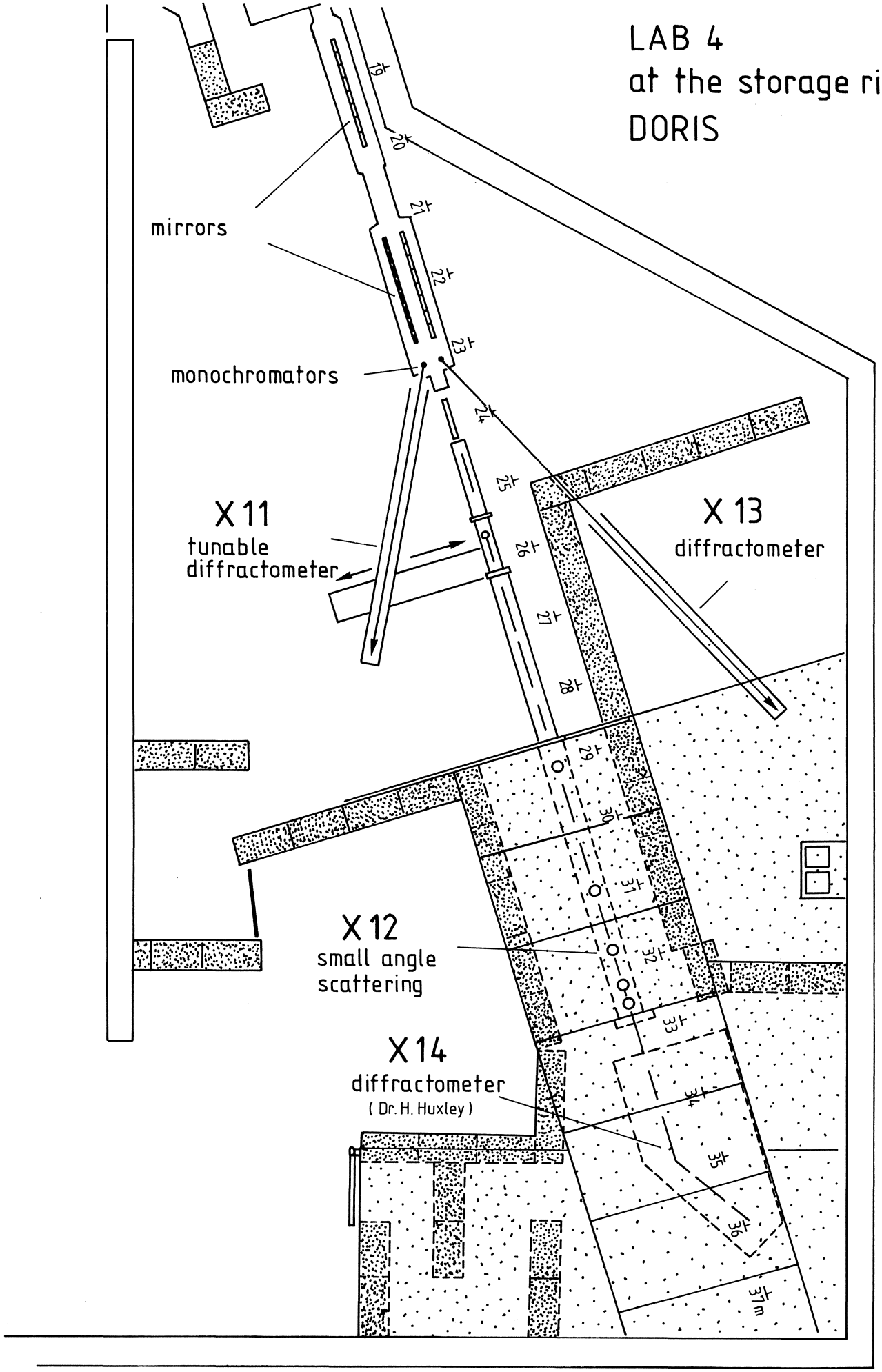
LAB 4
at the storage ring
DORIS
mirrors
monochromators
X 11
tunable
diffractometer
X 13
diffractometer
X 12
small angle
scattering
X 14
diffractometer
(Dr. H. Huxley)
19
20
21
22
23
24
25
26
27
28
29
30
31
32
33
34
35
36
37m

LAB 4
at the storage ring
DORIS

cross section of the hall
along the beam

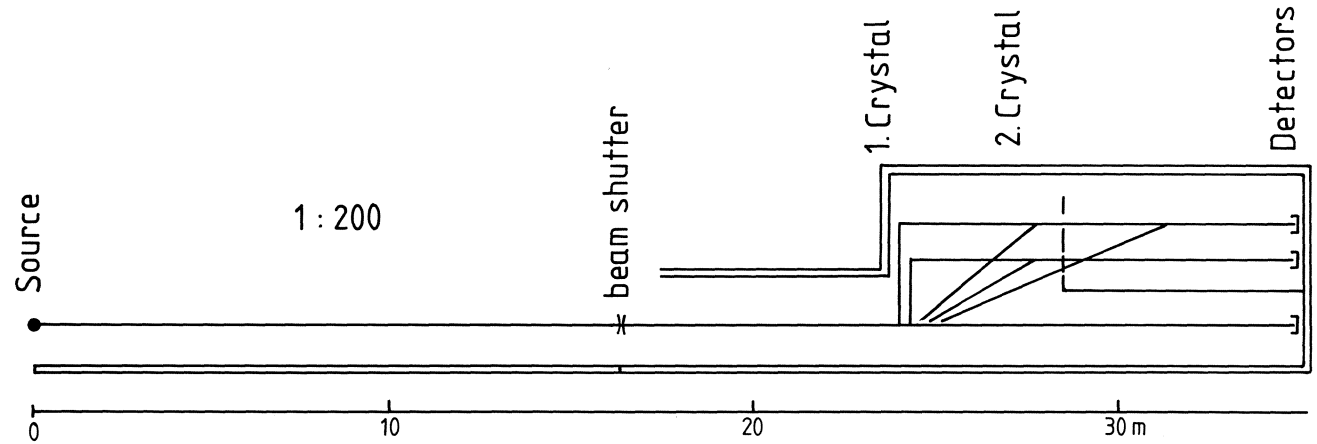

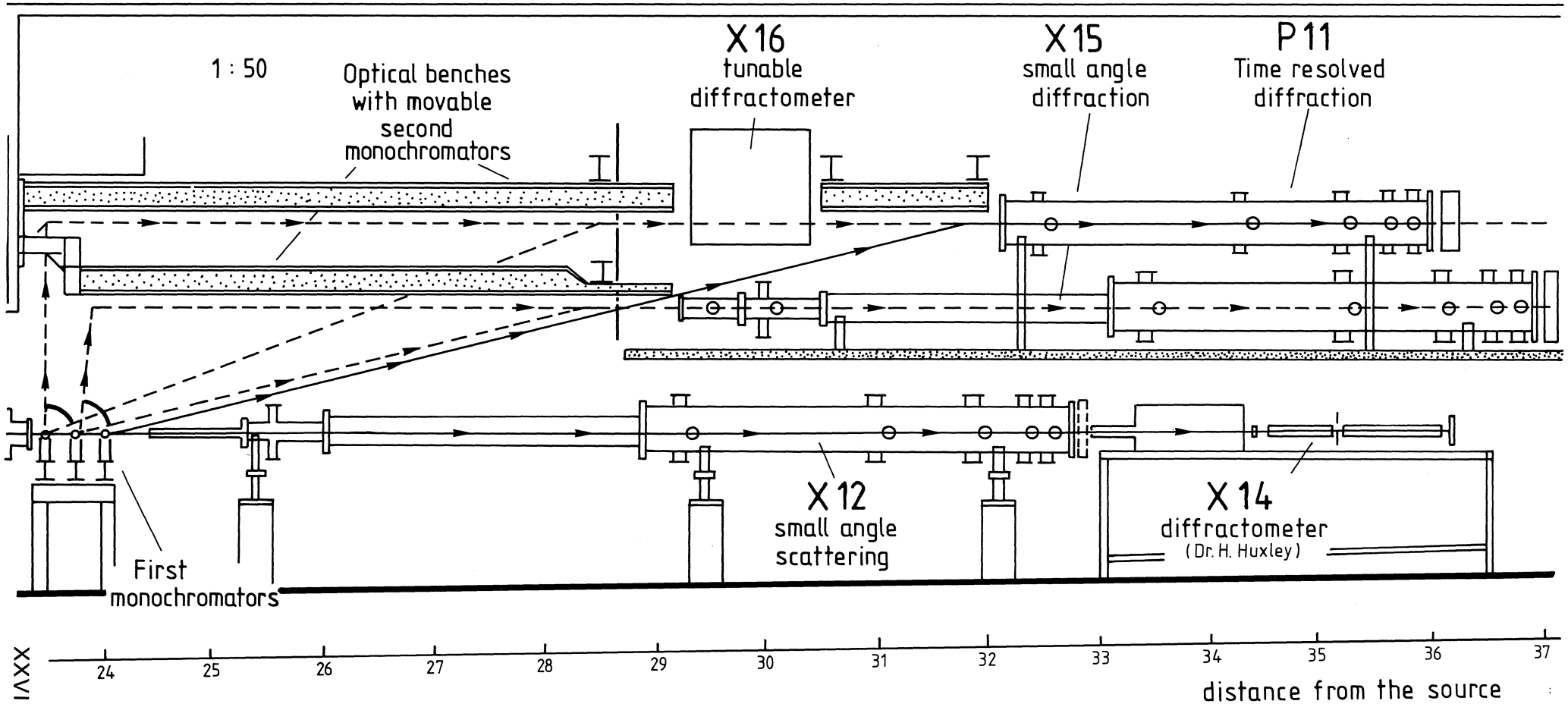

(d) Instruments at the synchrotron (Lab 2 at DESY)

The first diffraction experiments with synchrotron radiation were carried out in Lab 2 in the early 1970s using a small angle diffractometer. This instrument is remotely controlled and has produced diffraction patterns of muscles and collagen (see previous report). The existing mirrors and monochromators make use of only a small fraction of the beam, so a complete renewal of the optical system has been prepared during the last year and will be installed during the next shutdown of the synchrotron early in 1978. (For a description of the instruments in Lab 2 see Table 2.)

(e) Instruments at the storage ring (Lab 4 at DORIS)

The instruments on the ground floor of Lab 4 at DORIS are shown in Plate XXV. The optical system is more highly developed than that in Lab 2; it includes one double-focussing system with 8 mirrors and a Ge-monochromator, and two other sets of mirrors will be installed in March 1978.

The double monochromator system feeding a small angle instrument on the upper floor has been tested with flat asymmetrically-cut germanium crystals of small mosaic spread, and the stability of the beam leaving the second monochromator is very satisfactory. A list of existing and forthcoming instruments is given in Table 3. The instruments X11 and X13 may turn out to be more powerful than X14, and in this case we may envisage the installation of a spectroscopic instrument and/or a diffractometer for anomalous dispersion techniques in the area of X14. Moreover, we plan to focus the central beam also in horizontal direction by using cylindrical mirrors.

II. Experiments

(a) Experiments at X1 in Lab 2

(1) Muscles

J. Lowy, F.R. Poulsen and A. Harmsen

The aim is to elucidate the cross-bridge configuration changes in hypertonic muscles as a function of time.

The configuration of resting myosin cross bridges, in both smooth and striated intact living muscles, is changed by the osmolarity of the bathing medium. Extraction of water causes the cell volume to diminish and this seems to affect the cross bridges. Increased ionic strength is assumed to change the forces between the myosin heads from the same filament, as well as between those from different filaments and the forces between the backbone and myosin heads.

On taking muscles from isotonic to hypertonic media the myosin filaments assume a more ordered state. From the finding that the intensity of the central disc and the ring surrounding it decreases, and that a new layer line with a spacing of 280 Å appears, it is deduced that the myosin filaments aggregate side-to-side to form large ribbon-shaped structures (*taenia coli* of the guinea pig, a mammalian smooth muscle) and that the myosin heads become ordered in a pseudo-hexagonal lattice (anterior byssus retractor of *Mytilis*, a molluscan smooth muscle). The myosin filaments come very close together in the case of frog skeletal muscle; in patterns from hypertonic frog muscle the 1st and 2nd myosin layer lines disappear, the intensity distribution of the 3rd changes dramatically, the intensities of the 4th and 5th are greatly diminished, the meridional reflexions at 214, 106 and 85 Å disappear and the intensity of the 59 Å layer line is greatly reduced. The most important implications of these results are that estimates can be made of the contribution of the myosin backbone to the axial diffraction pattern. Time resolution of the changes in the scattering patterns is now being tried.

(2) Insect flight muscles

R.S. Goody, A. Harmsen, W. Hofmann, K.C. Holmes, M.K. Reedy, G. Rosenbaum

Using the low-angle diffraction optical bench X1, studies of the binding of nucleotides and soluble myosin fragments to glycerinated insect flight muscle fibres (see Research Reports 1976) were continued. Titrations of ATP (β,γ)-NH over a range of temperatures were performed to compare the

properties of the proteins in solution and in the organized state.

For the interpretation of the structure of insect flight muscle, additional detailed information is required from electron microscopy. This is not available at the resolution required, mainly because of sample damage during preparation. For this reason fixation and further processing procedures, including dehydration and embedding, were checked by low angle diffraction after each stage in the preparation. The use of the high intensity x-ray camera, giving short exposure times, appears to be the only rational approach to the problem of improving processing. It was found that in standard procedures essential information was already lost after the first fixation stage, and although this could be prevented by changing the fixation conditions, refinements of the further stages are needed to preserve the structure throughout processing.

(3) Dynamic experiments in solution

J. Barrington Leigh, R.S. Goody, A. Harmsen

A stopped-flow device has been constructed for the low-angle diffraction instrument X1. Using a one-dimensional position-sensitive detector and the proteins G-actin, F-actin and soluble fragments of myosin, a temporal resolution of about 10 seconds for low-angle scattering changes was estimated. These preliminary experiments indicate that by using a ring detector or 2-dimensional detector a resolution of under 1 second could be obtained.

(4) Collagen

A. Miller, S. White, A. Harmsen

Turkey bone collagen was studied by small angle diffraction in order to investigate the structure of collagen in various states of calcification. These experiments are accompanied by neutron small angle measurements (see report of the Outstation at Grenoble).

The relationship between the elasticity of collagen and its diffraction pattern was studied by Nemetschek, Riedl and Rosenbaum. First test experiments on corneal collagen were carried out by G. Elliott and P. Timmins.

(b) X-ray monochromators and flux measurements

S. Rek, A. Harmsen

Experiments have been continued on widening the band-width of germanium and silicon crystals by implanting the surfaces with ions. Different ion energies and annealing procedures have been tried in order to study their influence on the topography of the crystal. The rocking curves were measured with a precision of 0.02 seconds of arc. Ionization chambers were used for the measurement of the flux of x-ray photons. The intensity of the focussed beam of X11 at the storage ring (1.8 GeV, 200 mA) was 1.5×10^9 photons/sec, about five times more than at X1 on the synchrotron. (With the increased energy available since January 1978 - 3.86 GeV and 20 mA - the flux at X11 has increased to almost 10^{11} photons/second.)

(c) Experiments at X11 in Lab 4

(1) Protein crystallography

J. Drenth, A. Harmsen, M.H.J. Koch, G. Schulz

The optical bench X11 was first used in July 1977; an oscillation camera was aligned in the focussed beam, and though the intensity was not very high (energy of positrons: 1.8 GeV, 200 mA current), the preliminary results were very promising. We had to wait until January 1978 for the necessary changes at DORIS to give high energies and an intense x-ray spectrum. Crystallographers from Heidelberg (G. Schulz) and Groningen (J. Drenth) independently tried various protein crystals with unit cell dimensions between 20 and 200 Å, and there is agreement that the quality of the diffraction pattern, taken with an oscillation camera, is excellent after only a few minutes exposure, with resolution apparently well beyond what can be obtained with conventional x-ray

generators. Various protein crystals have been used by G.E. Schulz, M.P.I. Heidelberg, and A. Harmsen: glutathione reductase (form A and B), elongation factor Tu (orthorhombic and tetragonal) and the DNAase-actin complex. Radiation from positrons at 3.87 GeV and 15 mA was focussed by 8 flat mirrors in the vertical direction and by a bent Ge-monochromator in the horizontal direction, giving a beam about 1 mm x 0.5 mm. About $4 \cdot 10^9$ photons/sec were counted after the first collimator (ϕ = 0.6 mm). From the 21 oscillation pictures taken in the test it appears that in this case radiation damage may depend on the incident intensity in the same way as at ordinary CuK_α fluxes. The gain of intensity compared to the best conventional sources was 16.

Other tests have been carried out by J. Drenth (University of Groningen) and M.H.J. Koch. A crystal of the protein rhodanese, mounted in Groningen, was used for comparison*. 8 oscillation photos were taken, and there is no evidence of any major deterioration of the crystal during the series, though the 94.4 minutes total exposure time at DORIS would correspond to 25 hours with a rotating anode beam; this result was not expected in the light of prior data collection with rhodanese at Groningen. On the longest exposed films (31.5 minutes) spots corresponding to *d*-spacings less than 1.4 Å can still be observed, and reflexions could certainly be measured up to 1.7 Å. Comparison of the films taken at Groningen and at Hamburg give a gain factor of 15 at DORIS, in good agreement with the result mentioned above.

Plate XXVII a, b

It should be noted that a better alignment of the optical system of X11 would have doubled the gain factor, giving a factor of 20-30 under the present conditions. Higher positron energies, near 5 GeV and 50 mA, are expected soon and these would increase the intensity by another factor of 5, and should give higher resolution.

---

* Space group $C2$; a=156.1 Å, b=49.0 Å, c=42.2 Å, β=98·48°; MW 33,000.
Crystals grown in 3M ammonium sulphate, pH 7.3.
The same crystal (0.25 mm thick, volume 0.02625 mm^3) was used for all exposures.

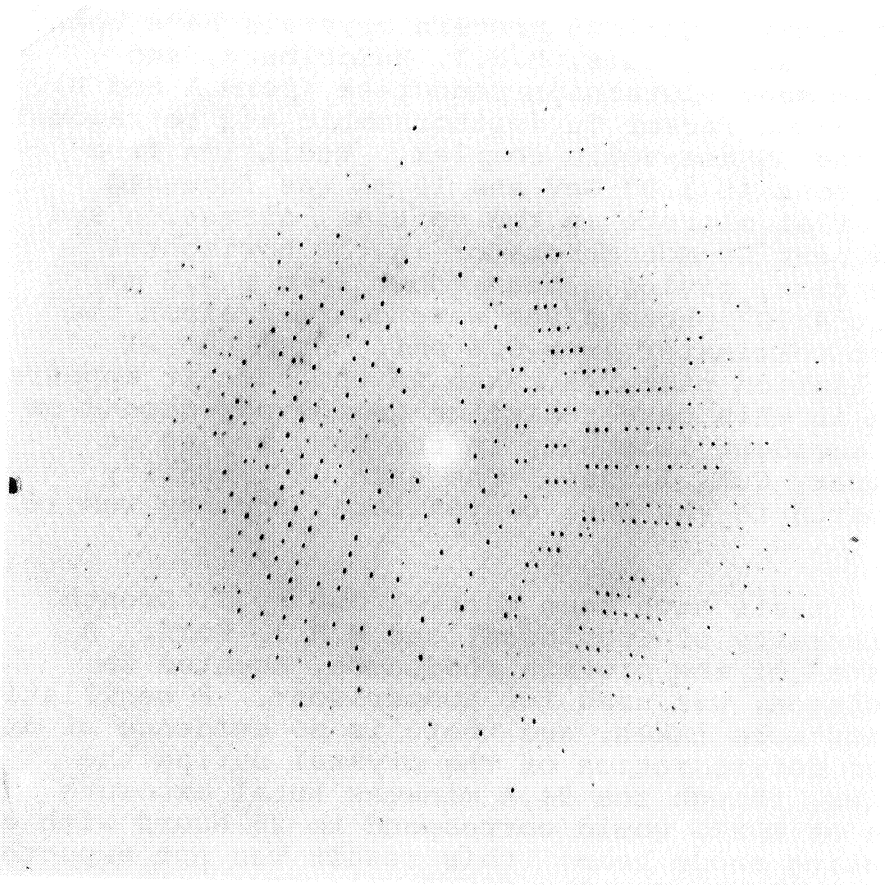

(a)

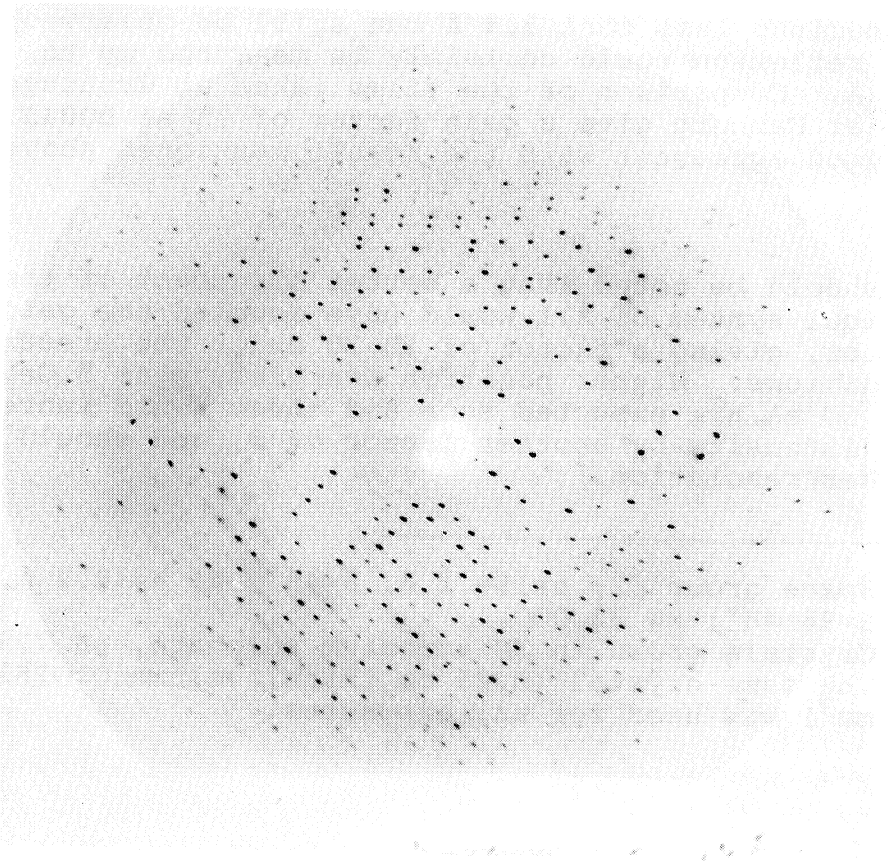

(b)

XXVII

Plate XXVII

3° oscillation photographs of the same crystal of the protein rhodanese for comparison between synchrotron storage-ring radiation and a conventional rotating-anode x-ray tube.

(a) At DORIS (positron energy 3.87 GeV, current 15 mA) - exposure time 4.6 min.

(b) Elliott GX6 rotating-anode x-ray tube (36 kV, 44 mA, graphite monochromator) - exposure time 100 min.

Note that the spots are sharper with synchrotron radiation.

(J. Drenth and M.H.J. Koch)

(2) Collagen

G.F. Elliott, A. Harmsen

With an average positron current of 18 mA at 3.87 GeV and a wavelength of 1.25 Å, a diffraction photograph from wet unstained cornea shows rings from the 3rd to 12th order after 30 minutes exposure. Shorter exposures showed the 2nd order of collagen diffraction, and with dry collagen rings from the 2nd to 18th order could be observed. This compares with the several hours needed to see only the 3rd and 5th order reflexions using a GX6 rotating anode and a (double Franks) focussing camera, although it must be pointed out that the rotating anode set-up will resolve first order diffraction up to 900 Å, unlike X11 as at present constituted.

Plate XXVIII a

Plate XXVIII b

(3) Time resolved experiments with a television-type x-ray detector on contracting frog muscle

H. Huxley, A. Harmsen, J. Milch

X-ray diagrams were recorded from contracting frog sartorius muscle using Dr. Milch's television-type x-ray detector (see p.102) and the X11 optical bench. Good pictures of the stronger equatorial and meridional reflexions could be taken in single exposures of as little as 100 milliseconds even with storage ring currents of only 10 to 20 mA (at 3.8 GeV). The behaviour of the layer lines during contraction was studied in a series of twitches with a total exposure time of a few seconds. The 430 Å layer line was found to disappear virtually completely during contraction and to reappear within about half a second afterwards. With more appropriate storage ring parameters and more usable beam time, an important range of new experiments on the structural changes in muscle during contraction and relaxation should be possible.

(d) Small angle scattering at X12 in Lab 4

H. Stuhrmann, M.H.J. Koch

First test experiments, with satisfactory results, were made in July 1977. Small angle scattering from various protein solutions was measured to

(a)

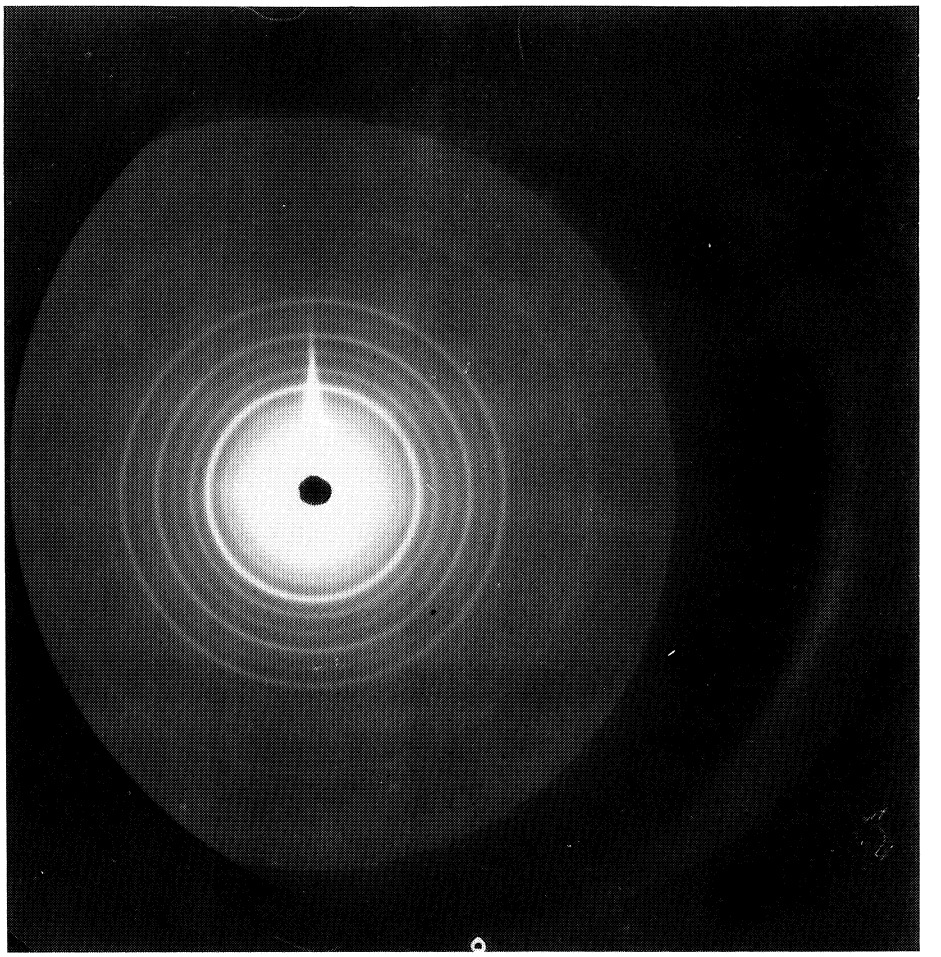

(b)

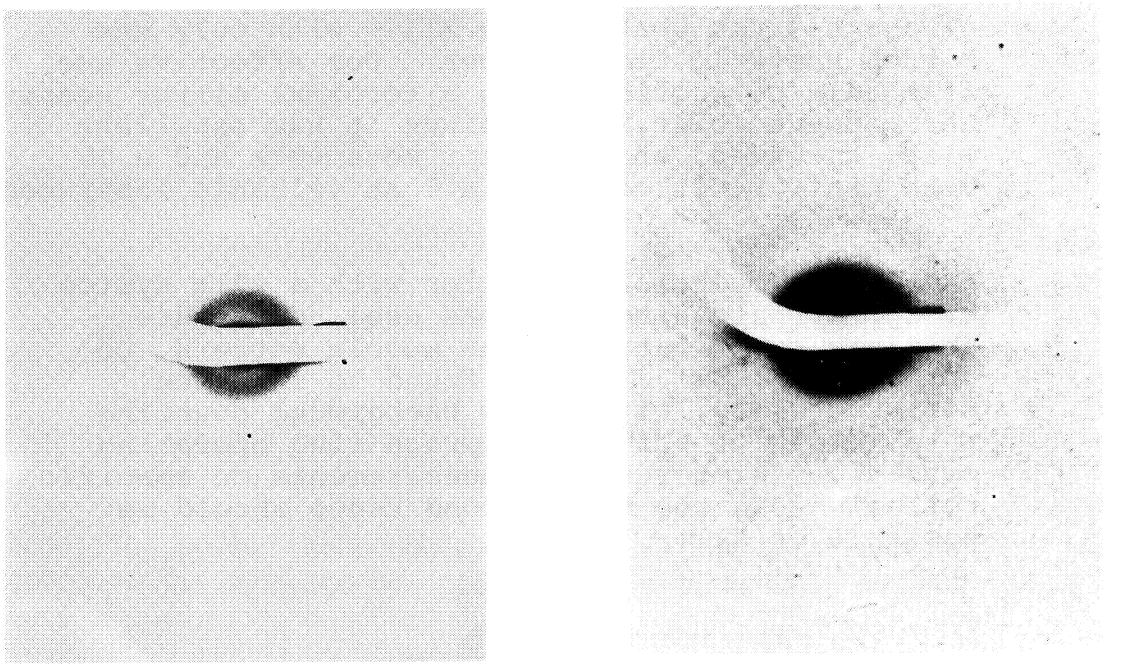

Plate XXVIII

(a) X-ray diffraction photograph of wet corneal collagen (DORIS, 3.87 GeV, 18 mA, wavelength 1.25 Å). Exposure time 30 min.

(b) For comparison, two x-ray photographs of a similar specimen using an Elliott GX6 rotating anode x-ray tube and a double-focussing Franks camera. Several hours' exposure are needed to see the third and fifth order reflexions in the two pictures. (G.F. Elliott)

investigate the ratio between the scattered intensity from the solute, from the solvent and from slits, windows and air. Measurements were made with "white" radiation, with a pinhole diameter of 0.4 mm, and a position-sensitive area detector (A. Gabriel).

(e) Experiments at X14

H. Huxley, A.R. Faruqi

X14 (property of the Medical Research Council, U.K.) was set up at the end of the storage ring beam line with a bent Ge-crystal monochromator and a single 20 cm long glass mirror. The count rate in the focussed beam at λ=1.54 Å was measured to be approximately 3 x 10^8 photons/sec with the storage ring operating at 20 mA and 3.8 GeV; this flux is somewhat below the theoretical value (>10^9) but the alignment of the beam from DORIS was uncertain at the time. However, since this camera is considerably further from the tangent point than X11, and since it has a maximum of two mirrors (as opposed to 8 in XII), the intensity it gives will always be much weaker than X11 - with only one mirror about 10 times weaker. For effective use it should be provided with a toroidal mirror nearer the tangent point, when, since it has excellent slit, specimen, and detector movements and a TV beam monitor, it could be a most valuable instrument.

A simple proportional counter with a slit system of appropriate dimension was used to measure absolute count rates on the muscle pattern, on both X14 and X11. It was found to function satisfactorily, with a low background counting rate, and with suitable storage ring operating conditions time-resolved measurements on specific reflexions in the millisecond range should be possible on X11.

(f) Test experiments at X15

H. Stuhrmann, A. Gabriel, M.H.J. Koch

The small angle instrument X15 receives radiation from a double monochromator. Alignment of the two monochromators, which may be between 1.30 m and nearly 6 m apart, was not difficult even with

rather perfect germanium crystals because the Ge_{111} reflexion could easily be found with the area detector. Using two asymmetric all-cut crystals the vertical beam width could be reduced by a factor of 3.

(g) Test experiments with an energy-dispersive counter

Sir John Randall, J. Bordas, M.H.J. Koch

It is well known that the ratio $\sin\theta/\lambda$ (2θ = scattering angle, λ = wavelength) is the relevant variable in all scattering experiments. Using "white" radiation the energy analysis of scattered photons at a given angle yields a scattering pattern equivalent to that taken at different scattering angles and constant wavelength. Energy-dispersive detectors are semiconductors which are sensitive to x-rays. The energy resolution is about 150 eV which corresponds to a wavelength resolution of about 1%. First test experiments with protein solutions yielded good results. As "white" radiation damages biological samples in a short time, the measurement has to be done quickly, and this can be achieved with an array of several energy-dispersive counters. A prototype with both spatial and energy resolution is being prepared in England and will be tested at one of our instruments in a few months.

(h) X-ray absorption fine structure (EXAFS) studies with S1 in Lab 2

M. Zeppezauer, J. Bordas

The instrument S1 was built at Daresbury and installed at the synchrotron in December 1977; it is being used jointly with physicists from Daresbury and DESY. First test experiments were done with alcohol dehydrogenase, which contains one zinc atom per 20,000 daltons. Though the zinc absorption edge is quite easy to observe, the statistics available were not good enough for a clear observation of the oscillatory structure. It is estimated that good data will be obtained from dilute solutions of metalloproteins in about 24 hours. S1 needs improvement for biological applications; measurement of the fluorescence radiation would be more convenient, and double-focussing mirrors would increase the intensity by nearly two orders of magnitude.

(j) Quaternary structure determination of polymeric proteins by nuclear resonance scattering

R.L. Mössbauer, F. Parak, Ch. Hermes, H. Stuhrmann

The aim is to develop a new method for the determination of the quaternary structure of polymeric proteins. The ^{57}Fe nucleus will be used as a label, and the Mössbauer scattering of this nucleus will be separated from the Rayleigh scattering of the atoms of the protein by using the time structure of the synchrotron radiation.

The first problem is to establish the time filtering procedure. In the first experiment synchrotron radiation from DORIS was reflected by two carbon monochromators on to a beam stop of metallic iron which was used at the same time as target. Energy close to 14.4 KeV was chosen so that Mössbauer scattering could not occur. The scattered radiation was registered by a fast plastic scintillator on a fast multiplier. The intensity of the synchrotron radiation was reduced by a diaphragm to about 5.10^5 c/min. The storage ring was working in the single bunch mode, i.e. 300 ps flashes of x-rays appear with a period of 1 μs. Coincidence electronics were used to measure the scattered x-rays during the flash, or at a definite time after it. In the first case an average counting rate of about 10^4 c/min. should be observed, whereas in the second there should be practically no counts, since no time-delayed processes are involved in this test experiment. The preliminary result, however, was a ratio between the two count rates of 100:1. The experiment has not yet been fully analysed, but it is possible that in the so-called single bunch mode of DORIS some "wrong" bunches are produced.

(k) Neutron scattering studies at the EMBL Outstation Grenoble and the Institut Laue-Langevin

M.H.J. Koch, H. Stuhrmann

Interpretation of neutron low-angle scattering data on *E. coli* ribosomes has continued.

Using the contrast variation method with 70 S particles reassembled from protonated and deuterated subunits, we have shown that the association of the two subunits occurs without major changes of shape or of protein and RNA distribution. It has further been demonstrated that the RNA is on average near the centres of the subunits, and the protein nearer the outside; also that the distance between the centres of the subunits is about 9 nm.

III. Detectors and data acquisition

J. Hendrix, H. Fürst, P. Clout, J. Milch

Hitherto use has been made of position-sensitive linear and area detectors designed by A. Gabriel. These detectors have now improved greatly, having almost homogeneous sensitivity and running for periods of months without breakdown. The maximum counting rate is of the order of 10^5 cps and the resolution in x and y direction is 1%. The amplitude signal from the electronic circuit of the detector is digitized and stored in a software-controlled multichannel analyzer IN90 (Intertechnique). The number of picture elements will shortly be increased from 8,000 to 16,000.

The demand for an area detector with still better resolution has led to a new concept of data acquisition, adapted from similar developments at the ILL. A CAMAC memory of 256K 16-bit words has been built at the ILL for the Hamburg Outstation; a special increment module allows fast addressing and incrementation of the memory, and the cycle time is less than 1 µs. A real time display, to be delivered shortly, allows a three-dimensional representation of the scattering pattern. The maximum counting rate will be 1-2 MHz.

(a) A new detector

The single bunch mode of the storage ring (one short pulse of 0.1 ns, each µs) has been regarded as a fatal nuisance for x-ray photon counters. However, this need not be true, as demonstrated by J. Hendrix in his proposal for a drift chamber.

To demonstrate the principle we consider a flat cylindrical detector with a central anode wire and an outer cylindrical cathode; a constant electrical field is necessary. An incoming flash of scattered x-ray photons will be absorbed in the gas of the drift chamber and the electrons created will move at a constant speed towards the anode wire. This takes a time which depends on the length of the path of the electrons, and each electron bunch will arrive after a different time which is a direct measure of the distance between the origin of the bunch and the centre of the detector. After 1 μs all electrons will have arrived at the central anode, and the next pulse starts the same game over again.

In practice the role of anode and cathode are changed so that the electrons drift towards the outer wires. This allows angular as well as radial resolution (expressed in polar coordinates). The electronics are designed so that 1024 photons per bunch can be processed, giving a counting rate of 10^9 cps. The construction of the detector is in progress and first tests are expected early in 1978.

(b) A fast x-ray detector based on scintillators, image intensifiers, and a TV camera

J. Milch (Princeton University, USA)

The principle of this detector is that a diffracted x-ray photon is converted to photons in the visible region by a thin scintillating phosphor; an image intensifier amplifies the light pattern, and a cooled silicon diode Vidicon (SIV) TV camera capable of on-target integration records the visible light pattern. A computer and associated electronics allow read-out of the TV camera, storage of data and control of experiments.

The present model, which was designed and built at Princeton University, is capable of recording x-rays over an area 40 mm in diameter without the count-rate limitation inherent in all x-ray counters. The system includes fast shutters which make possible time-resolved recording. Data from the camera are stored directly in digital form on a disc connected to a PDP-11 computer, so the results are available for immediate inspection as well as for later detailed analysis.

The detector has been used to record diffraction patterns from insect flight muscle (with R. Goody and W. Hofmann) and from frog sartorius muscle (with H.E. Huxley). Excellent data could be accumulated in only 1 - 10 sec., so it was possible to record diffraction from the frog sartorius muscle not only in the relaxed state, but also during and just after stimulation.

TABLE 1

THE PROPERTIES OF X-RAY SYNCHROTRON RADIATION AND ITS USES IN MOLECULAR BIOLOGY

Property	Use
High intensity	Though always desirable, it becomes essential in kinetic investigations (dynamics of diffraction, stopped flow techniques). Micro-diffractometry. Extension of diffraction patterns to very high resolution.
High degree of collimation (low divergence of the beam)	Diffraction of structures with unit cells larger than 100 Å (muscle, viruses, quarternary structures)
Linear polarization	Influences layout of x-ray optics.
Continuous spectrum (with beryllium windows from 4 Å to 0.01 Å)	Anomalous dispersion. Absorption and fluorescence spectroscopy
Time structure (0.1 ns pulse each μs)	Lifetimes of excited nuclei (Mössbauer diffraction). Molecular motions.

TABLE 2

INSTRUMENTS AT THE SYNCHROTRON

NAME	INSTRUMENT	OPERATION	PURPOSE
X1 until 20.2.1978	Small angle diffractometer; double focussing system with two mirrors and Ge-monochromator. Constant wavelength (1.54 Å)	Completely remote controlled	Diffraction experiments on muscle, collagen, membranes
from May 1978	Double focussing system with eight mirrors and Ge-monochromator. Constant wavelength (1.54 Å) corresponds to X13 in LAB 4.	New optical bench; freely accessible with remote control of mirror and monochromator.	
X2 from April 1978, test till Summer 1978	Small angle scattering with "white" radiation, with energy dispersive counters and position-sensitive Gabriel detectors.	Sample control and exchange through holes from the upper floor; remote control of mirrors and camera alignment.	Short time small angle scattering experiments on solutions and suspensions; stopped flow techniques.
X3* from May 1978	Movable optical bench (length 2 m). Double focussing system with two mirrors and Ge-monochromators, Wavelength 0.6 to 2.0 Å.	Completely remote controlled	Diffraction experiments (for test and development of instruments).
S1* ready	X-ray absorption spectrograph with two "locked" Ge-double monochromators. Energy resolution about 1 eV. (constructed at Daresbury, U.K.).	Completely remote controlled	X-ray absorption fine structure of metal proteins.

* X3 and S1 cannot run simultaneously

TABLE 3

INSTRUMENTS AT THE STORAGE RING

NAME	INSTRUMENT	OPERATION	PURPOSE
Ground Floor			
X11	Small angle diffractometer, double focussing system with eight mirrors and bent Ge-monochromator. Movable optical bench. Wavelengths: 0.5 to 2.2 Å.	Completely remote controlled	Diffraction experiments on muscle, collagen and other connective tissues, crystallography of proteins, viruses etc.
X12* (with mirrors in April 1978)	Small angle scattering with "white" radiation. Position-sensitive area detectors of A. Gabriel (20x20 cm). Distance sample-detector: 25, 45, 90, 180, 360 and 720 cm.	Sample control and exchange through holes from the upper floor; remote control of camera alignment.	Short time small angle scattering experiments. Stopped flow techniques.
X13 from April 1978	Small angle diffractometer, double focussing system with eight mirrors and (bent) Ge-monochromator. Fixed wavelength (1.5 Å). Delivery of optical bench and supplementary pieces in March 1978. Oscillation camera for Crystallography.	Optical bench freely accessible, remote control of mirror and monochromator.	Mainly diffraction experiments on proteins, viruses.
X14*	Diffractometer, double focussing system installed in X14 (brought from Daresbury, U.K., by H.E. Huxley, MRC, Cambridge)	Completely remote controlled	Diffraction experiments on muscles.
Upper Floor			
X15 (being tested)	Small angle diffraction; parallel upwards shift of the beam by 130 cm with two Ge-monochromators. Wavelengths: 0.7 to 4.5 Å. Position-sensitive area counter. Distance sample-detector: 25, 45, 90, 180, 360 and 720 cm.	Instrument freely accessible; remote control of monochromator crystals.	Diffraction from connective tissue, membranes, solutions.
X16 after May 1978	Place for a diffractometer. Wavelengths 1.3 to 4.5 Å.	Freely accessible, remote control of monochromators.	Anomalous dispersion.
P11 Test	Small angle diffraction. Detectors with a gating frequency adapted to the pulse structure of the radiation (one pulse of 0.1 ns each 1 μs).	Freely accessible, remote control of monochromator.	Mössbauer diffraction.

* X12 and X14 cannot run simultaneously

The Outstation at the ILL, Grenoble

Head: A. Miller

Members: C. Berthet, A. Gabriel, H. Lindley (part-time), D. Tocchetti

Fellows: S. Cusack, D. Hulmes

Visiting workers: B. Brodsky*,K. Piez*, G. Rogers*, I. Serdyuk*, A. Veis*
M. Carpenter*, M. Crifo*, G. Elliott*, J. Finney*, M. Greenwall*, B. Jacrot *et al.**, M. Koch*, M. Marett*, M. Marian*, R. Parfait*, M. Podo*, Sir John Randall*, D. Roger*, N. Roveri*, D. Sadler*, R. Stevens*, M. Strom*, P. Timmins*, R. Wade *et al.**, D. Worcester*

Technical assistants: J.-M. Bois, F. Dauvergne, H. Krischke, H. Ngotri, J. Sedita

The number of external users of the Outstation (i.e. not from EMBL or ILL) this year was fourteen groups from six countries. It is unlikely to grow vastly beyond this number since most of the groups carrying out approved ILL experiments now make some use of the Outstation. It appears that the equipment of the biochemistry laboratory is at about the right level for users; there were some occasions during the year when it became overcrowded if a full complement of resident visiting scientists and several user groups happened to be present simultaneously, but normally the load on equipment is reasonable. Plans were made during the year to start a laboratory devoted to the deuteration of organisms. This will start in 1978 and, like the rest of the Outstation, will be available to external users as well as to EMBL staff.

The research projects on connective tissue have continued and are described in the following sections. The main aim at present is to determine how the collagen molecules pack in three dimensions and to investigate how collagen and other molecules interact to produce different varieties of connective tissue. More generally, the application of neutron scattering to biology is being developed. The ways in which neutron scattering complements and extends x-ray and light scattering are of particular interest.

Neutron diffraction study of fibril packing in rat tail tendon

S. Cusack, T. Finney (Birkbeck College), D.J.S. Hulmes and A. Miller

In December 1975 a peak at 4000 $Å^{-1}$ was observed in the equatorial neutron scattering from rat tail tendon, using the D11 detector at 40 m. Since then more data have been collected to study the behaviour of this peak as a function of ionic strength, relative humidity, fixation and enzyme treatment. Electron microscopy shows that the cylindrical collagen fibrils in rat tail tendons have diameters ranging from 500 Å to 5000 Å (Parry and Craig, 1977), so the preliminary interpretation of the 4000 $Å^{-1}$ peak was either an interfibrillar interference maximum or a Bessel function maximum arising from the cylindrical fibrils. Since then, we have attempted to simulate the neutron diffraction observation by calculating the Fourier transforms of random arrays of parallel cylinders, with a diameter distribution taken from electron micrographs of rat tail tendon. The packing fraction of these arrays can be varied.

We have recently observed peaks corresponding to 4000 $Å^{-1}$ in the model calculations for the high density arrays. These peaks are interference maxima rather than Bessel function maxima. Besides being a function of the packing density, the appearance of the peak is highly dependent on the order in which different diameter discs are selected in generating the random array. If the diameters are selected either at random or in order of increasing size the calculated 4000 $Å^{-1}$ peak is very weak, even for packing fractions as high as 0.85. If the diameters are selected in order of decreasing size, however, the calculated peak is very strong and there are further maxima at higher scattering angles. Further work is necessary to characterize these observations as functions of packing fraction and the polydispersity of cylinder diameters. Besides providing a contribution to the study of small angle scattering from polydisperse systems, this work may allow the determination of the *in vivo* packing fraction of the fibrils in rat tail tendon. This could be compared with electron microscope observations on sectional material. If the packing fraction *in vivo* is known, then density measurements on whole tendons could be related to density within fibrils, thus permitting a more critical appraisal of molecular packing models.

Electron microscope/x-ray diffraction approach to the problem of molecular packing in collagen

C. Berthet, D.J.S. Hulmes, A. Miller and C. Wolff

Plate XXIX

X-ray diffraction has shown that there is lattice-like order in the molecular packing in rat tail tendon (Miller, 1976). Several solutions have been proposed for the indexing of the Bragg reflexions and, even where there is agreement on the indexing, there have been a number of suggestions for the unit cell contents. So far, electron microscopy has provided relatively little information on this problem. A regular three dimensional lattice has not been observed in electron micrographs of collagen fibrils, even though the x-ray measured equatorial spacings (up to 38 Å) are well above the limiting resolution of the microscope. The lattice is very labile, however, so it is possible that the ordered structure is destroyed during specimen preparation for electron microscopy. Our rationale in the present work is to use x-ray diffraction to monitor all stages of preparation and hence to find a preparation procedure which can be shown to preserve the regular lattice. It should then be possible to visualize this lattice in electron micrographs of ultra-thin sections of collagen fibrils.

Specimen preparation for ultra-thin sectioning consists of fixation, staining, dehydration and embedding. Since beginning this project in January 1977 we have shown that conventional glutaraldehyde fixation, in a variety of ionic and osmotic conditions, destroys the lattice-like order in the lateral molecular packing. Formaldehyde fixation, or formaldehyde followed by glutaraldehyde, preserves the lattice, however, provided the tendons are unstretched. Subsequent post-fixation with osmium tetroxide, bulk staining with a variety of heavy metal stains, and dehydration with either alcohol or acetone, leaves the main features of the lattice intact. Embedding in low viscosity epoxy resin (Spurr) causes a swelling of the 38 Å spacing to 50 Å. Embedding in Epon, however, causes no change in lattice dimensions, as monitored by x-ray diffraction. There is now available, therefore, a preparation for ultra-thin sectioning which preserves the lattice-like order in the lateral molecular packing.

Plate XXIX

(a)

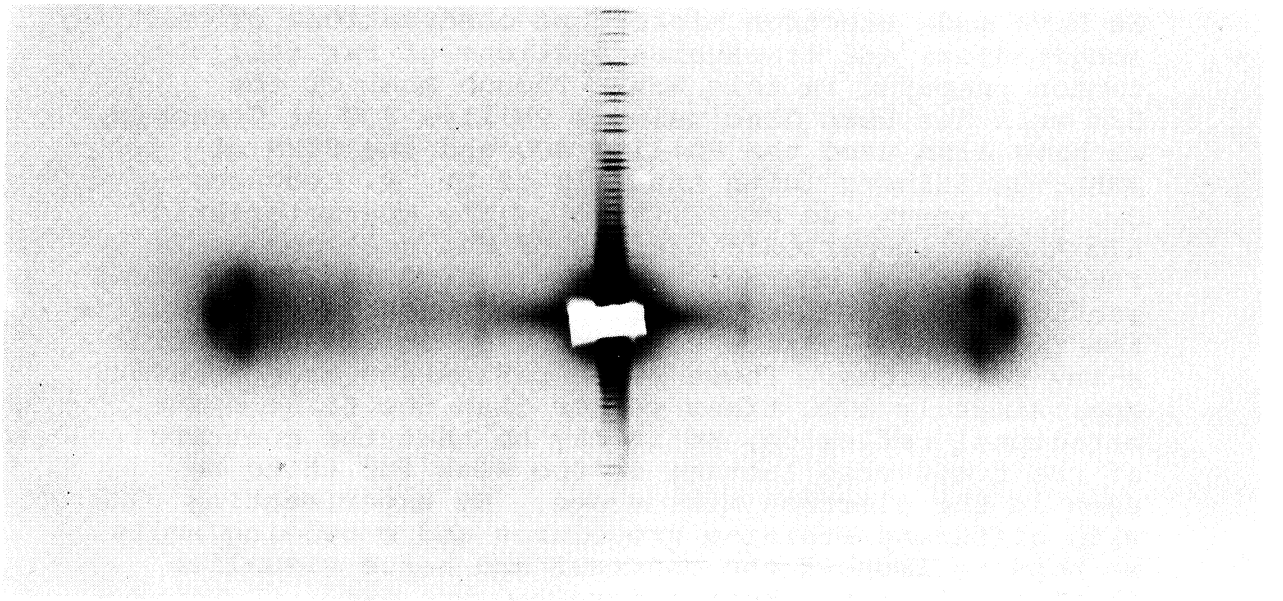

(b)

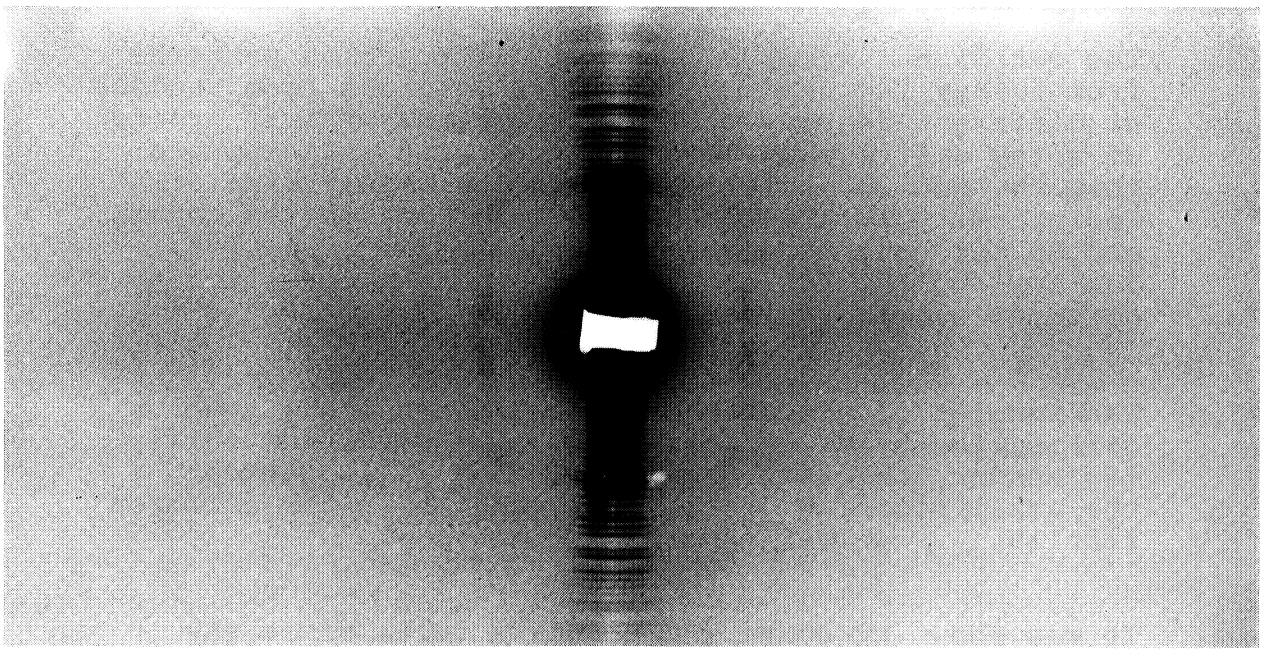

Plate XXIX

Medium-angle x-ray diffraction patterns of rat tail tendon: (a) under native conditions, (b) embedded in Epon. Fibre axis (meridian) vertical, equator horizontal.

We have made electron microscope observations of longitudinal and transverse sections of rat tail tendon prepared in this way. Though most of the E/M work has been done using a Philips 300 at Grenoble, we have also used the Philips 400 and the STEM at EMBL, Heidelberg (with the help of Dr. K. Leonard, Dr. R. Freeman and Mr. T. Arad). The characteristic 670 Å axially-periodic banding of the collagen fibrils can, of course, be clearly seen in longitudinal sections but, so far, we have not been able to visualize the transverse lattice corresponding to the equatorial x-ray reflexions. These Bragg reflexions are, however, approximately 1000 times weaker than the first order meridional reflexion, so it may be that the contrast of the transverse lattice is too weak for it to be seen in the electron microscope. By experimenting with different staining procedures and embedding media we hope to improve the contrast and hence visualize the lattice in the near future.

The mineralization of turkey leg tendon

D.J.S. Hulmes, A. Miller, S.W. White and P.A. Timmins (ILL)

The meridional x-ray and neutron diffraction patterns from turkey leg tendons have been obtained from tendons at different degrees of mineralization. Thirty orders of x-ray diffraction have been observed. It appears that the medium angle reflexions are rather similar in intensity to those obtained from uncalcified tendon and do not vary much with degree of mineralization. The low-angle reflexions on the other hand are strongly affected by mineralization.

The results of a combined low-angle x-ray and neutron diffraction study of calcified and uncalcified turkey leg tendon indicate that the mineral is located at the axial position of the "gap" region in the collagen fibrils.

It was shown by Hodge and Petruska that, since the molecular length of collagen is about 4.5 D where D is the intermolecular stagger, the axial period in the fibrils is divided into a "gap" region and an "overlap" region. Though it was suggested that these

"gap" regions might be the site of mineral crystallites in calcified collagen, this idea has been the subject of controversy and unambiguous experimental evidence has been lacking. We have re-investigated this problem by recording the low-angle meridional reflexions in the x-ray and neutron diffraction patterns from calcified und uncalcified turkey leg tendons.

Neutron diffraction is a particularly useful method for studying bicomposite materials at low resolution. This is because protons scatter neutrons very differently from deuterons, so by varying the D_2O/H_2O ratio in the medium surrounding the specimen different contrasts can be obtained. The average neutron scattering density from biological macromolecules lies between the scattering densities of D_2O and H_2O. Hence by making up mixtures containing the appropriate ratios of D_2O/H_2O, the scattering from selected parts of the specimen can be matched so that the neutron diffraction pattern is then dominated by the non-matched part of the structure. This contrast variation has been applied in a systematic and quantitative way to the low-angle meridional reflexions from calcified and uncalcified turkey leg tendon, and it is clear that at low-resolution the mineral component is scattering out of phase with the collagen "overlap" region.

The actual intensity values indicate that a volume of 30,000 $Å^3$ of mineral occurs in each gap. Taking the gap length as 230 Å, this indicates a cross-sectional area of 94 $Å^2$ for mineral, which corresponds reasonably well with the diameter of a collagen molecule (White *et al.*1977).

The low-angle x-ray reflexions from tendons at six different degrees of mineralization were analyzed further by comparing the observed intensities with those predicted by various models. The aim was to establish the most general type of model for the way the mineral deposit grows in the gap region. Four models were considered. (1) Mineral grows from a nucleus at the N-terminal end of the gap. (2) Mineral grows from a nucleus at the C-terminal end of the gap. (3) Mineral grows from a nucleus in the middle of the gap. (4) Mineral deposit grows by a uniform deposit over all of the gap. The comparison between observed and predicted intensities at different degrees of calcification strongly indicates the first model as accounting best for the way the mineralization takes place (White, 1978).

(Some x-ray studies were done in the EMBL Outstation at the DESY Synchrotron in Hamburg with the collaboration of A. Harmsen.)

The structure of collagen in cartilage of intervertebral disc

C. Berthet, D.J.S. Hulmes, A. Miller and P.A. Timmins (ILL)

Intervertebral disc contains three anatomically distinct regions, the cartilaginous end-plates, the hydrated gel-like *nucleous pulposus* and the fibrocartilaginous *annulus fibrosus*. The latter structure connects neighbouring vertebrae and is composed of 10-15 lamellae which are concentric cylindrical sheets. Collagen fibres in these sheets are oriented at 40-70° to the vertebral axis with opposite directions of tilt occurring in adjacent lamellae. Chemical studies reveal that the *annulus fibrosus* consists of much more non-collagenous material than tendon and also contains both Type I and Type II of the genetically distinct collagens. The distribution of these two types is not uniform; Type I predominates at larger radial locations while Type II predominates at smaller radial locations (Eyre and Muir, 1976).

We have studied the *annulus fibrosus* by small-angle x-ray and neutron diffraction to investigate the collagen in the tissue and the possible interaction between collagen and proteoglycans or glycoaminoglycans. The x-ray diffraction patterns were recorded both by a position-sensitive counter (J.-M. Bois) and by film. It proved possible to record up to 22 orders of the collagen meridional reflexions which index on a repeat distance of 670 Å. The intensities of these reflexions are similar to the corresponding intensities from collagen in tendon; however, a detailed examination shows that significant differences do exist. The intensities of the first few orders follow the pattern "strong odd - weak even" more closely in cartilage than in tendon, thus indicating that the gap/overlap ratio is closer to 1 in the former tissue. A difference Fourier synthesis using the intensities from the *annulus fibrosus* and the rat tail tendon and the phases from Model E in Hulmes *et al.* (1977) confirms this interpretation. Therefore either the collagen molecules in *annulus fibrosus* are longer than in rat tail tendon, or there is extra material bound to each end of the molecule in *annulus fibrosus*.

Plate XXX

The neutron diffraction pattern has not been obtained to such high resolution. It was recorded on the D17 instrument at ILL and a contoured pattern is shown in which the direction of the vertebral column may be regarded as vertical. The first six orders of the 670 Å collagen period may be clearly seen and are labelled 1-6. The second order is too weak to appear on the contour map. The direction of the line of reflexions indicates that the collagen fibrils are oriented about 70° to the direction of the vertebral column. A second less distinct line of reflexions reveals another population of collagen fibrils oriented again at 70° to the vertebral column but tilted in the opposite direction to the first set. Since the first set of reflexions are of similar intensity on both sides of the origin of the diffraction pattern, the collagen fibrils from which they originate must lie in the plane of the specimen. Since the specimen was cut at a fixed radius, these two sets of reflexions obviously originate from the radial lamellae of collagen fibres seen by optical polarization microscopy. Adjacent lamellae were seen by that method to be alternately tilted in opposite senses from the vertebral column direction. The neutron diffraction pattern confirms that the collagen fibrils follow the direction of the optically visible fibres. The intensities of the reflexions in Plate XXX are strikingly different from those in the neutron diffraction pattern from rat tail tendon in a D_2O solution of 0.15 M NaCl, particularly in the fifth order which is considerably stronger in the pattern from *annulus fibrosus* than in that from tendon.

These preliminary neutron diffraction results are consistent with the conclusion from the x-ray diffraction pattern, *viz.* that the differences between the diffraction patterns from tendon and *annulus fibrosus* may be either a difference in molecular length or that non-collagenous materials in the fibrocartilagenous tissue are regularly attached to the collagen. This latter possibility is being tested by the contrast variation method that neutron diffraction allows and we are also testing (C. Mason (EMBL) and D. Herbage (Lyon)) whether the dissected fibres used as specimens for x-ray diffraction are markedly different in chemistry and structure from the matrix in which they are embedded, and if differences are observable between fibres at differing radial positions in the *annulus fibrosus*.

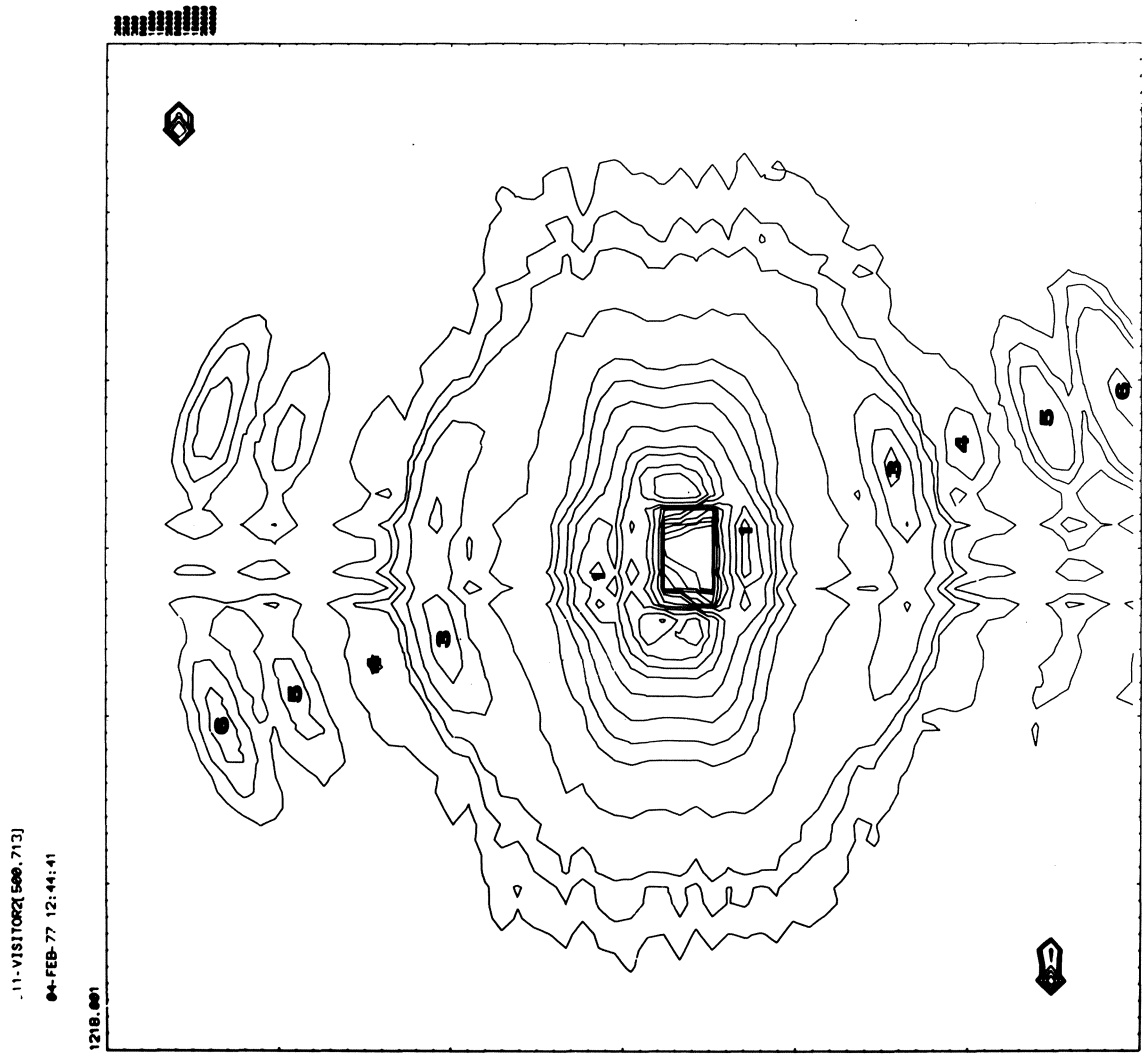

Plate XXX

Neutron diffraction pattern of collagen in cartilage of the intervertebral disc. For explanation see text.

Inelastic (Brillouin) light scattering from biopolymers

S. Cusack and A. Miller

Experiments using a triple-pass Fabry-Perot interferometer to frequency-analyse the light inelastically scattered by biological fibres are being continued by S. Cusack and R. Harley (Oxford), and with the encouragement of J.W. White (ILL). Inelastic scattering can occur when incident argon laser light (λ = 514.5 nm) interacts with sound waves propagating in the fibre, giving rise to intensity maxima in the scattered light spectrum at a frequency shift corresponding to that of the sound wave (typically 10 GHz). The scattering geometry determines the wavelength of the sound and thus a direct measure is made of the "hypersound" velocity in the fibre. This dynamic measurement can be related on the one hand to inter- and intra-molecular forces and molecular structure within the fibre and on the other hand to the mechanical (elastic) properties of the fibre.

The mechanical properties of fibrous proteins are of great biological importance and most of the work to date has been done on collagen fibres from rat-tail tendon. Results already published (Harley *et al.* (1977) show that longitudinally-polarized acoustic waves propagate along the fibre axis with a velocity dependent on relative humidity (3.9×10^5 cm/s at 0% decreasing to 2.6×10^5 cm/s at 85%). These results give values for the high frequency, microscopic Young's modulus of collagen which are nearly two orders of magnitude higher than those obtained by static, macroscopic stress/strain measurement. The decrease in sound velocity with increasing humidity can be partially explained by rigid loading of the collagen by water molecules but some softening of forces is also apparent. It is hoped to correlate these effects with inelastic neutron measurements on collagen. Recently a probable transversely polarized sound wave, also propagating along the fibre axis but with velocity 1.5×10^5 cm/s, has been observed. However the expected longitudinal accordion modes of vibration of the collagen molecule have not yet been detected.

More data are needed to help interpret these results. In particular work is in progress to observe hypersound waves in other fibrous proteins and synthetic polypeptides to try and relate the elasticity of polypeptide chains to their chain configuration.

X-ray cameras

C. Berthet

Two rotating anode x-ray generators (GX13-GX20) were installed at the beginning of 1977, and the following three x-ray cameras are now working: a medium angle camera with a sample-to-film distance of 17.5 cm and a cylindrical film, and two small-angle cameras, one with sample-to-film (or detector) distance variable in 10 cm increments up to 120 cm, and the other with sample-to-film (or detector) distance variable continuously from 40 cm to 130 cm. In all these cameras the focussing system is based on Huxley-Holmes optics. Different types and sizes of mirrors and monochromators can be used, depending on the kind of the focus desired. For example, gold mirrors are used to obtain maximum of intensity, or crown glass mirrors to obtain better resolution; the monochromators are quartz crystals cut so as to make an angle of either 3° or 6° with the 1011 planes according to the sample-to-film distance. It is also intended to instal a camera for solutions, in order to permit visitors using the neutron facilities to make complementary studies by x-ray techniques.

Computing

D. Tocchetti

The Norsk Data Nord 10 Computer was installed in April 1977, and a new version in September. In September the Optronics scanner and writer were also connected via a CAMAC interface, and operate satisfactorily. In the near future it is planned to connect a light scattering apparatus *via* the CAMAC interface. The software developed at EMBL in Heidelberg for image treatment is available, and has been implemented in Grenoble for particular needs - the determination of row lines and intensity measurements. The IN90 analyser has been linked *via* a TTY interface to the computer, to transfer data from the one-dimensional detector for further data treatment. Finally data from the Optronics scanner can be transferred on magnetic tape to a computer group at the CENG if it is desired to use their analysis facilities.

Detectors

J.-M. Bois

Several linear position-sensitive detectors with their associated equipment have been set up in the laboratory. The following installations are now working:

(1) one detector (Borkowski syst) 60 mm long or 100 mm long (overall resolution due to beam, detector, electronics: about 200 μm). It is easy to measure periodicities up to 700 Å.

(2) one minotor with bright transmission (90%).

(3) two diffraction patterns can be measured simultaneously.

(4) a device which automatically moves the sample chamber during an experiment. This allows continuous monitoring across a sample such as intervertebral disc where the structure changes from one side of the specimen to the other.

(5) dynamical acquisition up to 100 Hz.

(6) connection between IN90 analyser and N10 computer for data treatment.

References

Eyre, D.R. and Muir, H. (1976). *Biochem. J.*, *157*, 267.

Harley, R., James, D., Miller, A. and White, J.W. (1977). *Nature (London)*, *267*, 285-287.

Hulmes, D.J.S., Miller, A., White, S.W. and Doyle, B.D. (1977). *J. Mol. Biol.*, *110*, 643-666.

Miller, A. (1976). In *"Biochemistry of Collagen"* (Ramachandran, G.N. and Reddi, A.H. eds.)

Parry, D.A.D. and Craig, A.S. (1977). *Biopolymers*, *16*, 1015.

White, S.W., Hulmes, D.J.S., Miller, A. and Timmins, P.A. (1977). *Nature (London)*, *266*, 421-425.

White, S.W. (1978). Ph.D. Thesis, University of Oxford.

gedruckt bei az-werbung + weber offset druck, heidelberg